

**Final Report**

Texas Water Development Board Contract # 2003-483

**Quantification of Terrestrial and Marine Sediment Sources to a Managed Fluvial, Deltaic and Estuarine System: The Nueces-Corpus Christi Estuary, Texas.**

**December 2004**

Peter H. Santschi

The Laboratory for Oceanographic and Environmental Research  
Department of Marine Science  
Texas A&M University at Galveston

Kevin M. Yeager

The Laboratory for Oceanographic and Environmental Research  
Department of Marine Science  
Texas A&M University at Galveston

## TABLE OF CONTENTS

1. INTRODUCTION	6
1.1 Overview	6
1.2 Introduction	6
2. STUDY AREA AND RESEARCH DESIGN	6
2.1 Study are and hydrologic setting	6
2.2 Research design	8
3. MATERIALS AND METHODS	10
3.1 Materials and field methods	10
3.2 Sample processing and radiochemistry	10
4. RESULTS AND DISCUSSION	14
4.1 Surface sediment size distributions	14
4.2 Surface sediment radionuclide data	17
4.3 Deltaic sedimentation	30
4.4 Nueces Bay and Corpus Christi Bay sedimentation	33
5. CONCLUSIONS	42
5.1 Summary	42
5.2 Recommendations	44
6. REFERENCES	45
7. ACKNOWLEDGEMENTS	48
8. APPENDIX I: Nueces Delta sediment cores physical and radiochemical data	49
9. APPENDIX II: Nueces Bay and Corpus Christi Bay physical and radiochemical data, x-radiographs and supporting data	54

## FIGURES AND TABLES

Figure 1: Map of southwestern Texas, showing the Nueces River watershed, major rivers and tributaries and Texas county delineations.	7
Figure 2: Decay series for $^{238}\text{U}$ and $^{232}\text{Th}$ , y = years, d = days, m = minutes and s = seconds (modified from Kendall & McDonnell 1998).	9
Figure 3: Map of the greater Nueces River watershed showing locations where alluvial sediment samples were collected.	11
Table 1: Physical data for all surface sediment samples collected.	12
Figure 4: Map of the greater Nueces River watershed showing locations where interfluvial sediment samples were collected.	15
Figure 5: Map of the greater Nueces River watershed showing locations where slope sediment samples were collected.	16
Figure 6: Map of Nueces and Corpus Christi Bays showing locations where sediment cores were collected.	17
Figure 7: Ternary plot of grain size fractions for all surface sediment samples collected. Squares represent marine sediments, circles represent terrestrial sediments and triangles represent sediments in depocenters.	18
Figure 8: Ternary plot of mean grain size fractions for all surface sediment sample types collected. Squares represent marine sediments, circles represent terrestrial sediments and triangles represent sediments in depocenters.	18
Table 2: Radionuclide data for all surface sediments ( $\text{mBq g}^{-1}$ ).	19
Table 3: Mean lithogenic isotope ratios for all surface sediment sample compartments and terrestrial and marine composites.	21
Figure 9: Changing $^{226}\text{Ra}/^{232}\text{Th}$ signatures for alluvial sediments with increasing distance inland.	22
Figure 10: Changing $^{230}\text{Th}/^{232}\text{Th}$ signatures for alluvial sediments with increasing distance inland.	22
Figure 11: Changing $^{226}\text{Ra}/^{228}\text{Ra}$ signatures for alluvial sediments with increasing distance inland.	23
Figure 12: $^{226}\text{Ra}$ versus $^{232}\text{Th}$ signature for all surface sediment samples, by compartment. Circles (warm colors) delineate terrestrial, squares (cool colors) delineate marine and triangles (grey scale) delineate basin sediments.	23
Figure 13: Mean $^{226}\text{Ra}$ versus $^{232}\text{Th}$ signatures for all surface sediment compartments. Circles delineate terrestrial, squares delineate marine and triangles delineate basin samples.	24
Figure 14: Mean $^{226}\text{Ra}$ versus $^{232}\text{Th}$ signatures for composite marine and terrestrial sediment source compartments and basins.	24
Figure 15: Mean $^{226}\text{Ra}$ versus $^{230}\text{Th}$ signatures for composite marine and terrestrial sediment source compartments and basins.	25
Figure 16: Mean $^{228}\text{Ra}$ versus $^{232}\text{Th}$ signatures for composite marine and terrestrial sediment source compartments and basins.	25
Figure 17: $^{230}\text{Th}$ versus $^{232}\text{Th}$ signature for all surface sediment samples, by compartment. Circles (warm colors) delineate terrestrial, squares (cool colors) delineate marine and triangles (grey scale) delineate basin sediments.	26
Figure 18: Mean $^{230}\text{Th}$ versus $^{232}\text{Th}$ signatures for all surface sediment compartments. Circles delineate terrestrial, squares delineate marine and triangles delineate basin samples.	27
Figure 19: Mean $^{230}\text{Th}$ versus $^{232}\text{Th}$ signatures for composite marine and terrestrial sediment source compartments and basins.	27
Figure 20: Mean $^{228}\text{Th}$ and $^{232}\text{Th}$ signatures for composite marine and terrestrial sediment source compartments and basins.	28
Figure 21: Mean $^{228}\text{Th}$ versus $^{230}\text{Th}$ signatures for composite marine and terrestrial sediment source compartments and basins.	28
Table 4: Results of Pearson correlation for sediment compartments, comparing the % clay fraction with individual isotope concentrations, *indicates that the p value is $< 0.001$ .	29

## FIGURES AND TABLES

Table 5: Sediment accumulation rates and means, fallout isotope inventories and expected fallout inventories for each of the delta cores collected, *full depth of activity not resolved.	30
Figure 22: Fallout radionuclide ( $^{137}\text{Cs}$ , $^{210}\text{Pb}_{\text{xs}}$ ) profiles for Nueces Delta core 1.	31
Figure 23: Fallout radionuclide ( $^{137}\text{Cs}$ , $^{210}\text{Pb}_{\text{xs}}$ ) profiles for Nueces Delta core 2.	31
Figure 24: Fallout radionuclide ( $^{137}\text{Cs}$ , $^{210}\text{Pb}_{\text{xs}}$ ) profiles for Nueces Delta core 3.	32
Figure 25: Fallout radionuclide ( $^{137}\text{Cs}$ , $^{210}\text{Pb}_{\text{xs}}$ ) profiles for Nueces Delta core 4.	32
Figure 26: Fallout radionuclide ( $^{137}\text{Cs}$ , $^{210}\text{Pb}_{\text{xs}}$ ) profiles for Nueces Delta core 5.	33
Table 6: Sediment accumulation rates and fallout isotope inventories for each of the bay cores collected, nd = no or insufficient data, *complete profile for $^{137}\text{Cs}$ not available.	34
Figure 27: Fallout radionuclide ( $^{137}\text{Cs}$ , $^{210}\text{Pb}_{\text{xs}}$ ) profiles for Nueces Bay core 2.	35
Figure 28: Fallout radionuclide ( $^{137}\text{Cs}$ , $^{210}\text{Pb}_{\text{xs}}$ ) profiles for Nueces Bay core 3.	35
Figure 29: Fallout radionuclide ( $^{137}\text{Cs}$ , $^{210}\text{Pb}_{\text{xs}}$ ) profiles for Corpus Christi Bay core 1.	36
Figure 30: Fallout radionuclide ( $^{137}\text{Cs}$ , $^{210}\text{Pb}_{\text{xs}}$ ) profiles for Corpus Christi Bay core 2.	36
Figure 31: Fallout radionuclide ( $^{137}\text{Cs}$ , $^{210}\text{Pb}_{\text{xs}}$ ) profiles for Corpus Christi Bay core 3.	37
Figure 32: $^{210}\text{Pb}_{\text{xs}}$ profile for Corpus Christi Bay core 4.	37
Figure 33: $^{210}\text{Pb}_{\text{xs}}$ profile for Corpus Christi Bay core 5.	38
Figure 34: Semi-log plot of $^{210}\text{Pb}_{\text{xs}}$ data for Nueces Bay core 2.	38
Figure 35: Semi-log plot of $^{210}\text{Pb}_{\text{xs}}$ data for Nueces Bay core 3.	39
Figure 36: Semi-log plot of $^{210}\text{Pb}_{\text{xs}}$ data for Corpus Christi Bay core 1.	39
Figure 37: Semi-log plot of $^{210}\text{Pb}_{\text{xs}}$ data for Corpus Christi Bay core 2.	40
Figure 38: Semi-log plot of $^{210}\text{Pb}_{\text{xs}}$ data for Corpus Christi Bay core 3.	40
Figure 39: Semi-log plot of $^{210}\text{Pb}_{\text{xs}}$ data for Corpus Christi Bay core 4.	41
Figure 40: Semi-log plot of $^{210}\text{Pb}_{\text{xs}}$ data for Corpus Christi Bay core 5.	41
Figure 41: Mean sediment accumulation rate for each bay core versus distance from the Nueces River mouth.	42
Table AI1: Summary physical and radiochemical data for Nueces Delta core 1.	49
Table AI2: Summary physical and radiochemical data for Nueces Delta core 2.	50
Table AI3: Summary physical and radiochemical data for Nueces Delta core 3.	51
Table AI4: Summary physical and radiochemical data for Nueces Delta core 4.	52
Table AI5: Summary physical and radiochemical data for Nueces Delta core 5.	53
Table AII1: Summary physical and radiochemical data for Nueces Bay Core 1.	54
Table AII2: Summary physical and radiochemical data for Nueces Bay Core 2.	55
Table AII3: Summary physical and radiochemical data for Nueces Bay Core 3.	57
Table AII4: Summary physical and radiochemical data for Corpus Christi Bay Core 1.	58
Table AII5: Summary physical and radiochemical data for Corpus Christi Bay Core 2.	60
Table AII6: Summary physical and radiochemical data for Corpus Christi Bay Core 3.	61
Table AII7: Summary physical and radiochemical data for Corpus Christi Bay Core 4.	62
Table AII8: Summary physical and radiochemical data for Corpus Christi Bay Core 5.	63
Figure AII1: X-radiography and grain size distribution for Nueces Bay core 1, open circles denote % sand, grey boxes denote % silt and solid triangles denote % clay.	64
Figure AII2: X-radiography and grain size distribution for Nueces Bay core 2, open circles denote % sand, grey boxes denote % silt and solid triangles denote % clay.	65
Figure AII3: X-radiography and grain size distribution for Nueces Bay core 3, open circles denote % sand, grey boxes denote % silt and solid triangles denote % clay.	66
Figure AII4: X-radiography and grain size distribution for Corpus Christi Bay core 1, open circles denote % sand, grey boxes denote % silt and solid triangles denote % clay.	67
Figure AII5: X-radiography and grain size distribution for Corpus Christi Bay core 2, open circles denote % sand, grey boxes denote % silt and solid triangles denote % clay.	68

## FIGURES AND TABLES

Figure AII6: X-radiography and grain size distribution for Corpus Christi Bay core 3, open circles denote % sand, grey boxes denote % silt and solid triangles denote % clay.	69
Figure AII7: X-radiography and grain size distribution for Corpus Christi Bay core 4, open circles denote % sand, grey boxes denote % silt and solid triangles denote % clay.	70
Figure AII8: X-radiography and grain size distribution for Corpus Christi Bay core 5, open circles denote % sand, grey boxes denote % silt and solid triangles denote % clay.	71
Table AII9: Summary grain size data for Nueces Bay cores 1, 2 and 3 x-radiography sections.	72
Table AII10: Summary grain size data for Corpus Christi Bay cores 1, 2 and 3 x-radiography sections.	73
Table AII11: Summary grain size data for Corpus Christi Bay cores 4 and 5 x-radiography sections.	74

# 1. INTRODUCTION

## 1.1 Overview

This report describes the results of a cooperative research study by the Texas Water Development Board (TWDB) and the Department of Marine Science, Texas A&M University at Galveston. This study sought to apply radiochemical techniques to distinguish between terrestrial and marine sources of sediment to the greater Nueces-Corpus Christi Estuary. The study area includes the lower parts of the Nueces River watershed, Nueces Delta, Nueces-Corpus Christi Estuary, Gulf Intracoastal Waterway (GIW) and Gulf of Mexico (GOM). This report presents results, provides interpretations of data and observations, and concludes with recommendations.

## 1.2 Introduction

The purpose of this study was to investigate, specifically, whether radiochemical and complementary techniques could be utilized to allow for the delineation of terrestrial versus marine sources of sediment to the greater Nueces-Corpus Christi Estuary. An ancillary objective included the determination of sedimentation rates and mixing within the Nueces Delta and Nueces and Corpus Christi Bays.

# 2. STUDY AREA AND RESEARCH DESIGN

## 2.1 Study area and hydrologic setting

The study area includes portions of the Nueces River, primarily the southernmost reaches, the Nueces Delta, the Greater Nueces-Corpus Christi Estuary System, the GIW and the GOM (Fig. 1). The Nueces River originates in Edwards County, Texas and flows approximately 315 miles to empty into the Nueces-Corpus Christi Estuary. The Nueces River has several major tributaries, including the Atascosa River and the Frio River and its major tributaries, including San Miguel Creek, Seco Creek, Hondo Creek and the Sabinal and Leona Rivers. Its watershed is among the largest in the state of Texas, draining all or parts of 23 counties over approximately 45,000 km<sup>2</sup>. The hydrology of the Nueces River can be characterized as flashy with episodic flooding due to a semi-arid climate in this region. The principal cities within this basin include Corpus Christi, Hondo, Uvalde, Carrizo Springs, Crystal City, Tilden, Three Rivers, George West, Cotulla, Jourdanton, Pleasanton and Pearsall. The watershed covers three regions with distinct geographic and economic features, the Hill Country, Brush Country and Coastal Prairie. Approximately 200,000 people live within this basin, most of which are concentrated on the coastal plain, resulting in a relatively low overall population density.

The Nueces River, like most rivers in Texas, is a managed system. Three major reservoirs (capacity  $\geq$  5,000 acre-feet) have been constructed in this system, including the Upper Nueces Reservoir located north of Crystal City in Zavala County, the Choke Canyon Reservoir located west of Three Rivers in Live Oak and McMullen Counties and Lake Corpus Christi located north of Corpus Christi in Live Oak County. Management of the lower basin, nearest to Corpus Christi, began in 1934 with the construction of the Mathis Dam, built near the current site of the Wesley Seale Dam. This reservoir impounded  $6.66 \times 10^7$  m<sup>3</sup>, but decreased in capacity to  $4.86 \times 10^7$  m<sup>3</sup> by 1948 due to rapid sedimentation (Buckner *et al.* 1986). In 1958, the Wesley Seale Dam was completed at the same site, impounding  $3.45 \times 10^8$  m<sup>3</sup>, creating Lake Corpus Christi. Hydrologic management of the Lower Nueces River basin, the focus region for this work, is certain to continue and likely to increase in the near future. San Patricio, Jim Wells and Nueces, along with nine other counties, comprise the Texas coastal bend region. This region has among the most serious water problems in the state. By 2050, population is projected to increase 86% (505,097 to 938,000), with total water use increasing 61% (from  $2.32 \times 10^8$  to  $3.74 \times 10^8$  m<sup>3</sup> yr.<sup>-1</sup>) while at present this region has insufficient surface water supplies to meet the needs of the regional economy, whose core consists of heavy resource consuming industries including petroleum refining, chemical manufacturing, stone, clay and glass works and agriculture (hay, sorghum, cotton, corn) (TWDB 1997).

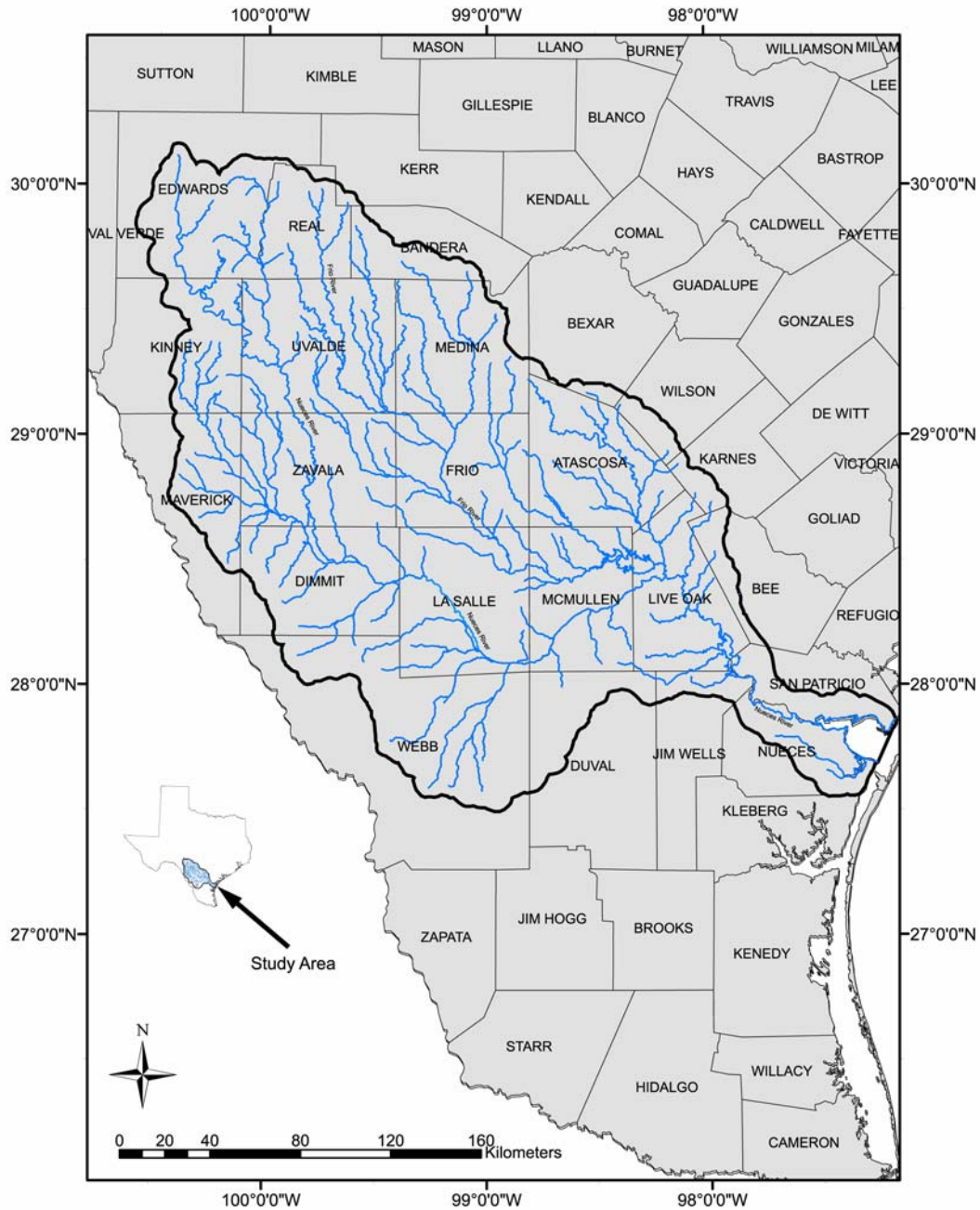


Figure 1: Map of southwestern Texas, showing the Nueces River watershed, major rivers and tributaries and Texas county delineations.

In direct competition with the aforementioned freshwater needs are the Nueces, Corpus Christi, Oso and Redfish Bays as well as Laguna Madre, estuaries and associated bay systems where the maintenance of ecological stability, sustainability and productivity is both an environmental and economic priority for the state. These systems are dependent upon freshwater inflows, which provide nutrients, sediment and salinity regulation. In turn, these coastal systems provide a beautiful and dynamic natural environment that serves as a vast resource base for minerals, sea foods and recreational opportunities; an environmental source of natural waste treatment for the by-products of modern society; and a navigational system of national significance

(TWDB 1997). The greater Nueces-Corpus Christi Estuary, the focus of this work, has a total surface area of 421 km<sup>2</sup> and volume of 1 x 10<sup>6</sup> m<sup>3</sup> with inflow to the system estimated at 16,060 x 10<sup>6</sup> m<sup>3</sup> yr.<sup>-1</sup> (Brock 2001). This estuarine system has and continues to attract state level resource management interest due to increasing water demands in the Texas coastal plain, which have and will continue to result in the reduction of freshwater inflow to the estuary.

The impoundments constructed throughout the basin have resulted in significant alterations to the Nueces Delta sediment budget and growth. The delta now receives much less sediment than before reservoir construction; more than 95% of the Nueces River Basin is upstream of Lake Corpus Christi (Longley 1994). Lake Corpus Christi is an effective sediment trap, between 1977-1985, Leibbrand (1987) showed that 97% of sediment entering the lake was retained in it. Photographic evidence shows that marsh progradation ceased between 1930-1959 (Morton and Paine 1984), similar observations were made by White and Calnan (1990a), who show net vegetated areas decreased by 133 acres between 1930-1959, increasing to a 185 acre loss between 1959-1979. While decreased sediment supply is the most important cause for delta retreat, other factors which play a role include relative rise in sea level in Corpus Christi Bay (White and Calnan 1990b) and subsidence (Brown *et al.* 1974; Ratzlaff 1980), likely due to significant withdrawals of oil and natural gas in the region. These reductions in freshwater and sediment inflow has resulted in pronounced impacts on the system in many ways, including reduction of overall productivity via reduced nutrient input and impacted water salinity regulation, delta retreat and loss of habitat for both terrestrial and estuarine flora and fauna, and degradation of water quality due to resulting changes of balance between freshwater inflows and wastewater discharges into the estuary.

## 2.2 Research design

The central objective of this research was to assess the ability of radio-isotopic techniques to differentiate terrestrial versus marine sources of sediment to the Nueces-Corpus Christi Estuary, and to model those inputs if possible. Ancillary objectives included attempting to discern discrete source compartments of terrestrial sediment to the system and to investigate sediment accumulation rates and mixing in the Nueces Delta and Nueces and Corpus Christi Bays. A suite of radionuclides were employed, including naturally occurring lithogenic and fallout isotopes (<sup>226</sup>Ra, <sup>228</sup>Ra, <sup>230</sup>Th, <sup>232</sup>Th, <sup>228</sup>Th, <sup>210</sup>Pb) as well as <sup>137</sup>Cs, which is derived from above ground nuclear weapons testing (Fig. 2). The research design was composed of three primary components:

### (1) The Nueces River Watershed, focused on the coastal plain:

This component focused on comprehensive sampling of landscape sediment compartments to accumulate a representative set of terrestrial sediment samples and to investigate the prospect of discerning discrete terrestrial sediment source compartments. While samples were collected throughout the watershed, sampling efforts were concentrated in the lower coastal plain region. Lithogenic radionuclides in the <sup>238</sup>U and <sup>232</sup>Th decay series have been used to address a range of problems in fluvial geomorphology, including provenance determination of coastal sediments (Roberts and Plater 1999); resolution of sedimentation rates of fluvial sands (Murray *et al.* 1990) and resolving fluvial sediment sources (Olley and Murray 1994, Yeager *et al.* 2002, 2004, Yeager and Santschi 2003) and source fluxes (Olley *et al.* 1993). These radionuclides have been used solely (Olley *et al.* 1997) and together with fallout radionuclides (Olley *et al.* 1993; He and Owens 1995) to address fluvial source and transport problems. This component required the collection of surface samples of river channel alluvium and upland sediments from varied landscape compartments (slopes, interfluves, deltaic).

### (2) The Gulf of Mexico and Gulf Intracoastal Waterway:

This component focused on comprehensive sampling of surface sediments in the GOM (within 3 km of the barrier island system) and GIW to accumulate a representative set of marine sediment samples to ascertain whether sediments in these environments carry characteristic radionuclide signatures that allow them to be differentiated from the terrestrial sediments collected in component (1). Lithogenic radionuclides in the <sup>238</sup>U

	$^{238}\text{U}$ Series						$^{232}\text{Th}$ Series					
<b>U</b>	$^{238}\text{U}$ 4.51x $10^9\text{y}$		$^{234}\text{U}$ 2.48x $10^5\text{y}$									
<b>Pa</b>	↓	$^{234}\text{Pa}$ 1.18m	↓									
<b>Th</b>	$^{234}\text{Th}$ 24.1d	↗	$^{230}\text{Th}$ 7.52x $10^4\text{y}$				$^{232}\text{Th}$ 1.39x $10^{10}\text{y}$		$^{228}\text{Th}$ 1.9y			
<b>Ac</b>			↓				↓	$^{228}\text{Ac}$ 6.13h	↓			
<b>Ra</b>			$^{226}\text{Ra}$ 1601y				$^{228}\text{Ra}$ 5.7y	↗	$^{224}\text{Ra}$ 3.64d			
<b>Fr</b>			↓						↓			
<b>Rn</b>			$^{222}\text{Rn}$ 3.825d						$^{220}\text{Rn}$ 54.5s			
<b>At</b>			↓						↓			
<b>Po</b>			$^{218}\text{Po}$ 3.05m		$^{214}\text{Po}$ 1.6x $10^{-4}\text{s}$		$^{210}\text{Po}$ 138.4d		$^{216}\text{Po}$ 0.158s		$^{212}\text{Po}$ 3.0x $10^{-7}\text{s}$	
<b>Bi</b>			↓	$^{214}\text{Bi}$ 19.7m	↓	$^{210}\text{Bi}$ 5.0d	↓		↓	$^{212}\text{Bi}$ 60.5m	↓	
<b>Pb</b>			$^{214}\text{Pb}$ 26.8m	↗	$^{210}\text{Pb}$ 21.4y	↗	$^{206}\text{Pb}$ stable		$^{212}\text{Pb}$ 10.6h	↗	↓	$^{208}\text{Pb}$ stable
<b>Tl</b>									$^{208}\text{Tl}$ 3.1m	↗		

Figure 2: Decay series for  $^{238}\text{U}$  and  $^{232}\text{Th}$ , y = years, d = days, m = minutes and s = seconds (modified from Kendall & McDonnell 1998).

and  $^{232}\text{Th}$  decay series in conjunction with fallout radionuclides ( $^{137}\text{Cs}$  and  $^{210}\text{Pb}$ ) have been used successfully to characterize and quantify sources of sediment to shelf environments (Santschi *et al.* 2001a) and to small estuaries (Baskaran and Santschi 1993; Benoit *et al.* 1999). This component required the collection of grab samples of surface sediments from the GOM and GIW.

### (3) Mixing and sediment accumulation in the Nueces Delta and Nueces-Corpus Christi Estuary:

This component focused on investigating rates of sediment accumulation and its spatial variability within the Nueces Delta and both Nueces and Corpus Christi Bays. The primary objectives were to ascertain where and at what rates sediments are being deposited or mixed at various locations within the estuary. Multi-radionuclide techniques have been successfully employed in deltaic and estuarine settings to determine both sediment geochronology and deposition rates. Examples considering a combination of  $^{210}\text{Pb}$ ,  $^{239,240}\text{Pu}$  and  $^{137}\text{Cs}$  include Ravichandran *et al.* (1995a) in the Sabine-Neches Estuary, Texas; Oktay *et al.* (2000) in the Mississippi River Delta; Huntley *et al.* (1995) at the Lower Passaic River, New Jersey, Santschi *et al.* (1999) in Lavaca Bay, Texas, Santschi *et al.* (2001b) in Galveston and Tampa Bays and the Mississippi River Delta and Hancock (2000) who used  $^{228}\text{Th}/^{232}\text{Th}$  to assess sediment mixing in the Bega Estuary, Australia. This component required the collection of delta sediment cores, Nueces and Corpus Christi Bay sediment cores and surface grab samples of delta and estuarine sediments.

## 3. MATERIALS AND METHODS

### 3.1 Materials and field methods

Extensive field sampling was undertaken throughout 2002-2003, focusing primarily on the southernmost portion of the Nueces River watershed in southwest Texas. Surface sediments (upper 2 cm) and sediment cores were collected. Surface sediment samples consisted of: channel alluvium from the Nueces River and associated tributaries (Fig. 3), floodplain and delta sediments (Table 1) and prospective source area soils predominantly throughout the lower watershed (divided into surface, interfluvial samples (Fig. 4) and subsurface or slope samples (Fig. 5)) as well as grab samples from Nueces Bay, Corpus Christi Bay, the GOM and GIW (Table 1). Sediment cores were collected from the Nueces Delta, Nueces Bay and Corpus Christi Bay (Fig. 6). Terrestrial sediment cores were collected in aluminum sleeves (inner diameter 7.3 cm) after being driven into the substrate to refusal. Bay cores were collected in 6" diameter PVC tubing after being driven into the sediment by a diver and small, rectangular x-ray trays (10.5 cm wide by 60 cm long) were collected within 2 m of the core for that station to provide representative x-ray images of the sediment profiles. Sediment grab samples were collected from the near surface (0-2 cm) using a trowel for sub-aerial samples and a small ponar type grab sampler for sub-aqueous samples. Prospective terrestrial source samples were focused at or adjacent to actively eroding sites throughout the basin, concentrating on A-horizons of upland interfluves and exposed sub-soils on slopes. All terrestrial and sub-aqueous sediment grab samples were combined in the field, consisting of eight to ten sub-samples collected over an approximately 10 m<sup>2</sup> area. Due to the duration and fiscal constraints of the contract, neither water samples nor suspended sediments were collected for this work.

### 3.2 Sample processing and radiochemistry

Bulk surface sediment grab samples were dried at 70-80 °C for 24 hours, then gently disaggregated with mortar and pestle and passed through 2 mm and 0.5 mm sieves. Delta sediment cores were sectioned at 1 cm intervals (or 2 cm intervals at depth), wet and dry weights were recorded to determine porosity and sediments were then dried and processed as previously described for surface sediments. Bay cores were similarly processed and x-ray images were obtained for them and were post processed using graphics software. Grain size analysis was undertaken to determine the quantities of sand, silt and clay in all sediment samples and cores, these methods included wet sieving and hydrometer analyses as summarized in Folk (1965).

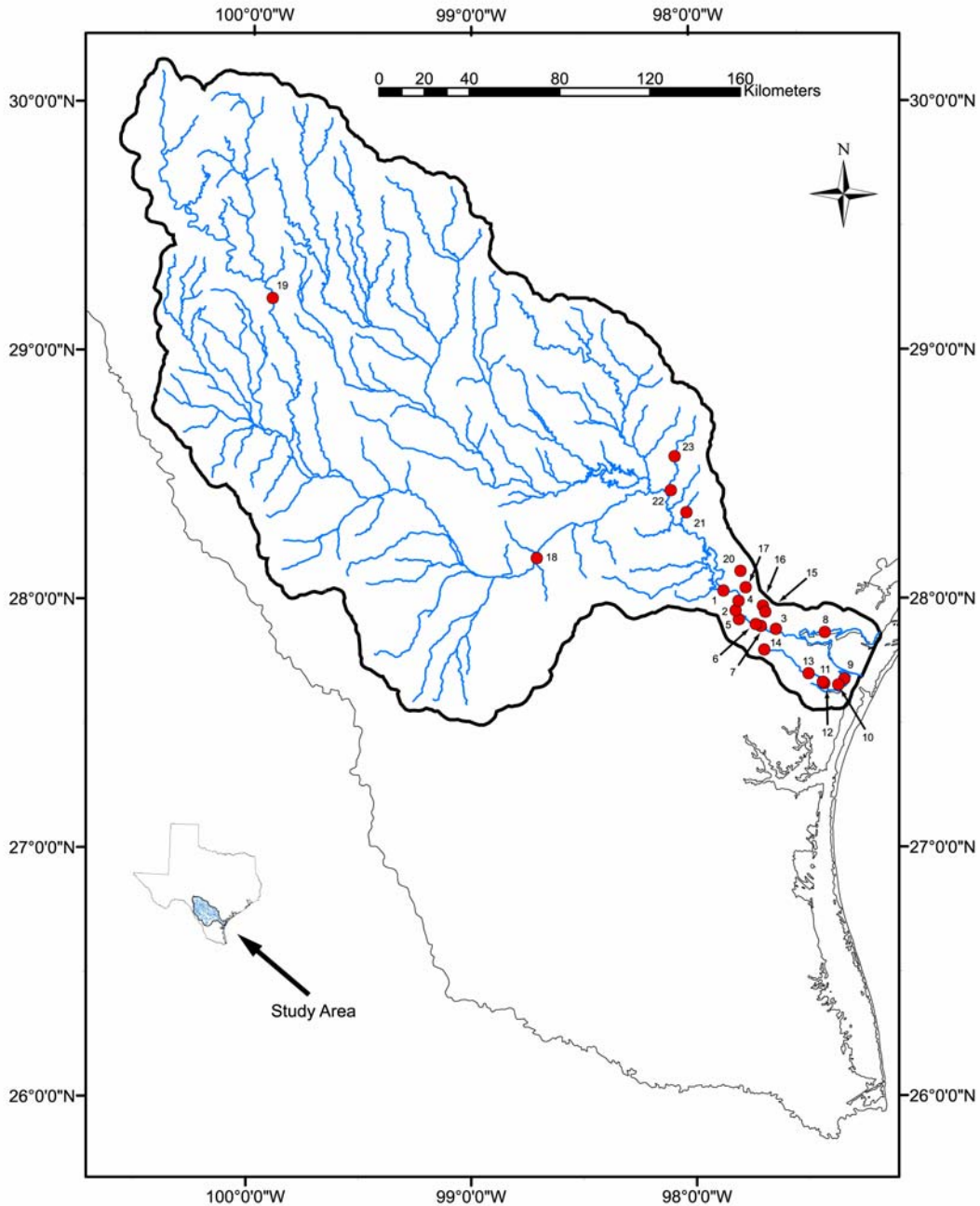


Figure 3: Map of the greater Nueces River watershed showing locations where alluvial sediment samples were collected.

High-resolution gamma spectrometry was employed to resolve  $^{228}\text{Ra}$  ( $t_{1/2} = 5.75$  yr., via  $^{228}\text{Ac}$   $E_g = 911$  keV),  $^{226}\text{Ra}$  ( $t_{1/2} = 1602$  yr., via  $^{214}\text{Pb}$   $E_g = 352$  keV) and  $^{137}\text{Cs}$  ( $t_{1/2} = 30$  yr.,  $E_g = 661$  keV) using either Canberra HPGe well detectors and multi-channel analyzer, model 747 or a Canberra planar detector and multi-channel analyzer, model DSA 1000. Samples were contained in either plastic test tubes for the well detectors (inner diameter 1.3 cm and height 9.4 cm) or plastic Petrie dishes for the planar detector (diameter 5.5 cm and height 1.5 cm) and sealed with epoxy for 20 days for equilibrium between  $^{226}\text{Ra}$  and its volatile daughter  $^{222}\text{Rn}$  ( $t_{1/2} = 3.8$  days), an inert gas, to be reached. Standards were prepared and run on each detector in a geometry identical to that for sediment samples to determine representative efficiencies for each nuclide.

Table 1: Physical data for all surface sediment samples collected.

Sample type/number	Date collected	Latitude	Longitude	% Sand	% Silt	% Clay
<b>Alluvium (km from river mouth)</b>						
1 (91.7)	2/15/2003	N28° 2.305'	W97° 51.65'	93.2	2.8	4.0
2 (72.5)	2/15/2003	N27° 57.61'	W97° 48.69'	59.8	19.0	21.2
3 (31.5)	2/15/2003	N27° 53.34'	W97° 37.66'	53.3	18.8	27.8
4 (77.4)	2/15/2003	N27° 59.16'	W97° 47.94'	78.0	10.6	11.4
5 (67.0)	2/15/2003	N27° 55.46'	W97° 47.95'	57.9	23.6	18.5
6 (48.9)	2/15/2003	N27° 54.92'	W97° 42.40'	66.8	11.9	21.3
7 (44.5)	2/16/2003	N27° 53.55'	W97° 41.89'	0.8	18.5	80.7
8 (5.1)	3/29/2003	N27° 52.40'	W97° 24.50'	78.1	10.9	10.9
9 (4.4)	4/26/2003	N27° 40.32'	W97° 19.37'	83.5	6.1	10.4
10 (7.1)	4/26/2003	N27° 39.57'	W97° 20.41'	10.1	24.6	65.2
11 (18.0)	4/26/2003	N27° 39.38'	W97° 24.12'	36.5	9.3	54.3
12 (18.0)	4/26/2003	N27° 39.38'	W97° 24.12'	29.3	53.8	16.9
13 (31.6)	4/26/2003	N27° 42.63'	W97° 30.12'	37.3	16.0	46.7
14 (48.1)	4/26/2003	N27° 47.98'	W97° 36.23'	66.9	13.2	19.9
15 (41.3)	4/27/2003	N27° 57.08'	W97° 40.62'	94.7	1.9	3.4
16 (44.5)	4/27/2003	N27° 58.53'	W97° 41.26'	36.4	19.8	43.8
17 (89.8)	4/27/2003	N28° 3.00'	W97° 45.83'	84.3	3.5	12.2
18 (242.3)	6/3/2003	N28° 10.81'	W98° 42.26'	20.7	23.3	56.0
19 (497.0)	6/3/2003	N29° 7.19'	W99° 55.03'	75.7	13.7	10.6
20 (140.9)	6/4/2003	N28° 6.99'	W97° 47.25'	61.0	16.7	22.4
21 (142.1)	6/4/2003	N28° 20.16'	W98° 2.04'	93.6	2.6	3.9
22 (163.4)	6/4/2003	N28° 26.82'	W98° 6.05'	93.4	1.7	5.0
23 (181.2)	6/4/2003	N28° 33.99'	W98° 2.80'	63.9	12.8	23.6
<b>Slope</b>						
1	2/15/2003	N28° 2.31'	W97° 51.65'	21.1	42.6	36.2
2	2/15/2003	N27° 53.34'	W97° 37.66'	40.6	27.6	31.8
3	2/15/2003	N27° 59.17'	W97° 47.79'	60.9	22.1	17.0
4	2/15/2003	N27° 55.46'	W97° 47.95'	40.9	35.4	23.7
5	2/15/2003	N27° 54.92'	W97° 42.40'	69.2	18.4	12.4
6	3/29/2003	N27° 52.40'	W97° 24.50'	32.2	24.5	43.3
7	3/30/2003	N27° 49.67'	W97° 32.35'	65.8	17.8	16.4
8	4/26/2003	N27° 40.32'	W97° 19.37'	26.8	28.8	44.4
9	4/26/2003	N27° 39.65'	W97° 20.38'	45.2	22.0	32.9
10	6/3/2003	N28° 38.34'	W99° 45.55'	35.6	28.3	36.1
11	6/4/2003	N28° 6.99'	W97° 47.25'	60.2	10.8	29.1
12	6/4/2003	N28° 34.71'	W98° 1.95'	56.1	14.9	29.1
<b>Interfluvial</b>						
1	2/15/2003	N28° 2.31'	W97° 51.65'	92.4	2.0	5.6
2	2/15/2003	N27° 53.34'	W97° 37.66'	61.6	21.0	17.5
3	2/15/2003	N27° 59.17'	W97° 47.79'	74.5	14.2	11.3
4	4/26/2003	N27° 40.32'	W97° 19.37'	61.8	10.7	27.5
5	4/26/2003	N27° 39.65'	W97° 20.38'	52.6	25.2	22.2
6	6/3/2003	N28° 10.81'	W98° 42.26'	42.8	21.5	35.7
7	6/3/2003	N28° 38.34'	W99° 45.55'	38.8	36.1	25.1
8	6/4/2003	N28° 2.03'	W97° 52.66'	71.3	14.4	14.3
9	6/4/2003	N28° 6.99'	W97° 47.25'	59.9	18.6	21.4
10	6/4/2003	N28° 20.16'	W98° 2.04'	83.6	9.2	7.3
11	6/4/2003	N28° 34.71'	W98° 1.95'	60.2	17.4	22.4

Table 1: Physical data for all surface sediment samples collected (continued).

Sample type/number	Date collected	Latitude	Longitude	% Sand	% Silt	% Clay
<b>GOM</b>						
1	7/27/2003	N28° 11.09'	W97° 44.54'	95.2	1.9	2.8
2	7/27/2003	N27° 52.99'	W97° 0.58'	92.5	3.1	4.5
3	7/27/2003	N27° 52.03'	W97° 0.70'	93.0	3.1	4.0
4	7/27/2003	N27° 51.24'	W97° 1.55'	92.8	2.5	4.7
5	7/27/2003	N27° 50.49'	W97° 1.75'	83.6	9.2	7.2
6	7/27/2003	N27° 49.36'	W97° 2.38'	94.1	1.8	4.1
7	7/27/2003	N27° 48.88'	W97° 3.11'	97.2	0.8	2.0
8	7/27/2003	N27° 48.27'	W97° 3.79'	96.7	0.9	2.5
9	7/27/2003	N27° 47.61'	W97° 4.84'	94.4	2.0	3.6
10	7/27/2003	N27° 46.93'	W97° 5.09'	96.7	1.3	2.0
<b>Nueces Bay</b>						
1	7/28/2003	N27° 50.79'	W97° 23.69'	97.0	0.3	2.7
2	7/28/2003	N27° 50.75'	W97° 24.83'	42.8	16.3	40.9
3	7/28/2003	N27° 50.56'	W97° 25.86'	30.3	20.5	49.1
4	7/28/2003	N27° 50.40'	W97° 26.97'	57.9	13.3	28.9
5	7/28/2003	N27° 50.39'	W97° 28.10'	22.3	57.3	20.4
6	7/28/2003	N27° 50.51'	W97° 28.98'	43.7	29.9	26.3
7	7/28/2003	N27° 50.98'	W97° 26.50'	64.3	19.6	16.1
8	7/28/2003	N27° 51.64'	W97° 25.42'	54.5	18.2	27.3
9	7/28/2003	N27° 51.65'	W97° 24.63'	10.7	27.6	61.7
10	7/28/2003	N27° 50.59'	W97° 24.15'	68.7	11.1	20.2
<b>Nueces Delta</b>						
1	2/16/2003	N27° 53.57'	W97° 31.55'	36.5	26.1	37.5
2	2/16/2003	N27° 53.56'	W97° 31.98'	54.7	11.6	33.8
3	3/29/2003	N27° 52.58'	W97° 33.76'	43.3	45.5	11.1
4	3/29/2003	N27° 51.82'	W97° 33.40'	6.1	2.7	91.2
5	3/29/2003	N27° 54.40'	W97° 32.82'	44.1	31.7	24.2
6	3/30/2003	N27° 49.67'	W97° 32.35'	73.0	13.5	13.5
7	3/30/2003	N27° 52.05'	W97° 34.45'	13.7	75.5	10.8
<b>Corpus Christi Bay</b>						
1	7/29/2003	N27° 49.99'	W97° 20.77'	3.7	45.5	50.9
2	7/29/2003	N27° 50.69'	W97° 18.93'	13.8	26.2	60.0
3	7/29/2003	N27° 49.30'	W97° 19.35'	5.5	32.2	62.3
4	7/29/2003	N27° 50.81'	W97° 16.83'	3.4	33.1	63.5
5	7/29/2003	N27° 47.47'	W97° 17.68'	6.3	22.6	71.1
6	7/29/2003	N27° 48.17'	W97° 15.62'	9.8	27.9	62.4
7	7/29/2003	N27° 45.71'	W97° 15.90'	16.0	23.5	60.5
8	7/29/2003	N27° 47.70'	W97° 13.56'	6.3	22.9	70.8
9	7/29/2003	N27° 43.96'	W97° 14.14'	2.5	23.2	74.2
10	7/29/2003	N27° 43.96'	W97° 18.06'	1.7	17.5	80.7
11	7/29/2003	N27° 46.27'	W97° 20.87'	3.4	22.9	73.8
12	7/29/2003	N27° 47.89'	W97° 22.60'	21.5	21.3	57.2
<b>GIW</b>						
1	7/27/2003	N27° 53.57'	W97° 5.96'	81.6	7.5	10.9
2	7/27/2003	N27° 53.38'	W97° 6.18'	63.8	16.5	19.7
3	7/27/2003	N27° 54.74'	W97° 7.59'	94.8	0.7	4.5
4	7/29/2003	N27° 40.09'	W97° 13.38'	88.4	4.4	7.2
5	7/29/2003	N27° 39.16'	W97° 14.06'	94.2	1.2	4.6

Table 1: Physical data for all surface sediment samples collected (continued).

Sample type/number	Date collected	Latitude	Longitude	% Sand	% Silt	% Clay
<b>GIW</b>						
6	7/29/2003	N27° 37.43'	W97° 14.79'	86.8	3.0	10.2
7	7/29/2003	N27° 35.11'	W97° 15.99'	88.5	4.1	7.4
<b>Delta Cores</b>						
1	3/29/03	N27° 54.40'	W97° 32.82'	--	--	--
2	3/29/03	N27° 52.58'	W97° 33.76'	--	--	--
3	3/29/03	N27° 51.82'	W97° 33.40'	--	--	--
4	3/30/03	N27° 49.67'	W97° 32.35'	--	--	--
5	3/30/03	N27° 52.05'	W97° 34.43'	--	--	--
<b>Nueces Bay Cores</b>						
1	7/28/03	N27° 50.51'	W97° 28.98'	--	--	--
2	7/28/03	N27° 50.98'	W97° 26.50'	--	--	--
3	7/28/03	N27° 50.59'	W97° 24.15'	--	--	--
<b>Corpus Christi Bay Cores</b>						
1	7/29/03	N27° 49.99'	W97° 20.77'	--	--	--
2	7/29/03	N27° 49.30'	W97° 19.35'	--	--	--
3	7/29/03	N27° 47.47'	W97° 17.68'	--	--	--
4	7/29/03	N27° 45.71'	W97° 15.90'	--	--	--
5	7/29/03	N27° 43.96'	W97° 14.14'	--	--	--

Efficiency errors based on standards were less than  $\pm 2\%$ .

Alpha spectrometry was employed to resolve  $^{232}\text{Th}$  ( $t_{1/2} = 1.39 \times 10^{10}$  yr.),  $^{230}\text{Th}$  ( $t_{1/2} = 7.52 \times 10^4$  yr.),  $^{228}\text{Th}$  ( $t_{1/2} = 1.91$  yr.) and  $^{210}\text{Pb}$  ( $t_{1/2} = 22.4$  yr.) via  $^{210}\text{Po}$  using a Canberra alpha spectrometer, model 7404, mated to a Canberra multi-channel analyzer, model 8224. Thorium samples were spiked with a  $^{229}\text{Th}$  tracer (NIST, SRM #4328B) and completely digested (HF, HCL and  $\text{HNO}_3$ ) over heat. The solution was passed through two sets of anion exchange columns to selectively isolate thorium isotopes as described by Buesseler *et al.* (1992). The elution was acidified with  $\text{H}_2\text{SO}_4$  and plated onto stainless steel planchets via sulfate electro-deposition prior to counting, according to methods described by Hallstadius (1984) and Buesseler *et al.* (1992). Chemical recoveries for thorium isotopes averaged 50%. Lead-210 samples ( $\approx 1$  g) were spiked with a certified  $^{209}\text{Po}$  tracer (Isotope Products Laboratory, #6209-100N) and completely digested (HF, HCL and  $\text{HNO}_3$ ) over heat. Ascorbic acid was then added to bind free Fe(III) and a silver disk was added to the solution over heat to provide a substrate for spontaneous deposition of polonium isotopes (Santschi *et al.* 1980, 1999; Ravichandran *et al.* 1995a,b).

## 4. RESULTS AND DISCUSSION

### 4.1 Surface sediment size distributions

Physical data for all samples are listed in Table 1. Figure 7 shows the distribution of sand, silt and clay in all surface sediment samples. These data are simplified in Figure 8, which shows the mean size distribution for each sediment type collected. While variability in grain size distributions are observed, particularly for terrestrial sediments, it is clear that the GOM sediments and those from the GIW are dominantly sands and conversely, those sediments from Corpus Christi Bay are dominantly clays. Sediments from both the Nueces Delta and Bay are similar to the terrestrial sediment types in that they have a more even distribution of the three size fractions. These size distribution data suggest that near shore oceanic sediments are sands derived

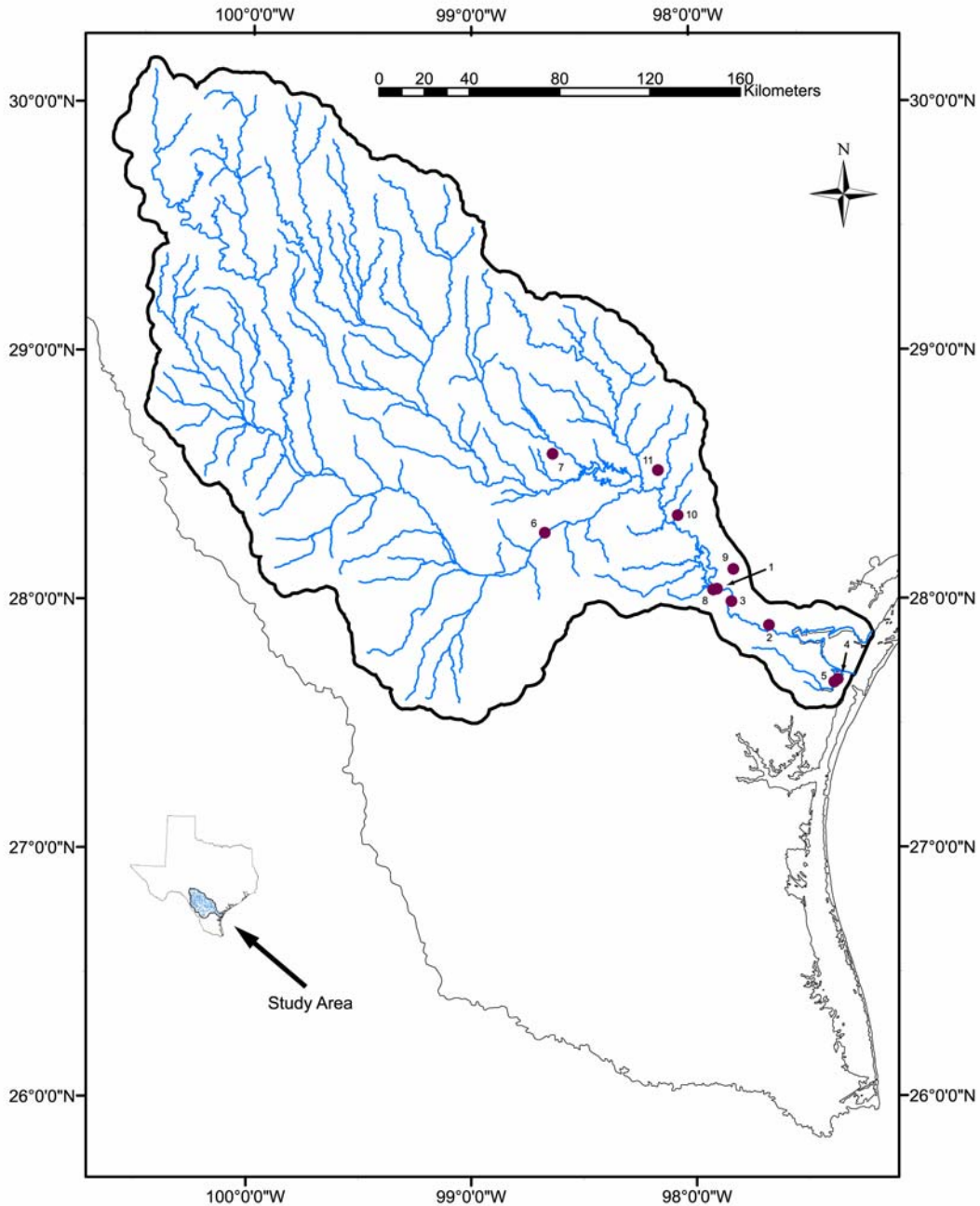


Figure 4: Map of the greater Nueces River watershed showing locations where interfluvial sediment samples were collected.

predominantly from long shore transport in the littoral zone in association with the barrier island system. Similarly, GIW sands are likely sourced from a combination of long shore transport and wash over the barrier island system in association with high energy storm events and wave action. Bed load and suspended sediments sourced from a combination of the Nueces River inflow and ephemeral tributaries, particularly to the east of the estuary, provide sand and fines to the Nueces Delta and Bay, where the coarser size fractions are effectively retained, as reflected by the size distributions of sediments from those areas. This scenario is maintained there by the “flashy” nature of the Nueces River and the very shallow depth of Nueces Bay (typically < 2 m). The larger and deeper ( $\approx 3 - 5$  m) Corpus Christi Bay is the primary depocenter for fine grained sediments, as

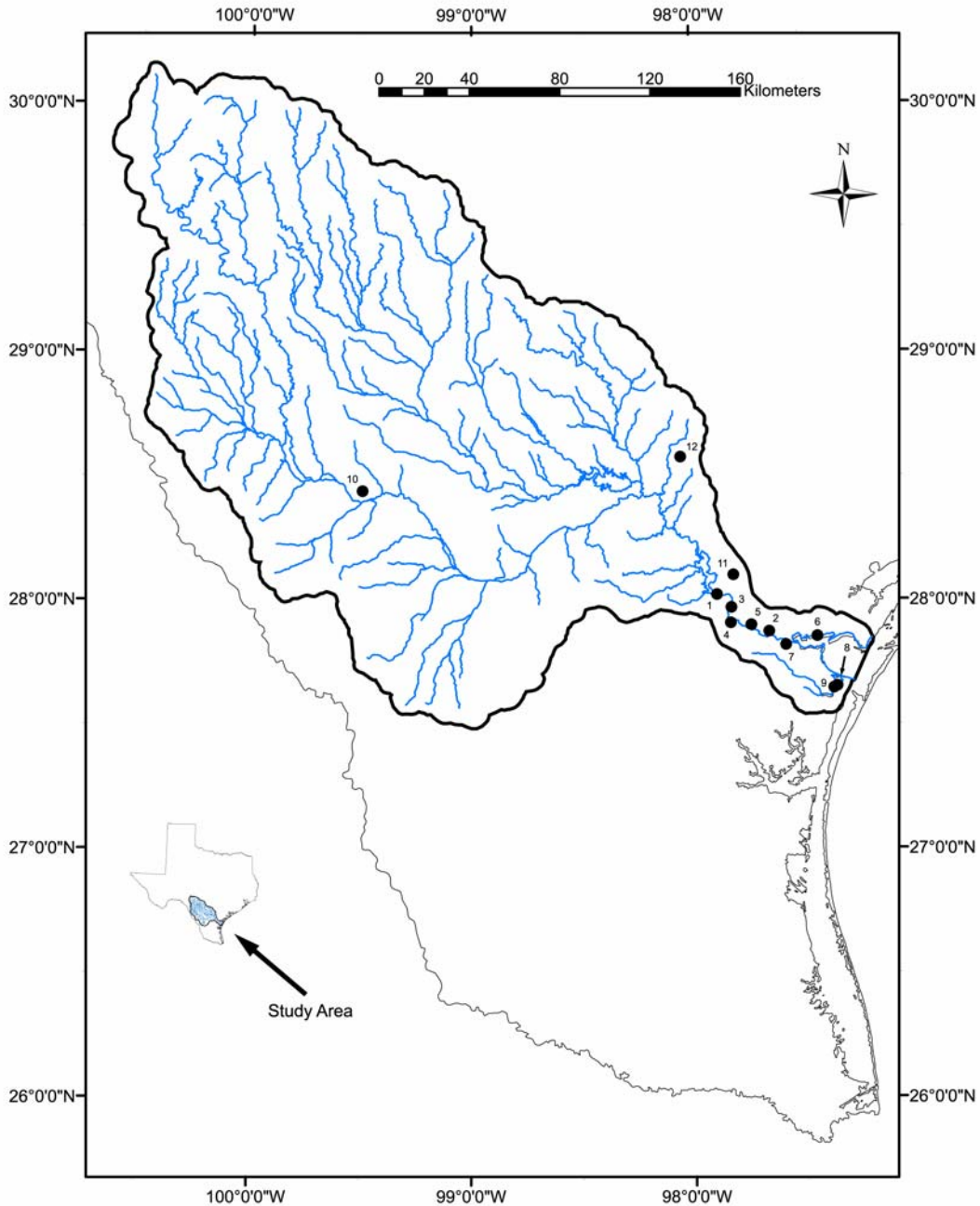


Figure 5: Map of the greater Nueces River watershed showing locations where slope sediment samples were collected.

evident from the dominance of the clay fraction there. Whatever sediment remains in suspension through Corpus Christi Bay is then transported to the shelf. Taken on their own, these data suggest, as expected, that marine sediment sources from the GOM or GIW do not provide a significant amount of sediment to the estuary system due to a small tidal variation combined with the armored nature (barrier island system) of the estuary mouth.

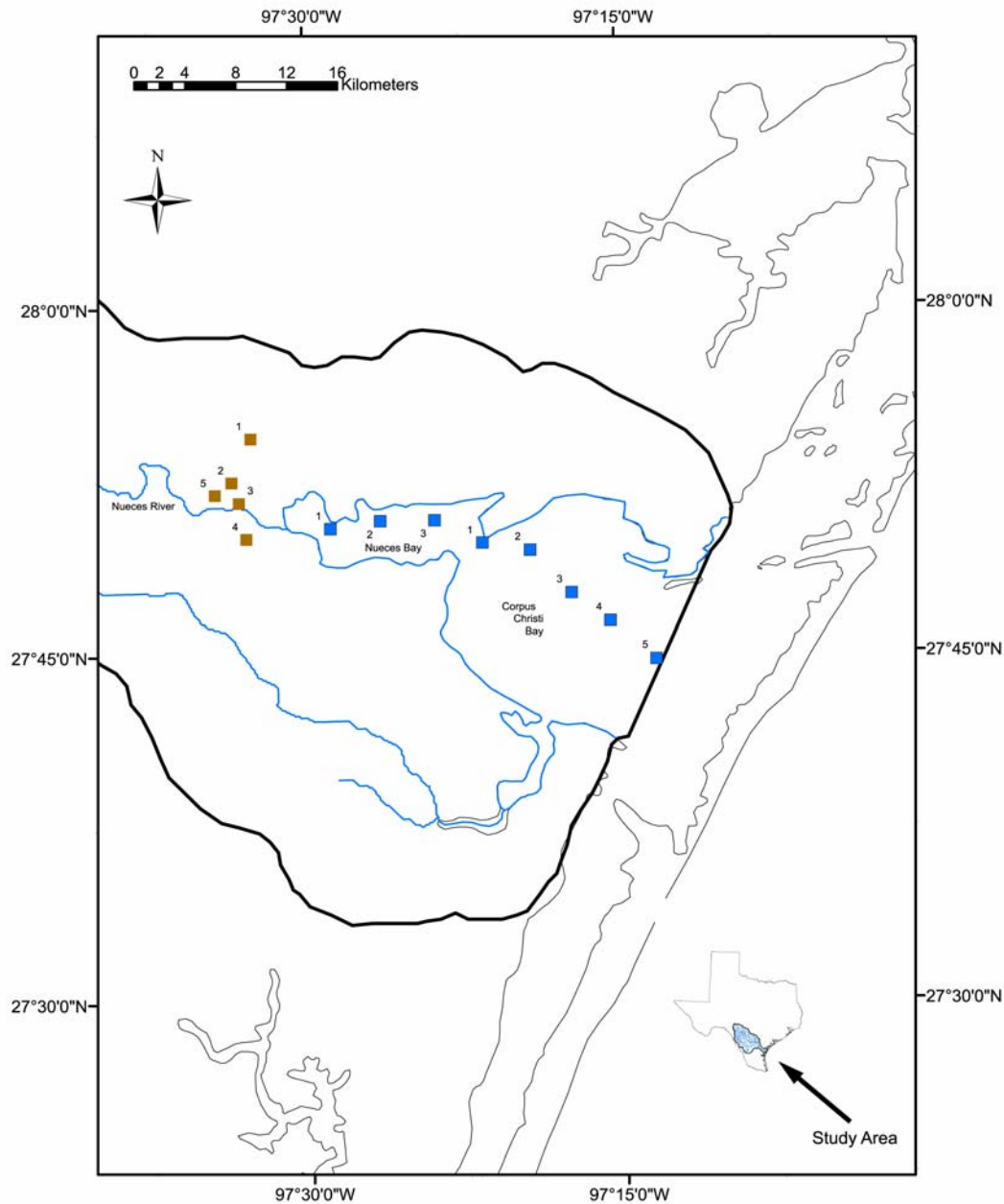


Figure 6: Map of Nueces and Corpus Christi Bays showing locations where sediment cores were collected.

#### 4.2 Surface sediment radionuclide data

Radionuclide data is presented in Table 2 for all surface sediment samples. Means of all sample compartment lithogenic isotope ratios are presented in Table 3. These data show that the fallout radionuclides  $^{137}\text{Cs}$  and  $^{210}\text{Pb}_{\text{xs}}$  are deficient in these sediments (Table 2), precluding their use to refine sources of sediment to the system. This is likely due to a combination of, 1) the wide range of sediment grain sizes represented (coarser sediments do not provide a substrate conducive to adsorption of these isotopes) and; 2) the semi-arid climate here, where sparse precipitation results in considerably less deposition of the fallout isotopes to the land surface. Upon examination of Table 3, it is apparent that the lithogenic isotope ratios are very similar in this

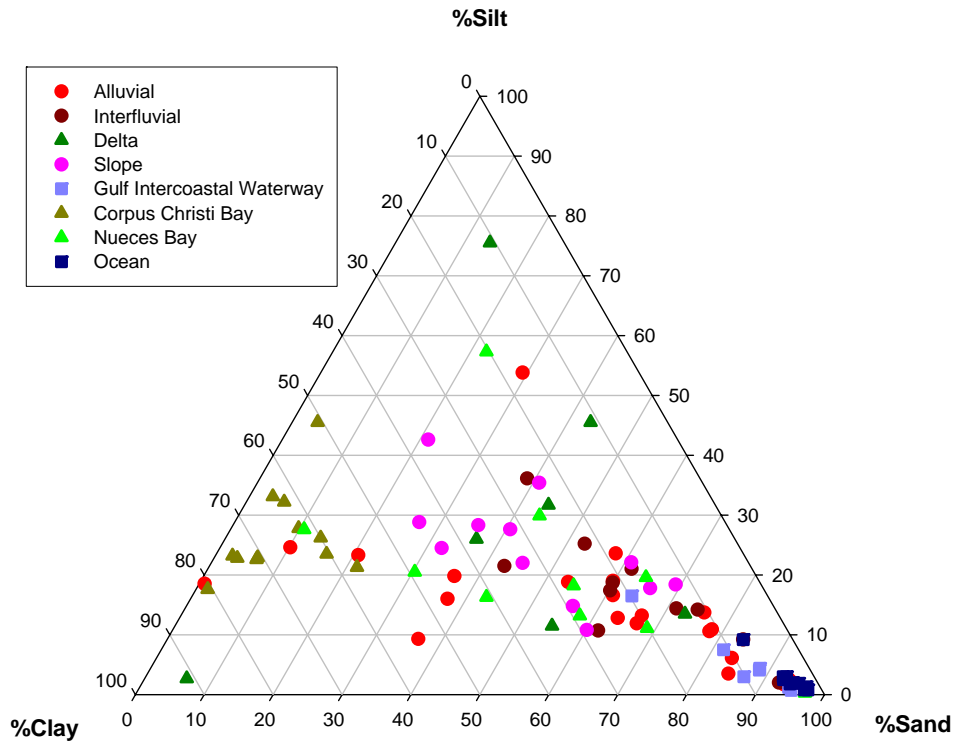


Figure 7: Ternary plot of grain size fractions for all surface sediment samples collected. Squares represent marine sediments, circles represent terrestrial sediments and triangles represent sediments in depocenters.

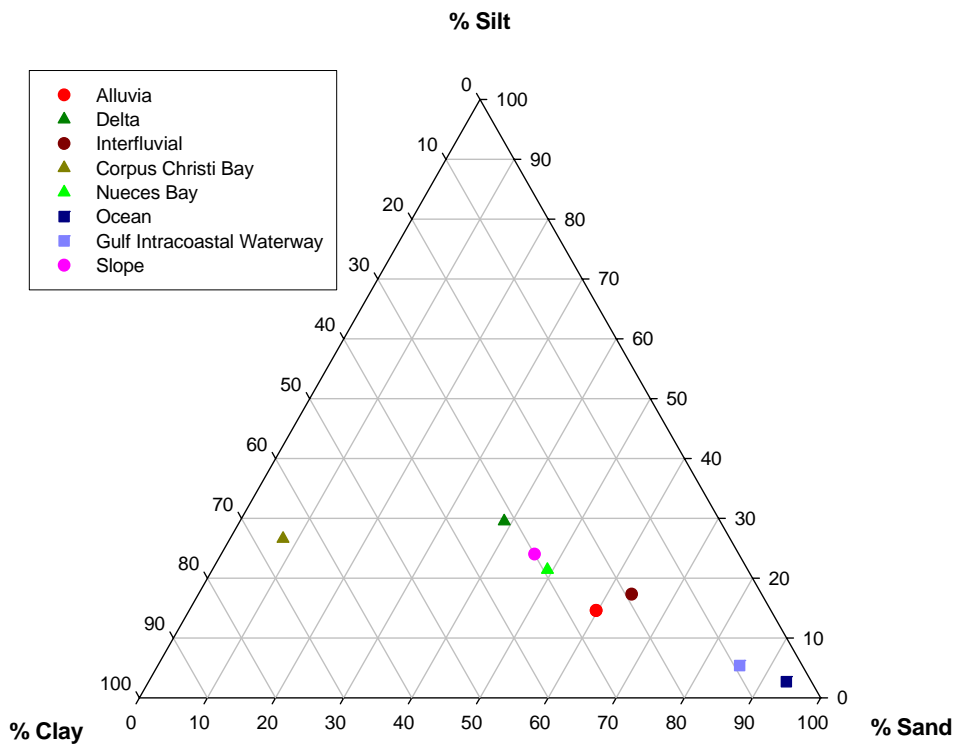


Figure 8: Ternary plot of mean grain size fractions for all surface sediment sample types collected. Squares represent marine sediments, circles represent terrestrial sediments and triangles represent sediments in depocenters.

Table 2: Radionuclide data for all surface sediments (mBq g<sup>-1</sup>).

Sample type/number	<sup>137</sup> Cs	<sup>210</sup> Pb <sub>xs</sub>	<sup>226</sup> Ra	<sup>228</sup> Ra	<sup>232</sup> Th	<sup>230</sup> Th	<sup>228</sup> Th
<b>Alluvium (km from mouth)</b>							
1 (91.7)	0	0	12.33 ± 0.60	9.41 ± 1.11	10.31 ± 0.83	14.05 ± 1.09	10.61 ± 0.85
2 (72.5)	0	0	22.24 ± 1.04	18.01 ± 2.02	32.01 ± 2.42	35.62 ± 2.69	34.19 ± 2.59
3 (31.5)	0	1.48 ± 0.96	24.22 ± 0.96	23.80 ± 2.23	38.93 ± 3.26	25.11 ± 2.21	38.77 ± 1.31
4 (77.4)	0	0	16.41 ± 0.77	15.70 ± 1.79	20.03 ± 1.82	36.38 ± 3.02	20.41 ± 1.80
5 (67.0)	0	0	22.71 ± 1.07	18.65 ± 2.09	40.64 ± 3.01	41.07 ± 3.05	44.16 ± 3.26
6 (48.9)	0	2.13 ± 0.94	18.51 ± 0.94	16.91 ± 1.82	29.10 ± 2.77	35.62 ± 3.32	27.85 ± 2.68
7 (44.5)	11.18 ± 1.28	23.17 ± 1.86	45.41 ± 1.86	39.19 ± 3.53	77.22 ± 5.61	79.28 ± 5.75	77.96 ± 5.66
8 (5.1)	0	0	13.75 ± 0.80	13.24 ± 1.14	13.06 ± 1.10	14.89 ± 1.26	11.60 ± 1.02
9 (4.4)	0	0	19.58 ± 0.80	17.37 ± 1.52	29.77 ± 2.33	33.61 ± 2.60	31.17 ± 2.47
10 (7.1)	0	0	29.04 ± 1.23	28.10 ± 2.77	39.25 ± 3.35	48.43 ± 4.09	44.21 ± 3.74
11 (18.0)	1.34 ± 0.13	0	32.61 ± 1.00	27.15 ± 1.89	44.68 ± 4.05	40.78 ± 3.75	45.16 ± 4.09
12 (18.0)	1.84 ± 0.18	9.38 ± 1.00	24.89 ± 1.00	22.05 ± 1.91	42.40 ± 3.60	48.03 ± 4.06	45.45 ± 3.85
13 (31.6)	1.61 ± 0.18	0	55.31 ± 1.71	30.73 ± 2.32	49.33 ± 4.20	57.66 ± 4.89	57.59 ± 4.86
14 (48.1)	0	0	20.61 ± 0.93	15.93 ± 1.21	50.96 ± 4.04	62.10 ± 4.90	45.53 ± 3.64
15 (41.3)	0	0	8.50 ± 0.56	8.91 ± 0.78	10.32 ± 0.93	11.64 ± 1.03	10.17 ± 0.92
16 (44.5)	2.57 ± 0.31	3.43 ± 0.92	22.49 ± 0.92	25.65 ± 2.15	56.02 ± 5.75	33.95 ± 3.73	58.15 ± 5.96
17 (89.8)	0	0	11.22 ± 0.68	10.80 ± 1.38	30.62 ± 2.99	45.31 ± 4.19	25.23 ± 2.56
18 (242.3)	0	0	36.85 ± 1.32	33.16 ± 2.62	52.90 ± 4.30	64.33 ± 5.19	48.45 ± 3.97
19 (497.0)	0	0	21.77 ± 0.81	5.04 ± 0.37	8.48 ± 0.65	33.08 ± 2.33	9.16 ± 0.70
20 (140.9)	0	0	16.19 ± 0.95	18.57 ± 2.07	29.35 ± 2.67	29.45 ± 2.69	31.96 ± 2.89
21 (142.1)	0	0	10.37 ± 0.67	10.62 ± 1.33	14.15 ± 1.14	14.73 ± 1.22	15.02 ± 1.21
22 (163.4)	0	0	32.89 ± 1.28	10.85 ± 1.53	16.86 ± 1.29	42.44 ± 3.07	16.32 ± 1.27
23 (181.2)	0	0	16.80 ± 0.94	15.40 ± 1.90	21.92 ± 1.66	24.18 ± 1.83	22.11 ± 1.68
<b>Slope</b>							
1	0	0	38.82 ± 1.52	26.98 ± 2.54	24.76 ± 1.97	30.55 ± 2.39	26.19 ± 2.08
2	1.82 ± 0.20	0	27.82 ± 0.91	25.38 ± 1.84	48.71 ± 3.84	50.47 ± 3.99	51.80 ± 4.05
3	2.56 ± 0.30	12.37 ± 0.84	24.37 ± 0.83	23.08 ± 1.75	19.36 ± 1.77	27.13 ± 2.41	22.02 ± 2.09
4	0	0	30.34 ± 1.37	25.10 ± 2.52	46.48 ± 3.90	47.33 ± 3.96	49.31 ± 4.12
5	2.51 ± 0.27	14.15 ± 0.71	14.93 ± 0.70	12.58 ± 1.31	34.66 ± 4.66	65.94 ± 8.34	36.83 ± 4.91
6	0	0	22.28 ± 1.17	24.07 ± 2.57	37.73 ± 3.15	39.99 ± 3.35	38.77 ± 3.25
7	0	0	15.42 ± 0.76	17.39 ± 1.38	30.30 ± 2.60	47.12 ± 3.89	34.30 ± 2.91
8	0	0	27.70 ± 0.98	28.21 ± 2.46	51.46 ± 4.45	52.09 ± 4.52	52.60 ± 4.41
9	0	0	21.49 ± 0.82	21.47 ± 1.78	28.43 ± 2.37	29.25 ± 2.43	29.84 ± 2.47
10	0	0	27.99 ± 1.05	18.19 ± 1.80	28.92 ± 2.63	44.41 ± 3.86	30.53 ± 2.77
11	0	0	18.36 ± 0.76	18.90 ± 1.67	28.24 ± 2.06	23.69 ± 1.74	30.16 ± 2.19
12	0	0	18.81 ± 0.99	19.98 ± 2.23	25.13 ± 2.18	21.08 ± 1.88	28.14 ± 2.41
<b>Interfluvial</b>							
1	0	0	11.27 ± 0.62	8.55 ± 1.05	15.68 ± 1.15	17.08 ± 1.25	15.70 ± 1.15
2	0	0	25.19 ± 0.97	22.52 ± 1.91	41.63 ± 3.24	59.21 ± 4.54	45.03 ± 3.48
3	7.71 ± 0.69	26.69 ± 0.81	21.02 ± 0.81	15.14 ± 1.63	20.93 ± 1.84	14.71 ± 1.37	22.15 ± 1.94
4	5.21 ± 0.63	38.74 ± 0.96	21.95 ± 0.96	18.80 ± 1.95	37.78 ± 3.23	57.64 ± 4.80	35.94 ± 3.12
5	1.62 ± 0.20	13.88 ± 1.05	25.00 ± 1.04	24.73 ± 2.05	41.39 ± 3.49	39.05 ± 3.33	44.19 ± 3.73
6	1.90 ± 0.21	3.74 ± 1.06	29.77 ± 1.06	24.33 ± 1.93	46.13 ± 3.77	49.81 ± 4.06	41.58 ± 3.43
7	0	0	26.60 ± 1.17	17.48 ± 1.51	29.19 ± 2.67	50.46 ± 4.39	28.56 ± 2.63
8	0	6.48 ± 0.71	20.09 ± 0.70	17.85 ± 1.38	17.79 ± 1.63	19.62 ± 1.80	19.43 ± 1.83
9	0	0	17.26 ± 0.80	15.77 ± 1.49	31.43 ± 3.03	24.40 ± 2.68	29.51 ± 2.87
10	1.80 ± 0.22	11.02 ± 0.67	13.58 ± 0.66	12.40 ± 1.16	21.54 ± 1.90	23.71 ± 2.07	22.63 ± 1.99
11	1.47 ± 0.18	3.81 ± 0.77	18.04 ± 0.76	19.86 ± 1.76	38.44 ± 3.03	51.64 ± 4.01	38.85 ± 3.10
<b>Ocean</b>							
1	0	0	19.38 ± 0.86	16.78 ± 1.80	14.99 ± 1.22	14.79 ± 1.21	16.01 ± 1.31
2	0	0	9.95 ± 0.59	9.48 ± 1.16	12.69 ± 1.07	16.44 ± 1.37	11.39 ± 0.99

Table 2: Radionuclide data for all surface sediments (mBq g<sup>-1</sup>) (continued).

Sample type/number	<sup>137</sup> Cs	<sup>210</sup> Pb <sub>xs</sub>	<sup>226</sup> Ra	<sup>228</sup> Ra	<sup>232</sup> Th	<sup>230</sup> Th	<sup>228</sup> Th
<b>GOM</b>							
3	0	0	13.74 ± 0.91	14.29 ± 1.28	30.19 ± 2.43	25.29 ± 2.07	26.67 ± 2.18
4	0	0	8.56 ± 0.61	8.94 ± 1.18	14.49 ± 1.17	12.74 ± 1.06	11.50 ± 0.96
5	0	0	14.44 ± 0.78	11.69 ± 1.49	16.47 ± 1.45	25.88 ± 2.16	20.40 ± 1.74
6	0	0	9.29 ± 0.69	9.92 ± 1.38	16.52 ± 1.47	13.87 ± 1.29	14.56 ± 1.36
7	0	0	18.83 ± 1.35	28.42 ± 3.04	49.64 ± 4.28	29.05 ± 2.65	45.82 ± 2.87
8	0	0	11.17 ± 0.54	7.93 ± 0.65	17.71 ± 1.37	16.26 ± 1.26	16.17 ± 3.57
9	0	0	9.53 ± 0.60	8.29 ± 0.67	15.46 ± 1.35	17.98 ± 1.59	13.01 ± 1.25
10	0	0	9.09 ± 0.62	5.52 ± 0.55	14.44 ± 1.20	16.48 ± 1.35	13.14 ± 1.13
<b>Nueces Bay</b>							
1	0	0	15.95 ± 0.65	7.18 ± 1.10	17.34 ± 1.49	27.28 ± 2.21	14.84 ± 2.94
2	1.11 ± 0.14	0	29.36 ± 0.99	21.08 ± 1.76	43.59 ± 3.38	42.74 ± 3.32	47.12 ± 3.64
3	1.55 ± 0.17	0	28.16 ± 1.01	25.25 ± 2.00	39.92 ± 3.32	40.71 ± 3.40	43.48 ± 3.58
4	0.86 ± 0.09	0	26.28 ± 0.94	19.35 ± 1.68	30.60 ± 2.68	33.64 ± 2.93	37.50 ± 3.21
5	0.69 ± 0.08	0	48.74 ± 1.40	31.88 ± 2.11	20.58 ± 1.83	22.67 ± 1.99	25.30 ± 2.19
6	0	0	38.15 ± 1.74	28.72 ± 3.07	41.21 ± 3.12	43.90 ± 3.33	46.77 ± 3.52
7	0.82 ± 0.08	0	21.33 ± 0.65	17.46 ± 1.23	29.87 ± 2.67	31.93 ± 2.82	32.30 ± 2.87
8	0.75 ± 0.07	0	26.95 ± 0.90	19.56 ± 1.64	24.57 ± 2.12	29.07 ± 2.47	22.37 ± 1.94
9	2.77 ± 0.30	0	35.74 ± 1.07	29.39 ± 2.01	56.88 ± 4.21	58.97 ± 4.36	53.88 ± 4.02
10	0.94 ± 0.11	0	18.52 ± 0.88	12.79 ± 1.19	27.11 ± 2.24	29.63 ± 2.39	24.17 ± 1.99
<b>Nueces Delta</b>							
1	3.26 ± 0.48	41.73 ± 0.85	22.08 ± 0.84	23.92 ± 1.85	33.25 ± 3.00	31.82 ± 2.90	32.76 ± 2.81
2	1.60 ± 0.19	0	31.31 ± 0.92	30.43 ± 1.98	29.34 ± 2.63	33.40 ± 2.96	36.82 ± 3.21
3	2.72 ± 0.37	7.96 ± 0.92	25.33 ± 0.91	24.50 ± 1.91	47.79 ± 4.01	67.43 ± 5.51	57.66 ± 4.79
4	7.87 ± 0.97	38.84 ± 1.49	34.05 ± 1.48	37.48 ± 3.16	33.48 ± 2.93	41.85 ± 3.60	33.79 ± 2.95
5	2.36 ± 0.25	32.92 ± 1.01	24.93 ± 1.00	22.11 ± 2.00	46.00 ± 3.80	48.34 ± 3.98	45.61 ± 3.77
6	0.93 ± 0.11	4.88 ± 0.78	15.22 ± 0.78	12.42 ± 1.46	30.73 ± 2.52	36.11 ± 2.92	30.04 ± 2.52
7	3.69 ± 0.26	16.59 ± 1.24	33.75 ± 1.24	36.72 ± 2.59	48.47 ± 3.82	52.44 ± 4.11	47.56 ± 3.75
<b>Corpus Christi Bay</b>							
1	1.82 ± 0.18	3.62 ± 0.80	26.05 ± 0.80	24.04 ± 1.73	47.26 ± 3.86	41.27 ± 3.40	37.47 ± 3.18
2	1.82 ± 0.17	5.83 ± 0.78	19.73 ± 0.76	22.17 ± 1.92	29.59 ± 2.61	34.32 ± 3.05	22.91 ± 2.10
3	2.27 ± 0.25	7.63 ± 0.82	22.41 ± 0.81	22.38 ± 1.81	50.51 ± 4.32	49.13 ± 4.21	37.21 ± 2.68
4	2.25 ± 0.22	6.58 ± 0.83	23.06 ± 0.82	24.25 ± 1.96	57.14 ± 4.02	61.85 ± 4.35	40.91 ± 2.91
5	3.53 ± 0.34	7.49 ± 1.07	22.21 ± 1.07	23.09 ± 2.52	33.09 ± 2.47	33.59 ± 2.50	22.40 ± 1.71
6	2.88 ± 0.28	9.47 ± 0.77	21.84 ± 0.76	20.78 ± 1.66	40.99 ± 3.32	48.87 ± 3.70	28.21 ± 2.37
7	2.31 ± 0.25	3.86 ± 0.87	22.95 ± 0.87	24.64 ± 1.96	43.33 ± 4.54	26.49 ± 5.60	33.34 ± 3.83
8	2.41 ± 0.23	14.75 ± 0.84	20.78 ± 0.83	23.71 ± 1.93	33.39 ± 2.95	31.36 ± 2.79	23.28 ± 2.20
9	3.63 ± 0.48	6.53 ± 0.90	24.21 ± 0.89	24.02 ± 1.94	47.35 ± 3.62	55.76 ± 4.23	35.34 ± 2.75
10	3.56 ± 0.41	22.77 ± 1.13	25.12 ± 1.11	27.35 ± 2.55	35.22 ± 3.08	32.74 ± 2.89	24.43 ± 2.25
11	3.13 ± 0.35	21.52 ± 0.95	23.62 ± 0.95	24.46 ± 2.11	43.86 ± 3.72	47.31 ± 4.01	37.36 ± 3.22
12	1.72 ± 0.18	4.82 ± 0.82	21.29 ± 0.82	22.40 ± 1.82	26.83 ± 2.13	25.24 ± 2.02	20.47 ± 1.67
<b>GIW</b>							
1	0	0	10.62 ± 0.56	8.88 ± 1.15	10.80 ± 0.92	12.13 ± 1.01	9.87 ± 0.97
2	1.13 ± 0.15	0	12.42 ± 0.64	10.33 ± 1.26	30.52 ± 2.56	35.68 ± 2.99	22.33 ± 5.35
3	0	0	6.71 ± 0.47	3.28 ± 0.75	3.64 ± 0.37	8.52 ± 0.76	3.86 ± 0.42
4	0	0	10.82 ± 0.74	8.37 ± 1.42	14.04 ± 1.13	14.99 ± 1.20	13.76 ± 3.30
5	0	0	12.10 ± 0.66	8.11 ± 1.08	8.63 ± 0.88	12.52 ± 1.09	9.82 ± 0.99
6	0.86 ± 0.10	0	11.90 ± 0.62	8.43 ± 1.08	15.14 ± 1.37	15.90 ± 1.43	14.63 ± 2.91
7	0	1.02 ± 0.48	8.11 ± 0.48	7.02 ± 0.60	4.69 ± 0.42	10.14 ± 0.85	4.94 ± 0.50

Table 3: Mean lithogenic isotope ratios for all surface sediment sample compartments and terrestrial and marine composites.

Sample Type	$^{226}\text{Ra}/^{232}\text{Th}$	$^{226}\text{Ra}/^{230}\text{Th}$	$^{228}\text{Ra}/^{232}\text{Th}$	$^{228}\text{Th}/^{228}\text{Ra}$	$^{230}\text{Th}/^{232}\text{Th}$	$^{228}\text{Th}/^{232}\text{Th}$	$^{228}\text{Th}/^{230}\text{Th}$
Alluvium	0.84 + 0.08	0.65 ± 0.06	0.63 ± 0.08	1.73 ± 0.22	1.31 ± 0.15	1.02 ± 0.12	0.90 ± 0.11
Slope	0.77 + 0.07	0.67 ± 0.06	0.69 ± 0.09	1.70 ± 0.22	1.21 ± 0.15	1.07 ± 0.13	0.94 ± 0.11
Interfluvial	0.71 + 0.07	0.67 ± 0.07	0.60 ± 0.08	1.74 ± 0.22	1.17 ± 0.14	1.01 ± 0.12	0.93 ± 0.11
Nueces Delta	0.72 + 0.07	0.63 ± 0.06	0.72 ± 0.09	1.66 ± 0.20	1.15 ± 0.14	1.06 ± 0.13	0.93 ± 0.11
Terrestrial composite	0.78 + 0.07	0.65 ± 0.06	0.65 ± 0.08	1.71 ± 0.22	1.24 ± 0.15	1.03 ± 0.12	0.92 ± 0.11
GOM	0.68 + 0.07	0.68 ± 0.07	0.62 ± 0.09	1.61 ± 0.24	1.02 ± 0.12	0.94 ± 0.12	0.97 ± 0.13
GIW	1.13 + 0.13	0.75 ± 0.08	0.81 ± 0.14	1.39 ± 0.32	1.48 ± 0.19	0.98 ± 0.18	0.71 ± 0.13
Oceanic composite	0.88 + 0.09	0.71 ± 0.07	0.70 ± 0.11	1.52 ± 0.28	1.21 ± 0.15	0.95 ± 0.14	0.86 ± 0.13
Corpus Christi Bay	0.58 + 0.05	0.60 ± 0.06	0.61 ± 0.07	1.28 ± 0.15	0.99 ± 0.12	0.74 ± 0.09	0.77 ± 0.10
Nueces Bay	0.96 + 0.09	0.86 ± 0.08	0.68 ± 0.08	1.71 ± 0.23	1.12 ± 0.13	1.05 ± 0.13	0.95 ± 0.12

system. This is true when examining discrete sediment compartments within the terrestrial setting (alluvium, slopes, etc.), the marine setting (GIW, GOM), or the two basins. This similarity continues when considering the two sediment source settings as composites of their individual sedimentary compartments. Consequently, a numeric approach to discerning the importance of each of the two large scale sediment source areas (terrestrial and marine) to sediments within Nueces and Corpus Christi Bays is not possible. However, the influence of upper basin geology on isotope ratio signatures does appear. Examination of alluvial signatures of  $^{226}\text{Ra}/^{232}\text{Th}$  (Fig. 9),  $^{230}\text{Th}/^{232}\text{Th}$  (Fig. 10) and  $^{226}\text{Ra}/^{228}\text{Ra}$  (Fig. 11) all show consistent change moving inland, a likely effect of proximity to the uranium rich rocks of the upper coastal plain of Texas (e.g., the Catahoula Fm.), where lithogenic isotopic signatures would be expected to contrast with those derived from other rocks of the coastal plain (Galloway 1977, Hobday and Galloway 1999).

A stepwise, graphical examination of discrete lithogenic isotope signatures shows considerably more promise in determining the importance of terrestrial versus marine sources of sediment to the Nueces-Corpus Christi Estuary system. Figure 12 depicts the concentrations of  $^{226}\text{Ra}$  versus  $^{232}\text{Th}$  for all surface sediment samples collected, by compartment. In order to better see the separation of individual sediment compartments, Figure 13 depicts the means of each for the same two isotopes. It is clear (Fig. 13) that terrestrial and marine sediment source components have significantly different signatures and that sediment deposited in Nueces and Corpus Christi Bays are indistinguishable from the terrestrial component, suggesting they are composed entirely of sediment derived from terrestrial sources, shown in the simplest terms by Figure 14. The same conclusions are made by examining activities of  $^{226}\text{Ra}$  versus  $^{230}\text{Th}$  and  $^{228}\text{Ra}$  versus  $^{232}\text{Th}$  (Figs. 15, 16), which consider both daughter to parent isotope relationships within decay series as well as isotope comparisons between decay series ( $^{238}\text{U}$  and  $^{232}\text{Th}$ , Fig. 2).

Additional evidence is required. While a considerable amount of research has been done which shows that radium and thorium isotopes behave conservatively, i.e., remain particle bound, in aquatic systems (radium; Tanner 1964, Riese 1982, Ames *et al.* 1983; thorium; Kaufman 1969, Ivanovich and Harmon 1982, 1992), it is known that when moving from relatively low ionic strength river water to considerably higher ionic strength, brackish estuarine waters, radium isotopes in particular can quickly be desorbed from inorganic mineral matter (e.g., Li *et al.* 1977, Key *et al.* 1985, Elsinger and Moore 1984). The desorption of radium isotopes is primarily controlled by the concentration of radium in the system, the suspended sediment concentration and the salinity (Webster *et al.* 1995) and is a rapid, ion exchange dominated process. The Nueces-Corpus Christi Estuary, like most estuarine systems, has salinities which are stratified horizontally and vertically. Generally, the horizontal gradient of fresh to brackish to marine salinities (0, 15, 35 parts per thousand (ppt)) progresses from the river

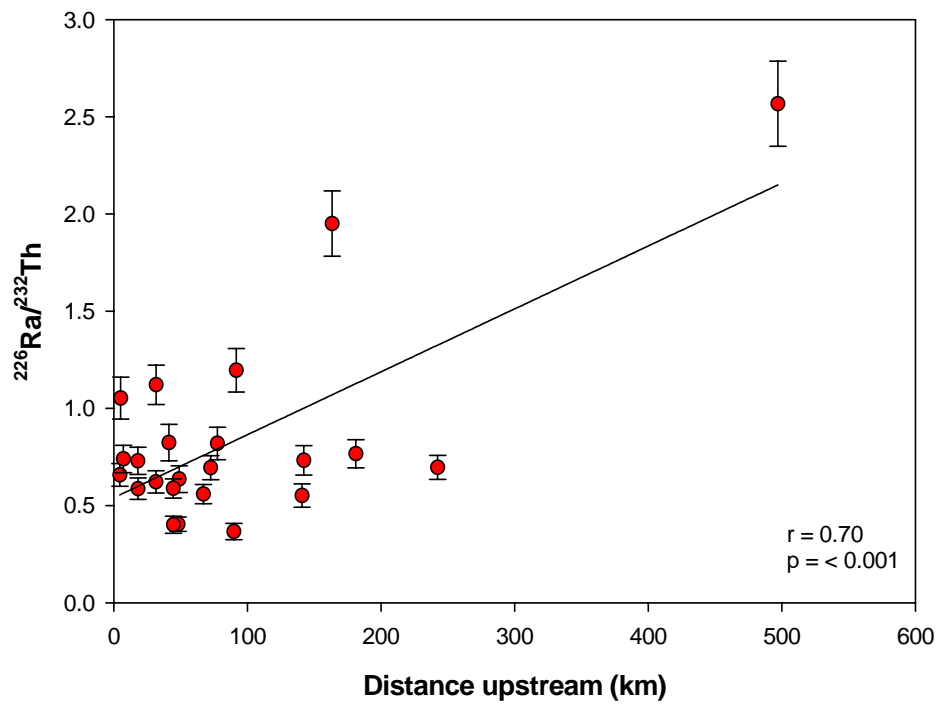


Figure 9: Changing  $^{226}\text{Ra}/^{232}\text{Th}$  signatures for alluvial sediments with increasing distance inland.

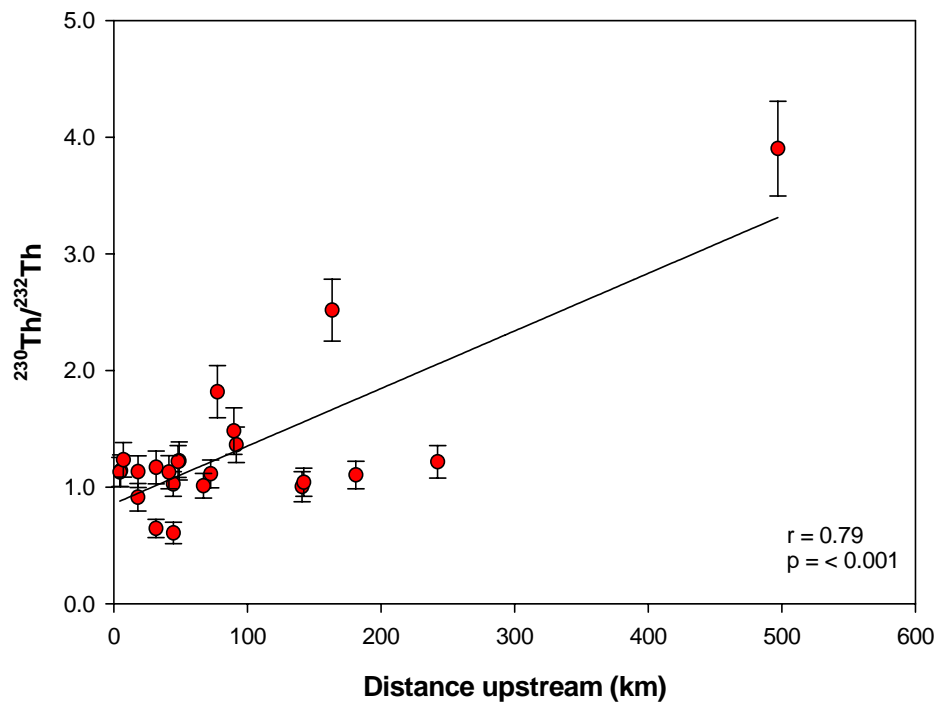


Figure 10: Changing  $^{230}\text{Th}/^{232}\text{Th}$  signatures for alluvial sediments with increasing distance inland.

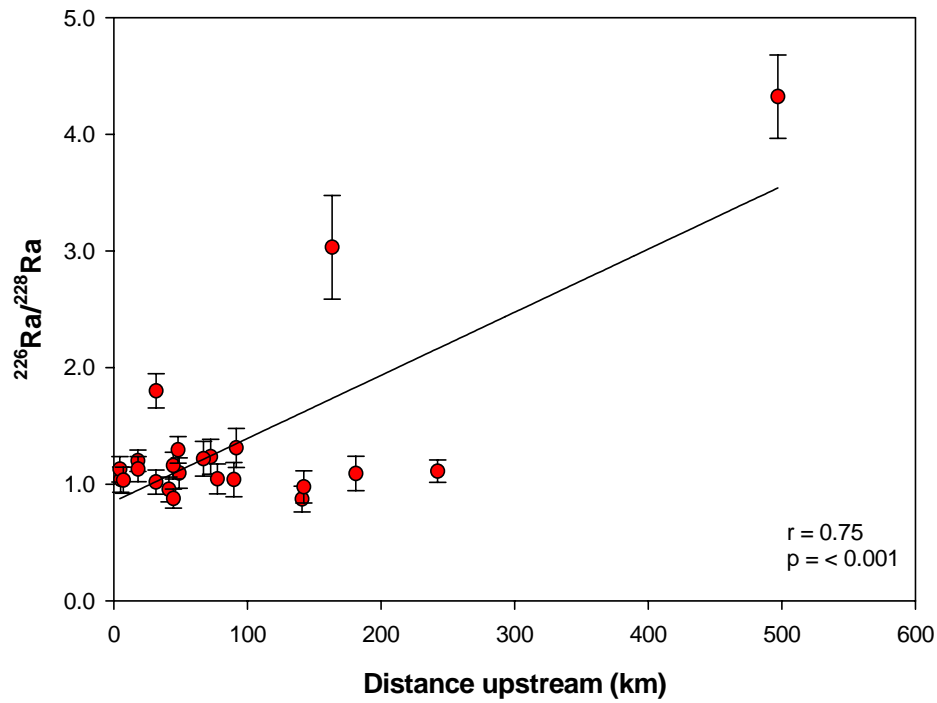


Figure 11: Changing  $^{226}\text{Ra}/^{228}\text{Ra}$  signatures for alluvial sediments with increasing distance inland.

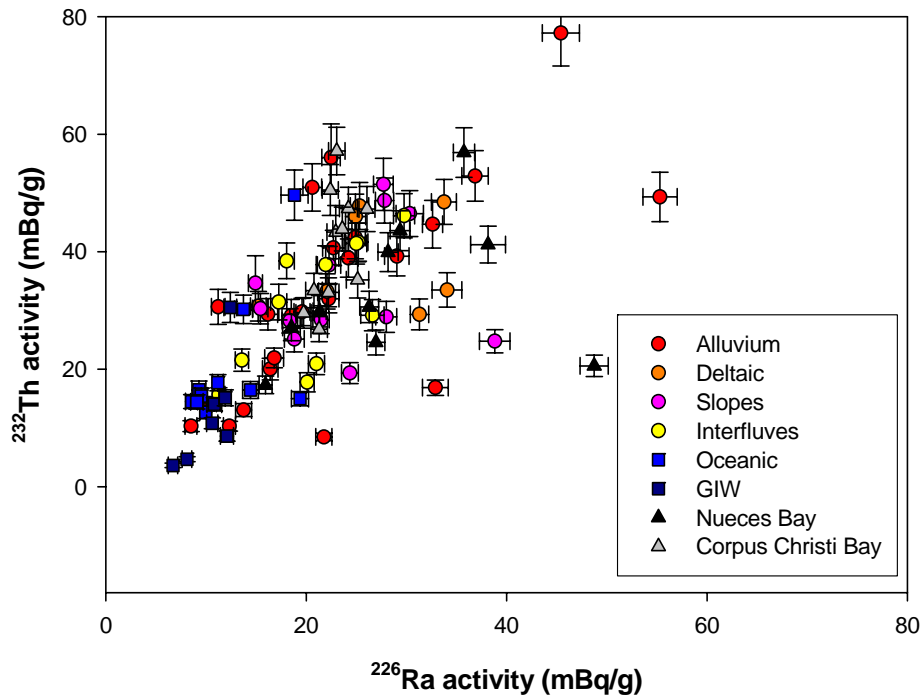


Figure 12:  $^{226}\text{Ra}$  versus  $^{232}\text{Th}$  signature for all surface sediment samples, by compartment. Circles (warm colors) delineate terrestrial, squares (cool colors) delineate marine and triangles (grey scale) delineate basin sediments.

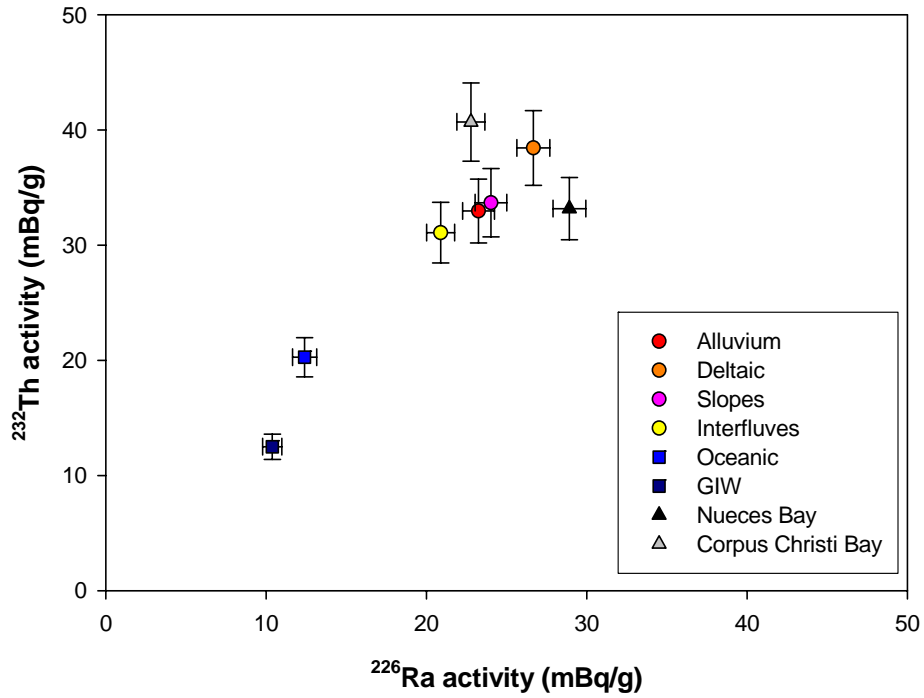


Figure 13: Mean  $^{226}\text{Ra}$  versus  $^{232}\text{Th}$  signatures for all surface sediment compartments. Circles delineate terrestrial, squares delineate marine and triangles delineate basin samples.

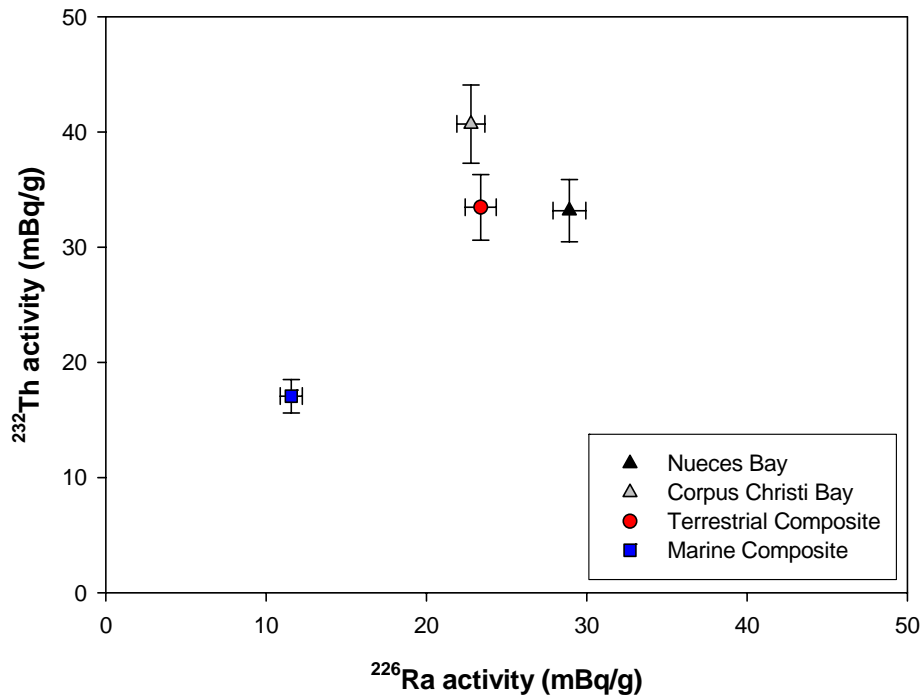


Figure 14: Mean  $^{226}\text{Ra}$  versus  $^{232}\text{Th}$  signatures for composite marine and terrestrial sediment source compartments and basins.

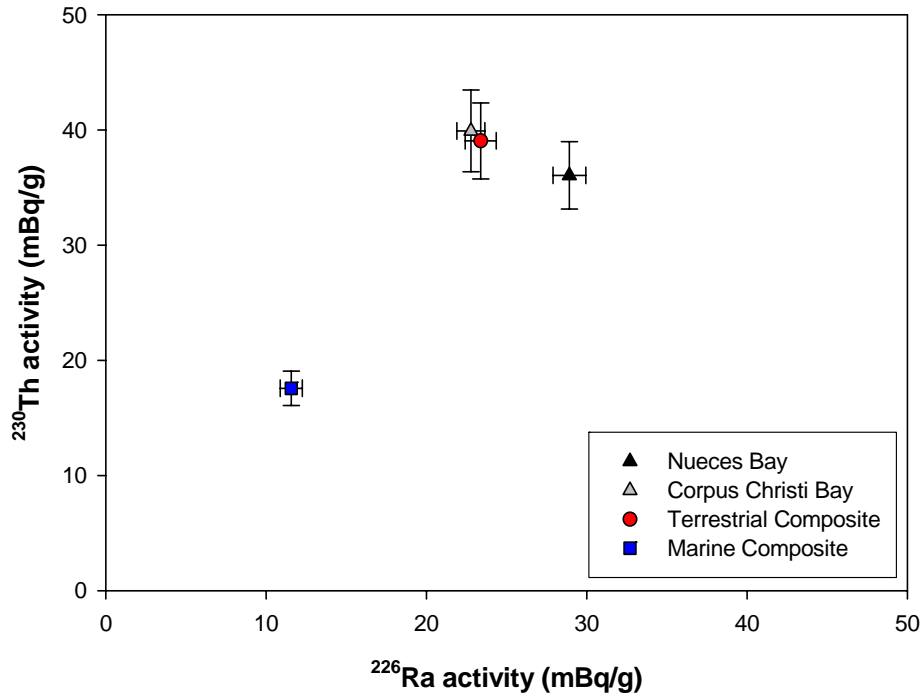


Figure 15: Mean  $^{226}\text{Ra}$  versus  $^{230}\text{Th}$  signatures for composite marine and terrestrial sediment source compartments and basins.

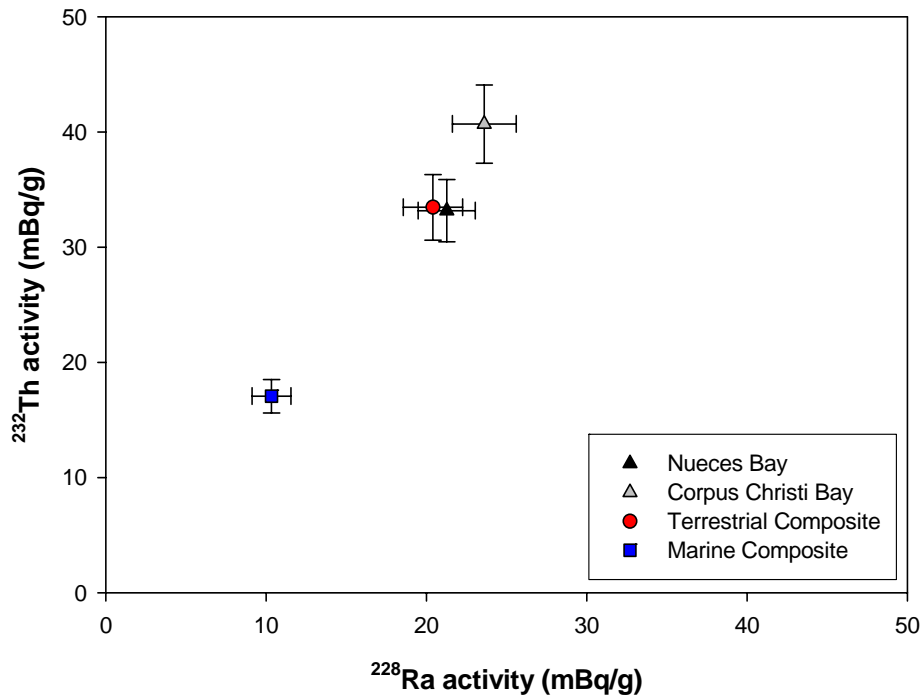


Figure 16: Mean  $^{228}\text{Ra}$  versus  $^{232}\text{Th}$  signatures for composite marine and terrestrial sediment source compartments and basins.

delta and mouth to the secondary bay (Nueces), then to the primary bay (Corpus Christi). In this setting, radium isotopes that could be lost by desorption from sediments, would begin moving into solution upon arrival at Nueces Bay and this process would continue as the sediments move into Corpus Christi Bay and salinity continues to rise towards marine levels.

Thorium isotopes have the advantage of being particle reactive and remaining particle bound, even when moving across the salinity gradient from river to estuarine or marine conditions. Figure 17 depicts the

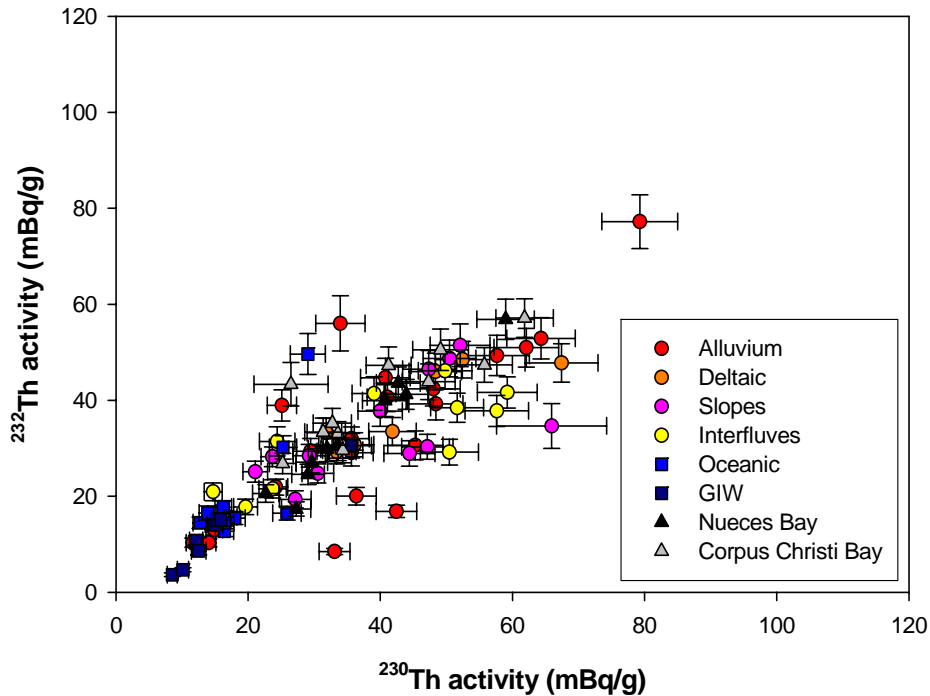


Figure 17:  $^{230}\text{Th}$  versus  $^{232}\text{Th}$  signature for all surface sediment samples, by compartment. Circles (warm colors) delineate terrestrial, squares (cool colors) delineate marine and triangles (grey scale) delineate basin sediments.

concentrations of  $^{230}\text{Th}$  versus  $^{232}\text{Th}$  for all surface sediment samples collected, by compartment and Figure 18 depicts the means of each for the same two isotopes. As with Ra/Th data, it is clear (Fig. 18) that terrestrial and marine sediment source components have significantly different signatures and that sediment deposited in Nueces and Corpus Christi Bays are indistinguishable from the terrestrial component, suggesting they are composed entirely of sediment derived from terrestrial sources, shown in the simplest terms by Figure 19. The same conclusions are made by examining activities of  $^{228}\text{Th}$  versus  $^{232}\text{Th}$  and  $^{228}\text{Th}$  versus  $^{230}\text{Th}$  (Figs. 20, 21), which consider both daughter to parent isotope relationships within decay series as well as isotope comparisons between decay series ( $^{238}\text{U}$  and  $^{232}\text{Th}$ , Fig. 2). The fact that both Ra/Th and Th/Th isotopic data are in unanimous agreement, both showing that terrestrial and marine sediments are distinctly different and that sediments deposited in Nueces and Corpus Christi Bays are derived predominantly from terrestrial sources, suggests that these isotopic signatures are reflective of differences in the sediment source compartments themselves and not a function of geochemical processes which are known to effect the elements considered in starkly contrasting ways.

So, what are the causes of the differences between the terrestrial and marine settings that might explain why sediment from each is distinctly different with respect to these isotopic signatures? Two possible explanations include grain size distribution and differences in large scale sourcing of sediments comprising the terrestrial and marine sources as defined herein. Firstly, differences in sediment surface area as a function of grain size have been shown to influence radionuclide adsorption (Megumi *et al.* 1982), which is particularly

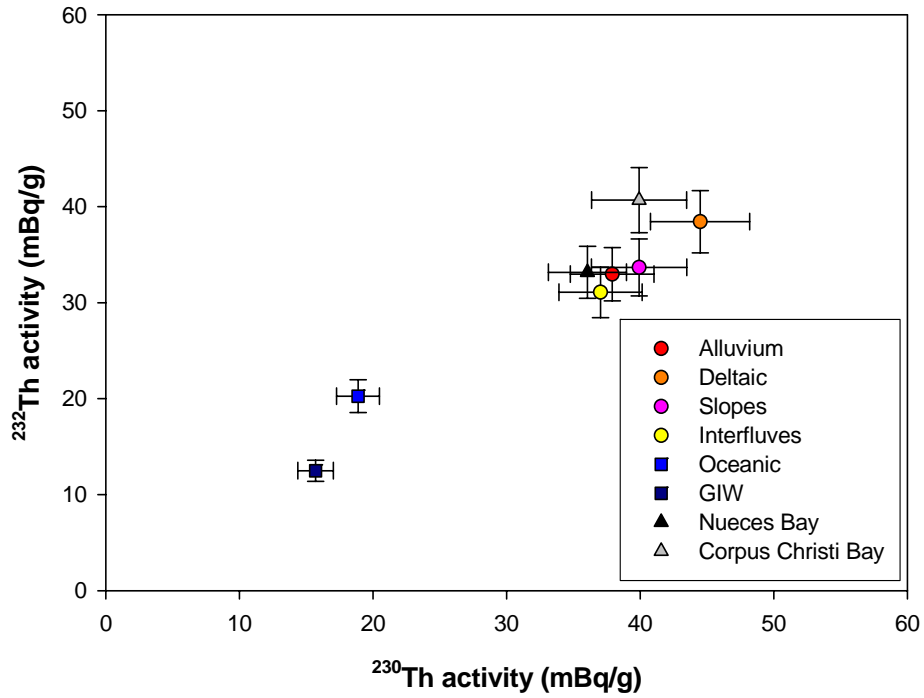


Figure 18: Mean  $^{230}\text{Th}$  versus  $^{232}\text{Th}$  signatures for all surface sediment compartments. Circles delineate terrestrial, squares delineate marine and triangles delineate basin samples.

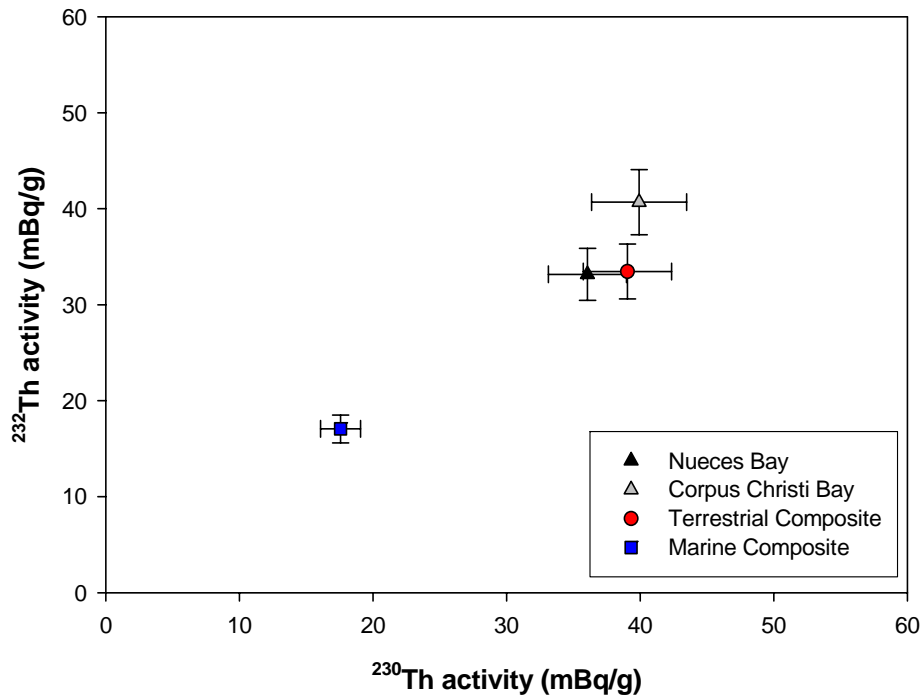


Figure 19: Mean  $^{230}\text{Th}$  versus  $^{232}\text{Th}$  signatures for composite marine and terrestrial sediment source compartments and basins.

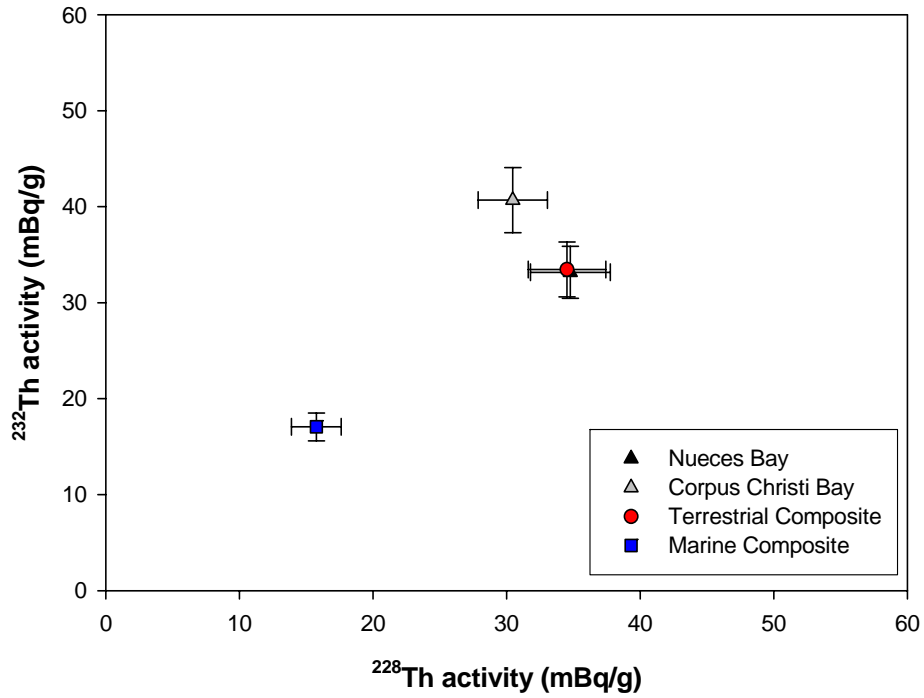


Figure 20: Mean  $^{228}\text{Th}$  and  $^{232}\text{Th}$  signatures for composite marine and terrestrial sediment source compartments and basins.

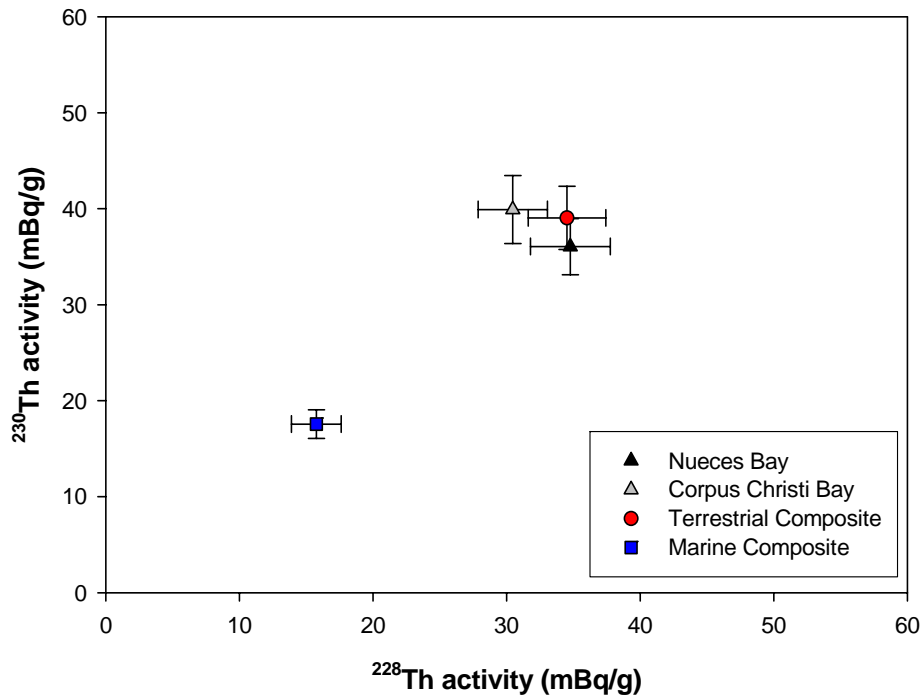


Figure 21: Mean  $^{228}\text{Th}$  versus  $^{230}\text{Th}$  signatures for composite marine and terrestrial sediment source compartments and basins.

important in fluvial systems, where transport results in sorting of materials by particle size and density (Paola *et al.* 1992). While an individual radionuclide's activity can be a function of substrate surface area, daughter/parent ratios remain constant within analytical uncertainty (e.g., Murray *et al.* 1990, 1991, Olley *et al.* 1997, Yeager and Santschi 2003). Upon inspection of the grain size data presented here (Table 1, Figs. 7, 8), a clear influence is not obvious. While the marine sediment compartments are dominantly sands, considerable grain size variability exists in all terrestrial sample compartments and a strong contrast is evident between the two bays. Nueces Bay sediments are similar to terrestrial sediments, having a relatively even mix of grain sizes and Corpus Christi Bay sediments are almost entirely clay. Statistical analyses were somewhat mixed (Table 4), showing that in freshwater, the influence of grain size is clear in most cases, but that in brackish or marine

Table 4: Results of Pearson correlation for sediment compartments, comparing the % clay fraction with individual isotope concentrations, \*indicates that the p value is < 0.001.

Sample Type	<sup>230</sup> Th	<sup>226</sup> Ra	<sup>232</sup> Th	<sup>228</sup> Ra	<sup>228</sup> Th
<b>Terrestrial Composite</b>	r = 0.405 p = 0.001 n = 53	r = 0.656 p = *	r = 0.587 p = *	r = 0.780 p = *	r = 0.578 p = *
<b>Nueces Bay</b>	r = 0.834 p = 0.001 n = 10	r = 0.365 p = 0.150	r = 0.885 p = *	r = 0.611 p = 0.030	r = 0.837 p = 0.001
<b>Corpus Christi Bay</b>	r = 0.127 p = 0.355 n = 11	r = 0.149 p = 0.321	r = -0.091 p = 0.395	r = 0.539 p = 0.035	r = -0.161 p = 0.318
<b>Marine Composite</b>	r = 0.396 p = 0.058 n = 17	r = -0.077 p = 0.384	r = 0.038 p = 0.443	r = -0.181 p = 0.243	r = -0.063 p = 0.406

settings, the relationship is weakened or absent altogether, regardless of how dominant the clay size fraction might be (such as Corpus Christi Bay). Most importantly, the radio-isotopic signatures for sediments in terrestrial domains, many of which are comprised predominantly of sandy sediments (e.g., interfluvial, alluvium, etc.), are very different than those in coastal domains (e.g., GOM, GIW), strongly suggesting that sediment sources for the two provinces are indeed different and that winnowing of fine grained sediments is not the primary cause of these differences we observe. Secondly, unlike the terrestrial source component, which is a mix of lithologies and diagenetic alteration products of the weathering and transport of rocks comprising the land surface of the Nueces River basin, the marine component consists of a mix, to a minor degree of these same constituents, in addition to sediments derived from transport and delivery to the GOM by the Mississippi River. The Mississippi River provides 83% of all sediment delivered to the continental shelf, and while Texas rivers have a significantly higher suspended sediment load as compared to the Mississippi River (820 versus 510 mg/L, respectively), they cannot compete with the overwhelming volume and mass of water and sediment delivered to the coast by the Mississippi River (Curtis *et al.* 1973, Walker and Colman 1987). Some of these sediments are then transported west, by the long shore current of the northern GOM and contribute to the composition of sediments sampled here, off the south west coast of Texas, along with sediments provided to the GOM by east Texas rivers (e.g., Sabine, Neches, Trinity, Brazos and Colorado). Since the Mississippi River watershed is enormous and drains a host of North American lithologies not represented in the Nueces River watershed (as is also the case for the Brazos and Colorado Rivers in particular), it is reasonable to presume that different lithologic isotope signatures for those sediments may be reflected.

Based on the combined data presented, it is our conclusion that the overwhelming majority of sediment deposited in both Nueces and Corpus Christi Bays are derived from terrestrial sources. While marine sources of sediment to estuaries can be significant, even dominant in some instances (e.g., Eyre *et al.* 1998, Cooper 2001, Jenkins *et al.* 2002), the physiographic settings for those estuaries and embayments can generally be characterized as open as compared to what we find in southwest Texas. Marine sources of sediment are often important in estuaries that have wide, un-obstructed openings to the sea, experience significant tidal variation or

are well mixed due to a combination of significant tidal variation, wind action and the influence of shelf or open ocean currents. The Nueces-Corpus Christi Estuary, in contrast, can be characterized as micro-tidal, has an extensive barrier island system armoring and restricting communication with the GOM and is not significantly affected by shelf or open ocean currents. Based on these considerations, the evidence suggests that marine sources of sediment to this estuary are insignificant.

### 4.3 Deltaic sedimentation

As described previously (sections 2.2, 3.1 and Fig. 6), a set of five sediment cores were collected from the southern portion of the Nueces Delta to investigate sediment accumulation rates using  $^{137}\text{Cs}$  and  $^{210}\text{Pb}_{\text{xs}}$ . Appendix I (Tables AI1 – AI5) summarize the physical and radiochemical data for each of these delta cores. These cores were composed of predominantly fine grained sediments throughout (silts and clays), with the exception of cores 1 and 2, which had a considerable sand fraction, particularly in the upper region of the profile. Sediment accumulation rates have been determined using  $^{137}\text{Cs}$  by:

$$S = (D_{\text{pk}}/T) \quad (1)$$

where  $S$  = sediment accumulation rate ( $\text{g cm}^{-2} \text{ yr.}^{-1}$ ),  $D_{\text{pk}}$  = mass depth ( $\text{g cm}^{-2}$ ) at which the  $^{137}\text{Cs}$  maxima occurs and  $T$  = time since 1963 (yr.). This model is based on the assumption of limited vertical mobility of cesium in sediments and gives accumulation rates representative of the average rate of sediment accumulation since 1963 (Huntley *et al.* 1995, Winkels *et al.* 1998, Valero-Garces *et al.* 1999).  $^{210}\text{Pb}_{\text{xs}}$  is defined as total  $^{210}\text{Pb}$  – deepest  $^{210}\text{Pb}$  values in the core, where equilibrium is assumed between  $^{210}\text{Pb}$  and its progenitor,  $^{226}\text{Ra}$  (Walsh and Nittrouer 2003, Kim and Rejmankova 2002, Craft and Richardson 1993, Binford 1990). Sedimentation rates have been determined using  $^{210}\text{Pb}_{\text{xs}}$  by the constant flux model (Robbins 1978), which is most appropriate for settings where input of  $^{210}\text{Pb}$  from atmospheric fallout may be constant, but sedimentation is not. The  $^{210}\text{Pb}_{\text{xs}}$  distribution as a function of mass depth is:

$$^{210}\text{Pb}_{\text{xs}} = F_{210} e^{-\lambda t}/S_a \quad (2)$$

where  $F_{210}$  =  $^{210}\text{Pb}$  flux,  $\lambda$  = decay constant ( $0.031 \text{ yr.}^{-1}$ ),  $t$  = time (yr.) and  $S_a$  = sediment accumulation rate. The sediment accumulation rate, as a function of mass depth is:

$$S_a = \Delta m/\Delta t \quad (3)$$

where  $m$  = mass depth ( $\text{g cm}^{-2}$ ). Table 5 lists the sediment accumulation rates, inventories determined and the fallout isotope inventories expected from fallout alone (discussed in section 4.4), and Figures 22 – 26 show the profiles of  $^{137}\text{Cs}$  and  $^{210}\text{Pb}_{\text{xs}}$  for each core.

Table 5: Sediment accumulation rates and means, fallout isotope inventories and expected fallout inventories for each of the delta cores collected, \*full depth of activity not resolved.

Delta Core	$^{137}\text{Cs}$ rate ( $\text{g cm}^{-2} \text{ yr.}^{-1}$ )	$^{210}\text{Pb}_{\text{xs}}$ rate ( $\text{g cm}^{-2} \text{ yr.}^{-1}$ )	Mean rate ( $\text{g cm}^{-2} \text{ yr.}^{-1}$ )	$^{137}\text{Cs}$ inventory ( $\text{mBq cm}^{-2}$ )	$^{210}\text{Pb}_{\text{xs}}$ inventory ( $\text{mBq cm}^{-2}$ )
1	$0.22 \pm 0.04$	$0.31 \pm 0.02$	$0.27 \pm 0.04$	$120 \pm 11$	$524 \pm 2$
2	$0.47 \pm 0.03$	$0.54 \pm 0.08$	$0.51 \pm 0.09$	$79 \pm 7$	$434 \pm 3$
3	$0.14 \pm 0.03$	$0.21 \pm 0.02$	$0.18 \pm 0.04$	$147 \pm 13$	$650 \pm 4$
4	$0.07 \pm 0.01$	$0.17 \pm 0.02$	$0.12 \pm 0.02$	$20 \pm 2$	$340 \pm 5$
5	$0.39 \pm 0.03$	$0.32 \pm 0.06$	$0.36 \pm 0.07$	$83 \pm 8^*$	$485 \pm 4$
Expected fallout inventory	--	--	--	$118 \pm 9$	$270 \pm 18$

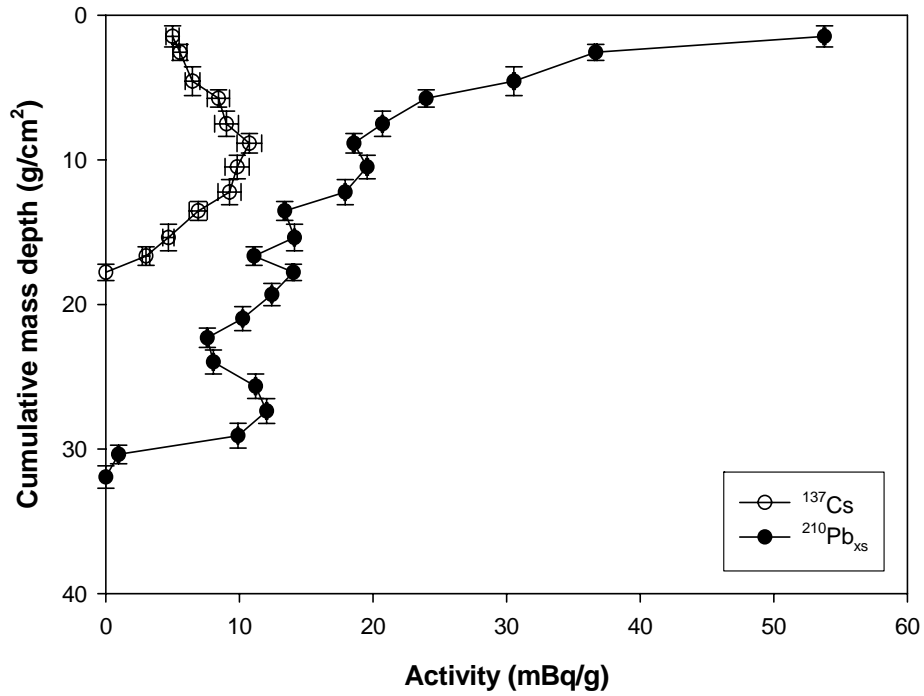


Figure 22: Fallout radionuclide (<sup>137</sup>Cs, <sup>210</sup>Pb<sub>xs</sub>) profiles for Nueces Delta core 1.

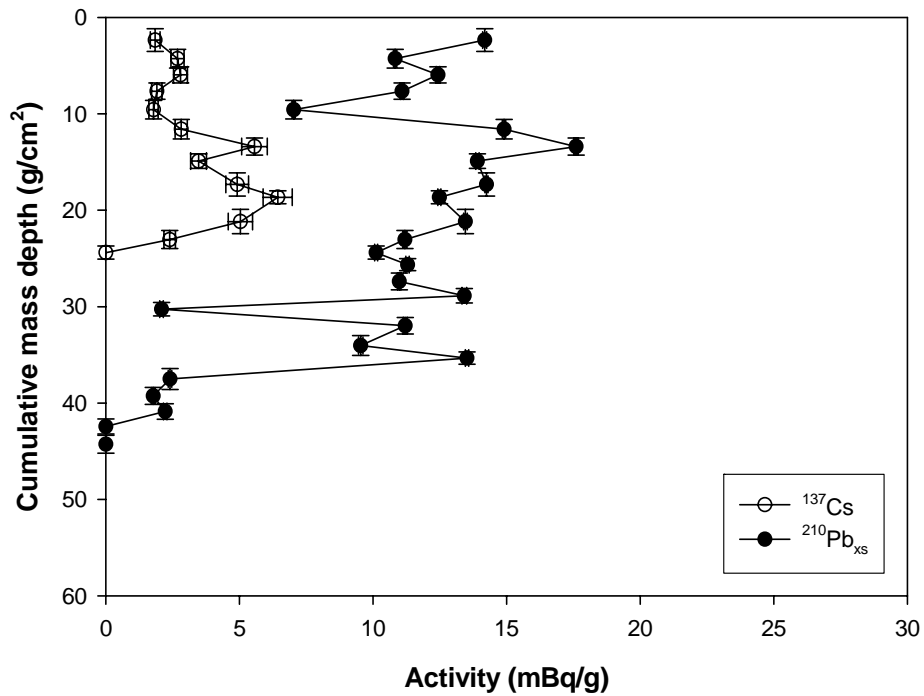


Figure 23: Fallout radionuclide (<sup>137</sup>Cs, <sup>210</sup>Pb<sub>xs</sub>) profiles for Nueces Delta core 2.

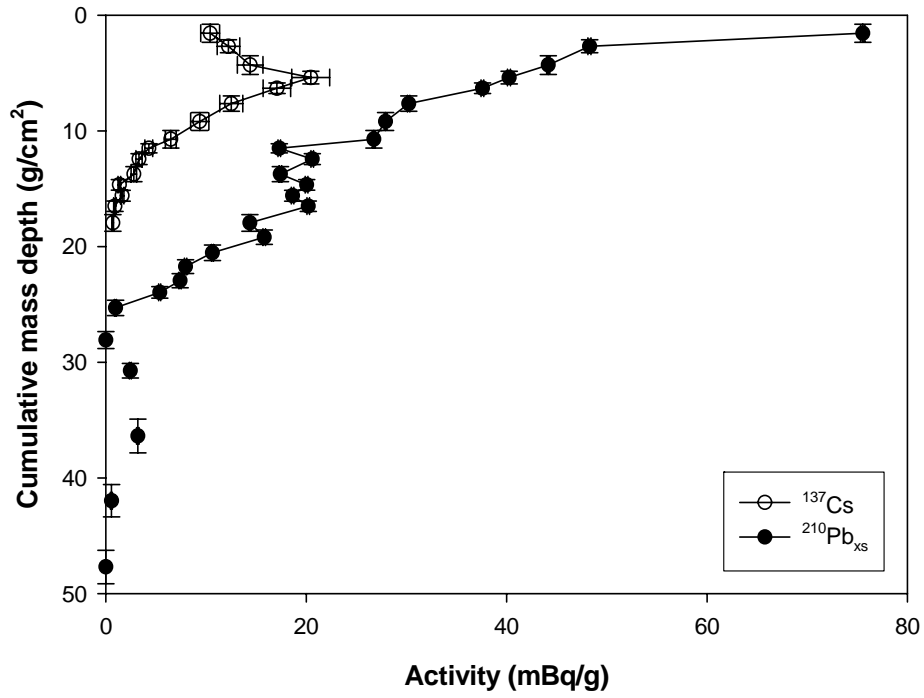


Figure 24: Fallout radionuclide ( $^{137}\text{Cs}$ ,  $^{210}\text{Pb}_{\text{xs}}$ ) profiles for Nueces Delta core 3.

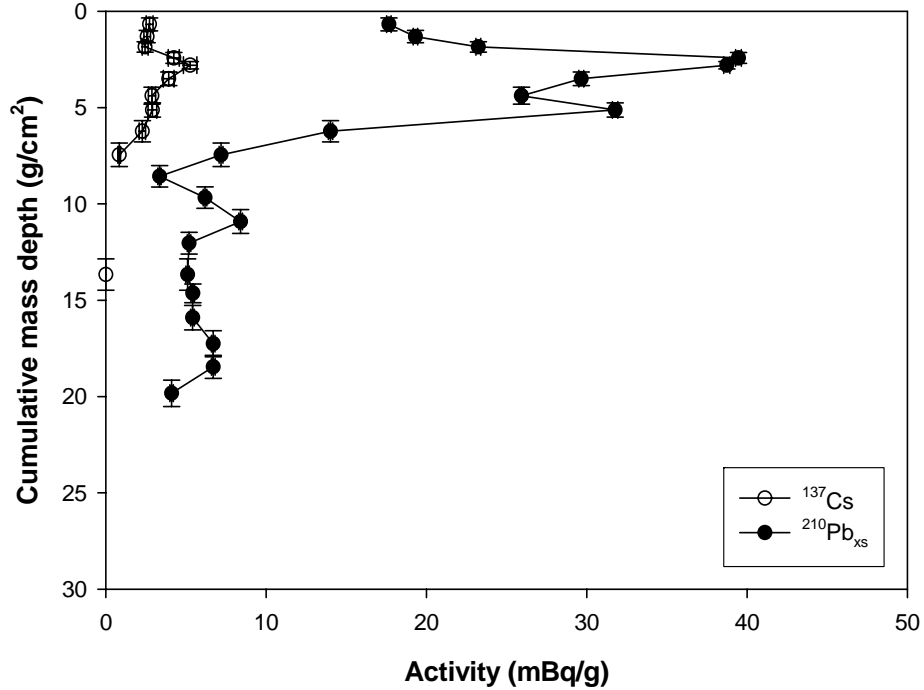


Figure 25: Fallout radionuclide ( $^{137}\text{Cs}$ ,  $^{210}\text{Pb}_{\text{xs}}$ ) profiles for Nueces Delta core 4.

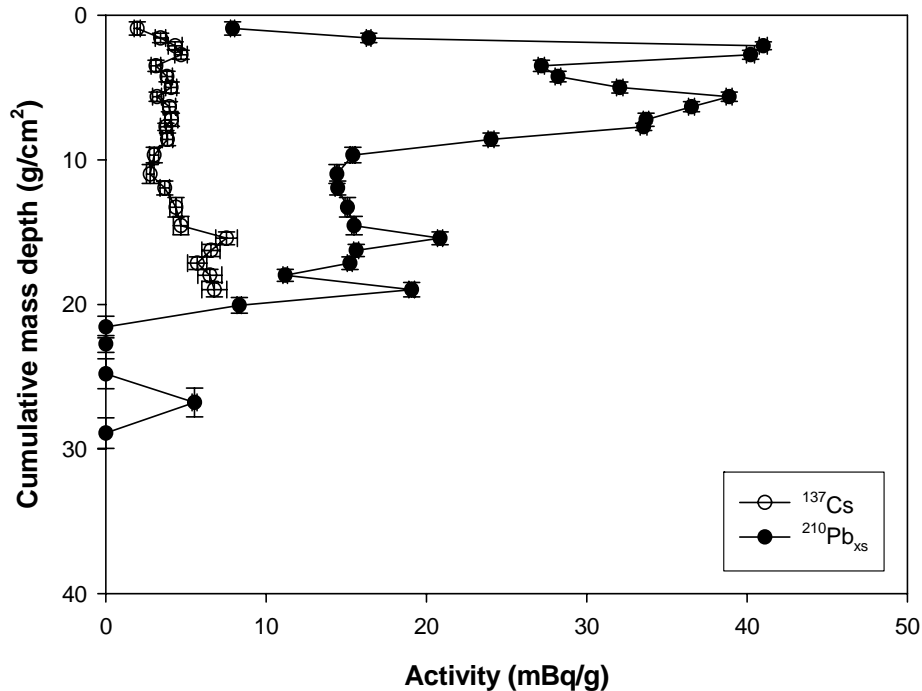


Figure 26: Fallout radionuclide ( $^{137}\text{Cs}$ ,  $^{210}\text{Pb}_{\text{xs}}$ ) profiles for Nueces Delta core 5.

The sediment accumulation rates determined by the two isotopes and approaches are in close agreement. The rates determined here are well within the range (when converted to units of  $\text{cm yr}^{-1}$ ) of those presented for the Nueces Delta by White *et al.* (2002), who determined sedimentation rates employing only  $^{210}\text{Pb}_{\text{xs}}$ . Upon inspection, a subtle gradient in sediment accumulation across the delta is evident, with rates that are generally lower in the west and progressively higher moving east. While White *et al.* (2002) discussed the large scale gradient of decreasing sedimentation moving from east to west across the Texas coastal plain as a function of such influences as changing regional precipitation, watershed size and hydrologic management in the form of dams, this small scale gradient is likely a reflection of contrasts in land use and topography on either side of the Nueces Delta here. The western side has a comparatively subdued topography and most importantly, is dominated by industrial and residential land uses which create impervious surfaces and provide little sediment to be eroded and transported by runoff. In contrast, the eastern border of the delta is delineated by a sharp bluff line, with mixed agricultural land at its summit. This combination of land use and topography would be expected to supply much more sediment for erosion, transport and deposition on the eastern side of the delta. Inventories of  $^{210}\text{Pb}_{\text{xs}}$  are, as expected, well above predicted fallout values (Table 4), due to lateral particle inputs from the watershed. However,  $^{137}\text{Cs}$  inventories are only at approximately the same levels as expected from atmospheric fallout, indicating some losses (see later discussion).

#### 4.4 Nueces Bay and Corpus Christi Bay sedimentation

As described previously (sections 2.2, 3.1, 3.2 and Fig. 6), a set of eight sediment cores and accompanying x-radiographs were collected from the northern portion of Nueces Bay, near the mouth of the Nueces River, through Nueces Bay and out into Corpus Christi Bay, moving toward the GOM. These cores and x-radiographs were collected to investigate sediment mixing and accumulation rates using  $^{137}\text{Cs}$  and  $^{210}\text{Pb}_{\text{xs}}$ . Appendix II lists summary tables (Tables AII1 – AII8), which include physical and radiochemical data for each of the bay cores collected, all x-radiographs and matching grain size distributions (Figures AII1 – AII8) and summary tables for x-radiograph physical data (Tables AII9 – AII11).

The Nueces Bay sediment cores differ from those collected in Corpus Christi Bay in two ways; 1) sands comprise a larger percentage of their composition, particularly over the first 10 – 20 cm (Figs. AII1 – AII8, Tables AII1 – AII11), and 2) they are mixed over greater depth (Fig. 27 - 33). These differences are attributable to geographic and physiographic effects, 1) the proximity of Nueces Bay to the Nueces River and terrestrial sources of sandy sediment and 2) Nueces Bay, being shallower and in direct communication with the Nueces River, is more easily mixed by physical processes (wind, high river discharge, etc.) as compared to Corpus Christi Bay.

Sediment accumulation rates for these cores have been determined using  $^{137}\text{Cs}$  where possible by the same method discussed previously (section 4.3). Sedimentation rates using  $^{210}\text{Pb}_{\text{xs}}$  have been determined for these cores using the constant flux-constant sedimentation (CF-CS) model, where sedimentation rates can be calculated assuming steady state conditions and at relatively constant porosity, using:

$$[^{210}\text{Pb}_{\text{xs}}(z)] = [^{210}\text{Pb}_{\text{xs}}(0)]\exp(-\alpha z) \quad (4a)$$

$$\alpha = (\lambda/S) \quad (4b)$$

where  $[^{210}\text{Pb}_{\text{xs}}(z)]$  and  $[^{210}\text{Pb}_{\text{xs}}(0)]$  represent  $^{210}\text{Pb}_{\text{xs}}$  concentration at depth  $z$  and at the sediment interface, respectively;  $S$  = sediment accumulation rate ( $\text{g cm}^{-2} \text{yr}^{-1}$ ) and  $\lambda$  = decay constant of  $^{210}\text{Pb}$  ( $0.031 \text{ year}^{-1}$ ). Table 6 lists the inventories, mixing depths and sediment accumulation rates determined for each core, Figures 27 –

Table 6: Sediment accumulation rates and fallout isotope inventories for each of the bay cores collected, nd = no or insufficient data, \*complete profile for  $^{137}\text{Cs}$  not available.

Core	$^{137}\text{Cs}$ rate ( $\text{g cm}^{-2} \text{yr}^{-1}$ )	$^{210}\text{Pb}_{\text{xs}}$ rate ( $\text{g cm}^{-2} \text{yr}^{-1}$ )	Mean rate ( $\text{g cm}^{-2} \text{yr}^{-1}$ )	$^{137}\text{Cs}$ inventory ( $\text{mBq cm}^{-2}$ )	$^{210}\text{Pb}_{\text{xs}}$ inventory ( $\text{mBq cm}^{-2}$ )
Nueces Bay 1	nd	Mixed	--	--	--
Nueces Bay 2	$0.32 \pm 0.01$	$0.52 \pm 0.28$	$0.42 \pm 0.28$	$25 \pm 2^*$	$354 \pm 5$
Nueces Bay 3	$0.33 \pm 0.03$	$0.38 \pm 0.09$	$0.36 \pm 0.10$	$16 \pm 2$	$194 \pm 2$
Corpus Christi Bay 1	$0.31 \pm 0.01$	$0.39 \pm 0.11$	$0.35 \pm 0.11$	$35 \pm 3^*$	$384 \pm 3$
Corpus Christi Bay 2	$0.16 \pm 0.02$	$0.21 \pm 0.08$	$0.19 \pm 0.08$	$21 \pm 2^*$	$239 \pm 2$
Corpus Christi Bay 3	$0.19 \pm 0.02$	$0.23 \pm 0.03$	$0.21 \pm 0.04$	$30 \pm 3^*$	$303 \pm 2$
Corpus Christi Bay 4	nd	$0.28 \pm 0.08$	$0.28 \pm 0.08$	--	$173 \pm 2$
Corpus Christi Bay5	nd	$0.26 \pm 0.08$	$0.26 \pm 0.08$	--	$356 \pm 3$
Expected fallout inventory	--	--	--	$118 \pm 9$	$270 \pm 18$

33 show the profiles of  $^{137}\text{Cs}$  and  $^{210}\text{Pb}_{\text{xs}}$  and Figures 34 - 40 show the semi-log plots of  $^{210}\text{Pb}_{\text{xs}}$  over depth, from which sediment accumulation rates were derived. Expected inventories from fallout alone were estimated for both isotopes by pro-rating published fallout data for  $^{210}\text{Pb}_{\text{xs}}$  (Baskaran *et al.* 1993) and  $^{137}\text{Cs}$  (Santschi *et al.* 1999) in consideration of the average annual rainfall in the Nueces River basin ( $57 \text{ cm yr}^{-1}$ ); the  $^{137}\text{Cs}$  fallout value was also decay corrected to 2003. These expected values are only an approximation of what might be expected to accumulate on the earth's surface through dry and wet deposition alone. The  $^{137}\text{Cs}$  values are well below the expected fallout inventory, which is not surprising considering that the full depth of the profile was not resolved in most cores and also that the location of these cores are in saline waters, which leads to greater

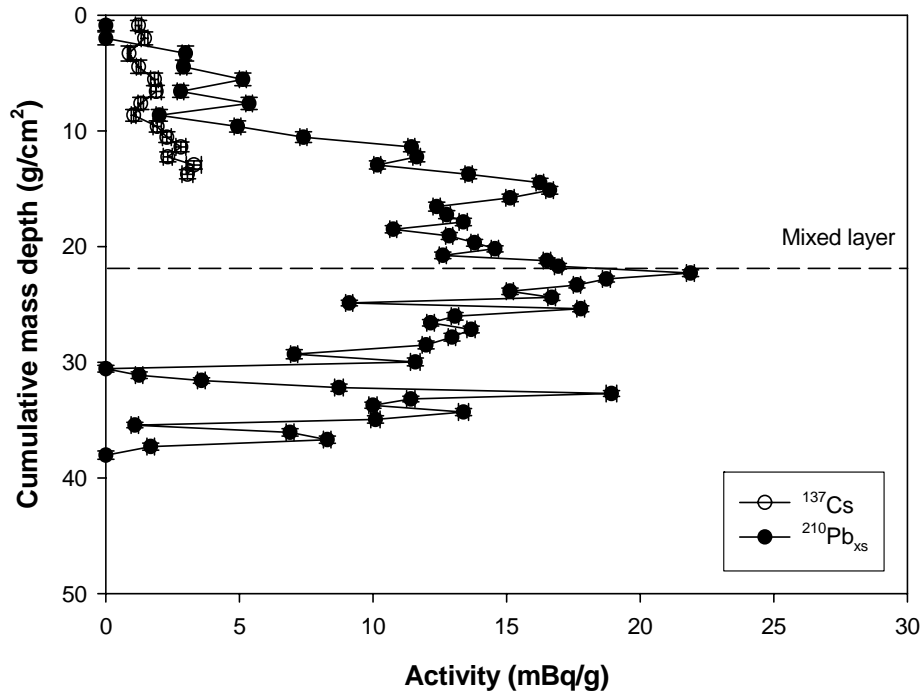


Figure 27: Fallout radionuclide ( $^{137}\text{Cs}$ ,  $^{210}\text{Pb}_{\text{xs}}$ ) profiles for Nueces Bay core 2.

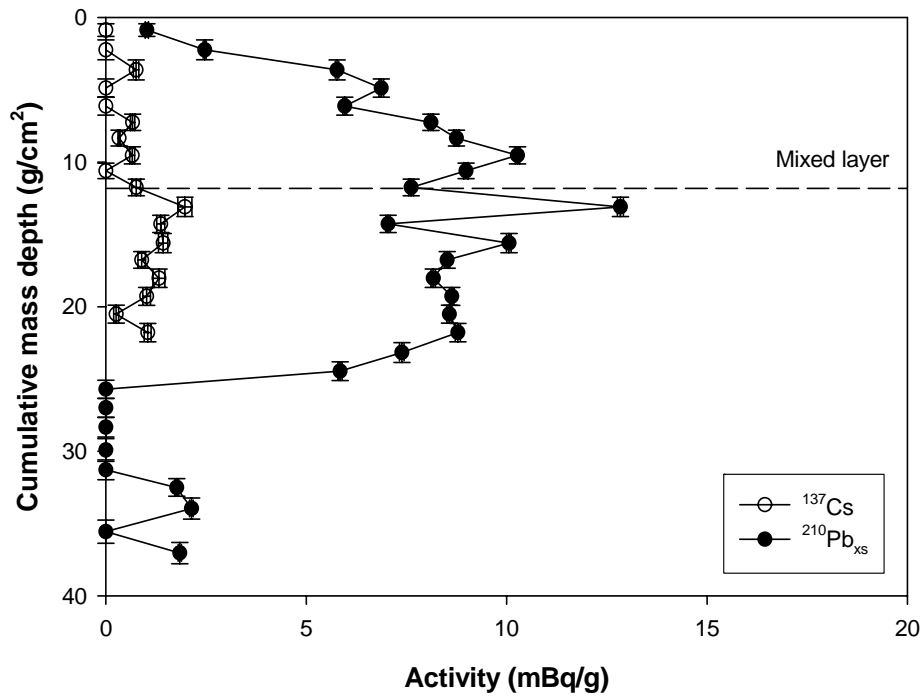


Figure 28: Fallout radionuclide ( $^{137}\text{Cs}$ ,  $^{210}\text{Pb}_{\text{xs}}$ ) profiles for Nueces Bay core 3.

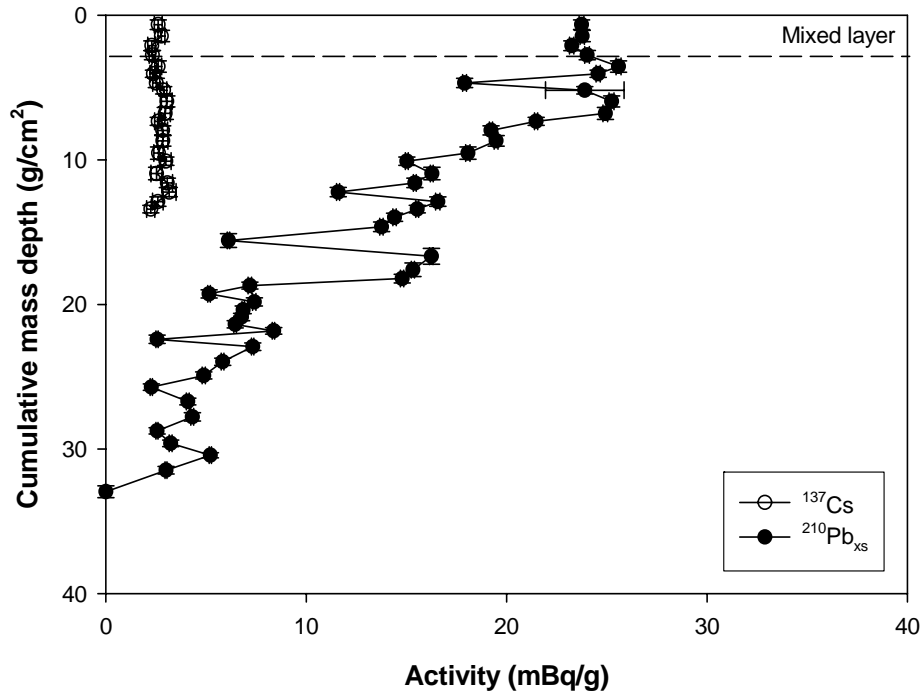


Figure 29: Fallout radionuclide ( $^{137}\text{Cs}$ ,  $^{210}\text{Pb}_{\text{xs}}$ ) profiles for Corpus Christi Bay core 1.

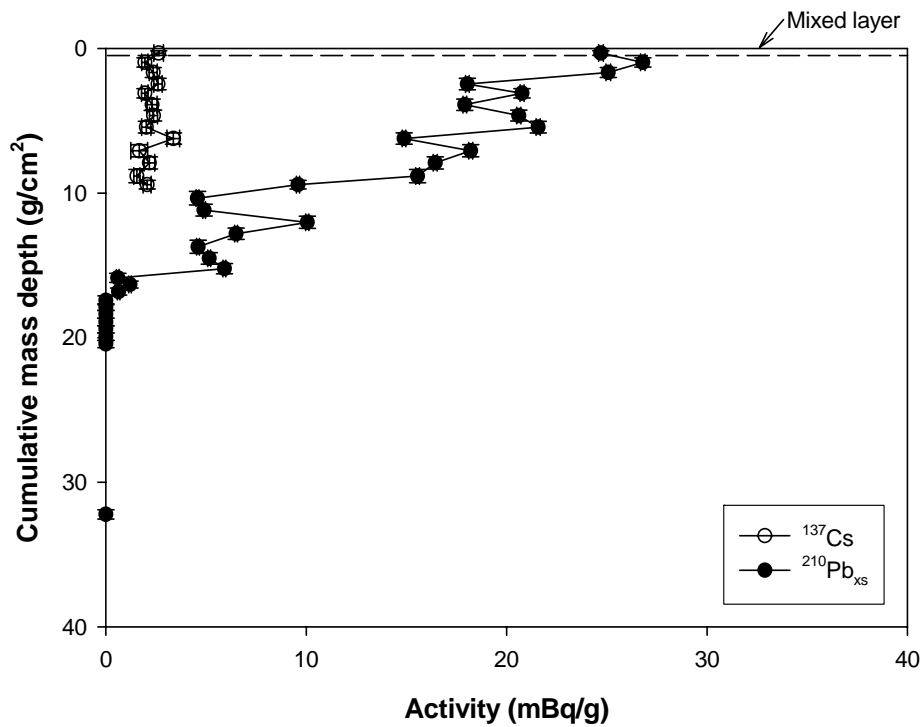


Figure 30: Fallout radionuclide ( $^{137}\text{Cs}$ ,  $^{210}\text{Pb}_{\text{xs}}$ ) profiles for Corpus Christi Bay core 2.

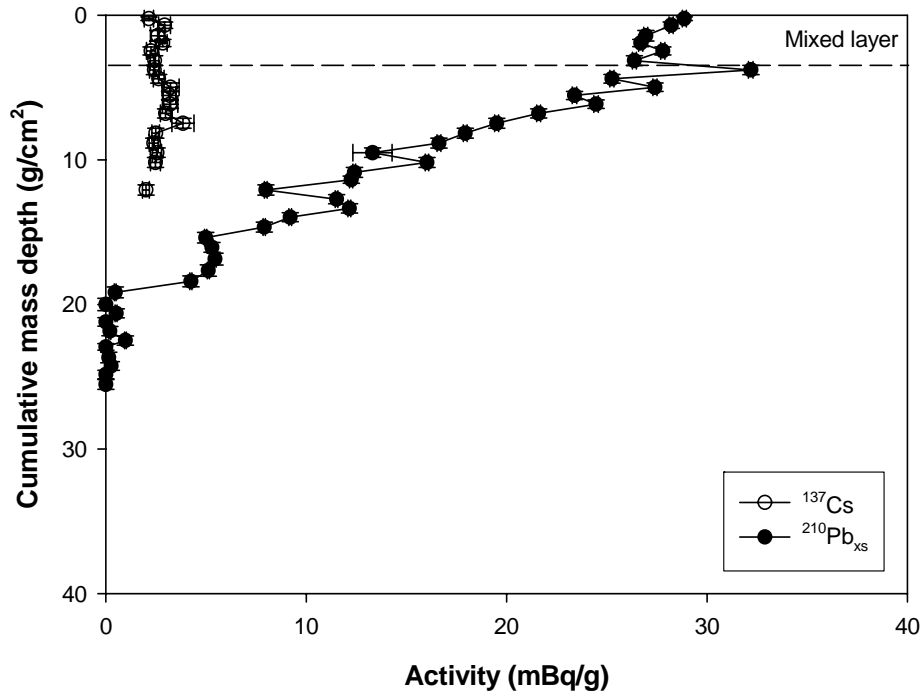


Figure 31: Fallout radionuclide (<sup>137</sup>Cs, <sup>210</sup>Pb<sub>xs</sub>) profiles for Corpus Christi Bay core 3.

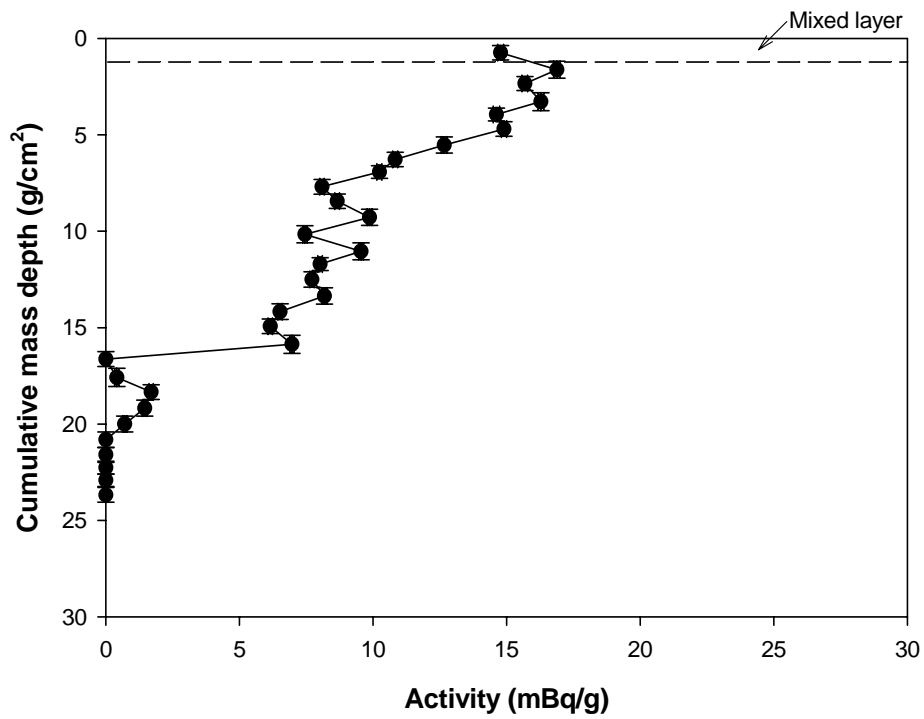


Figure 32: <sup>210</sup>Pb<sub>xs</sub> profile for Corpus Christi Bay core 4.

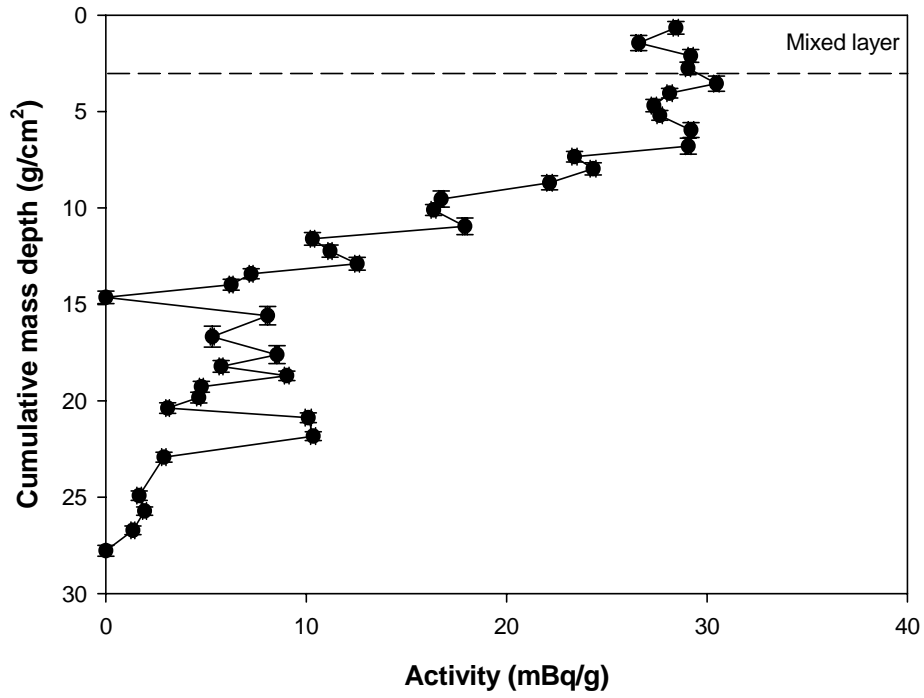


Figure 33:  $^{210}\text{Pb}_{\text{xs}}$  profile for Corpus Christi Bay core 5.

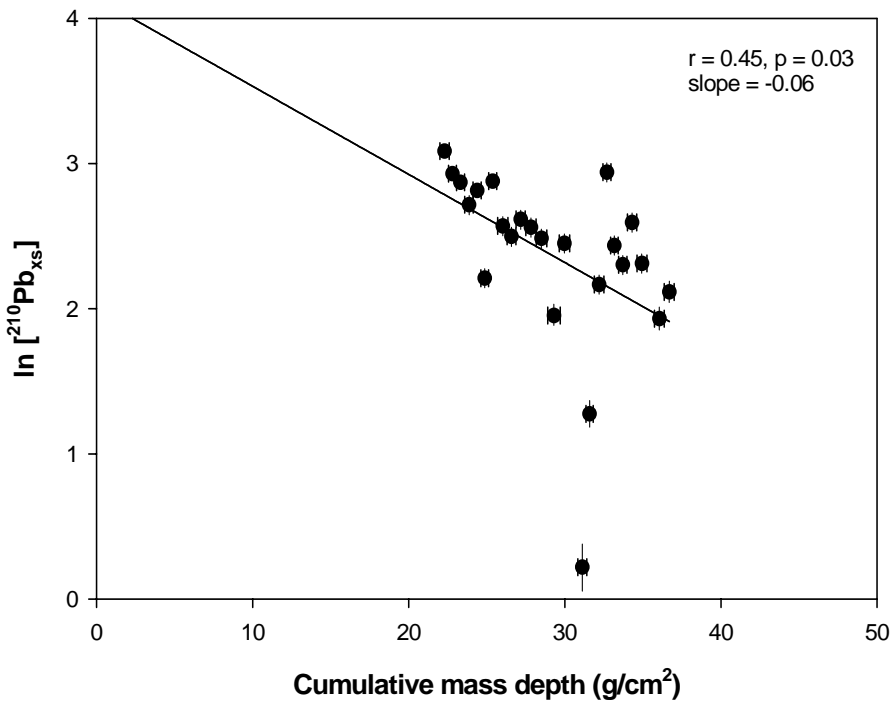


Figure 34: Semi-log plot of  $^{210}\text{Pb}_{\text{xs}}$  data for Nueces Bay core 2.

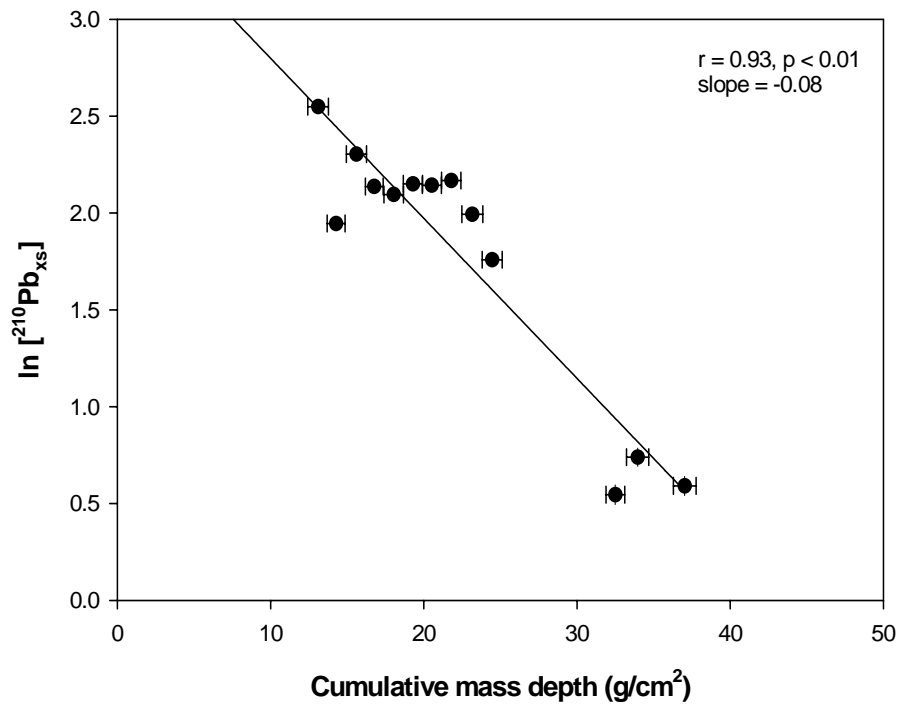


Figure 35: Semi-log plot of  $^{210}\text{Pb}_{\text{xs}}$  data for Nueces Bay core 3.

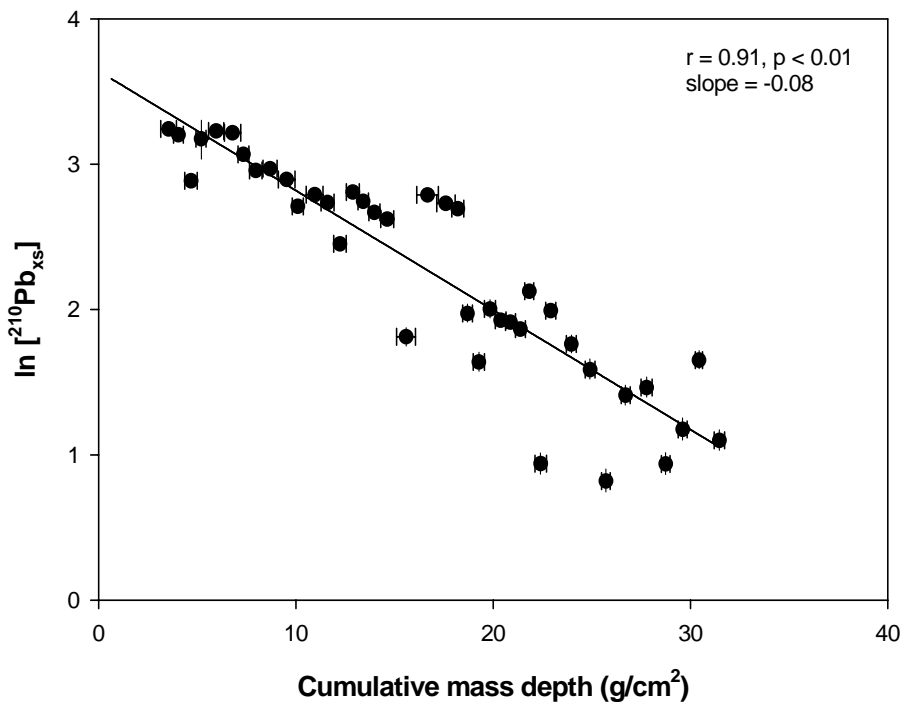


Figure 36: Semi-log plot of  $^{210}\text{Pb}_{\text{xs}}$  data for Corpus Christi Bay core 1.

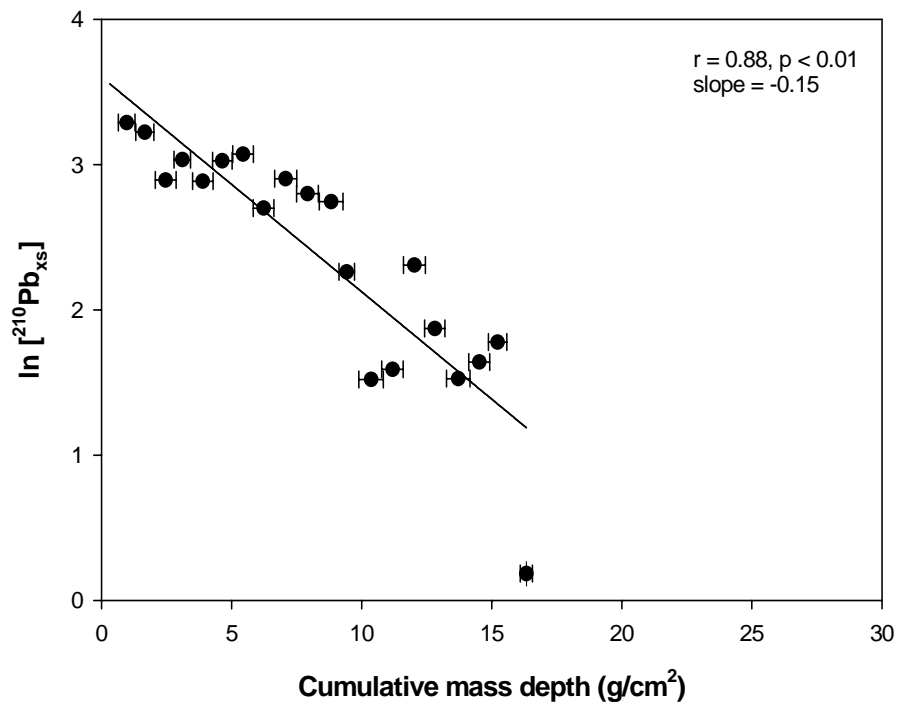


Figure 37: Semi-log plot of  $^{210}\text{Pb}_{\text{xs}}$  data for Corpus Christi Bay core 2.

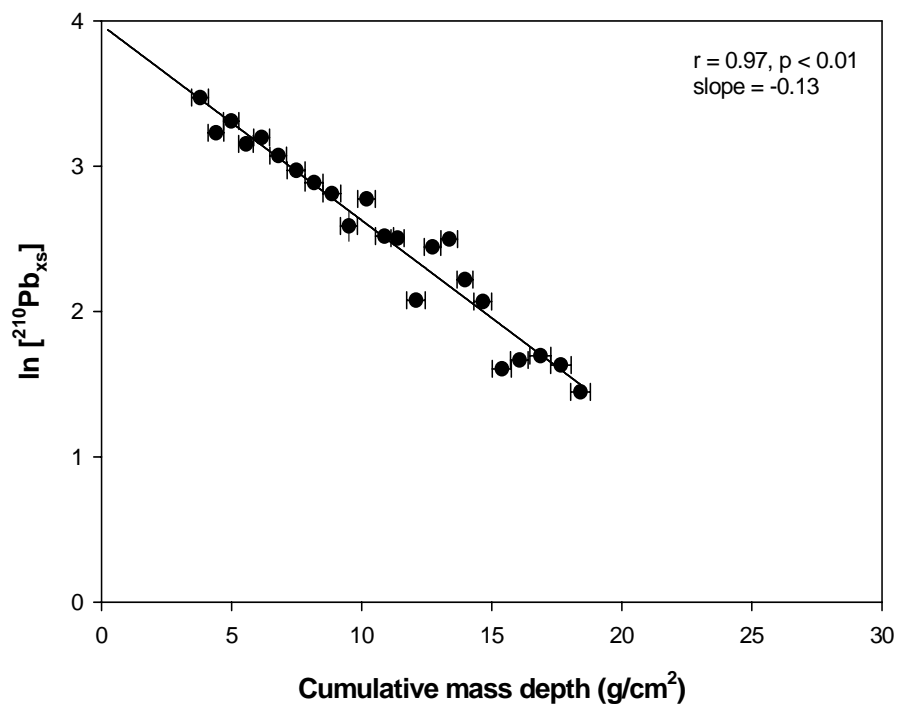


Figure 38: Semi-log plot of  $^{210}\text{Pb}_{\text{xs}}$  data for Corpus Christi Bay core 3.

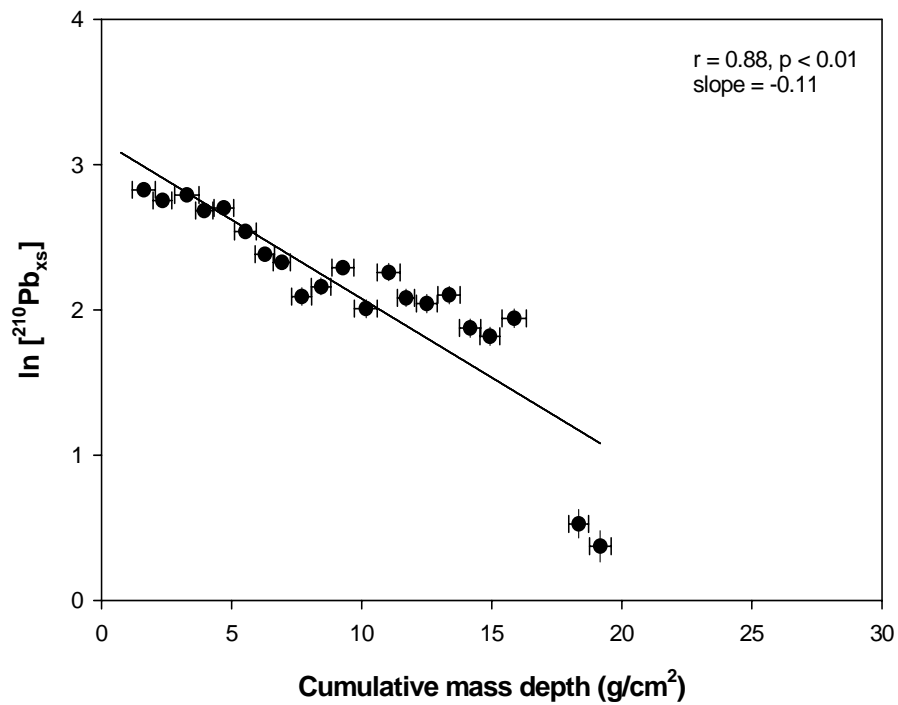


Figure 39: Semi-log plot of  $^{210}\text{Pb}_{\text{xs}}$  data for Corpus Christi Bay core 4.

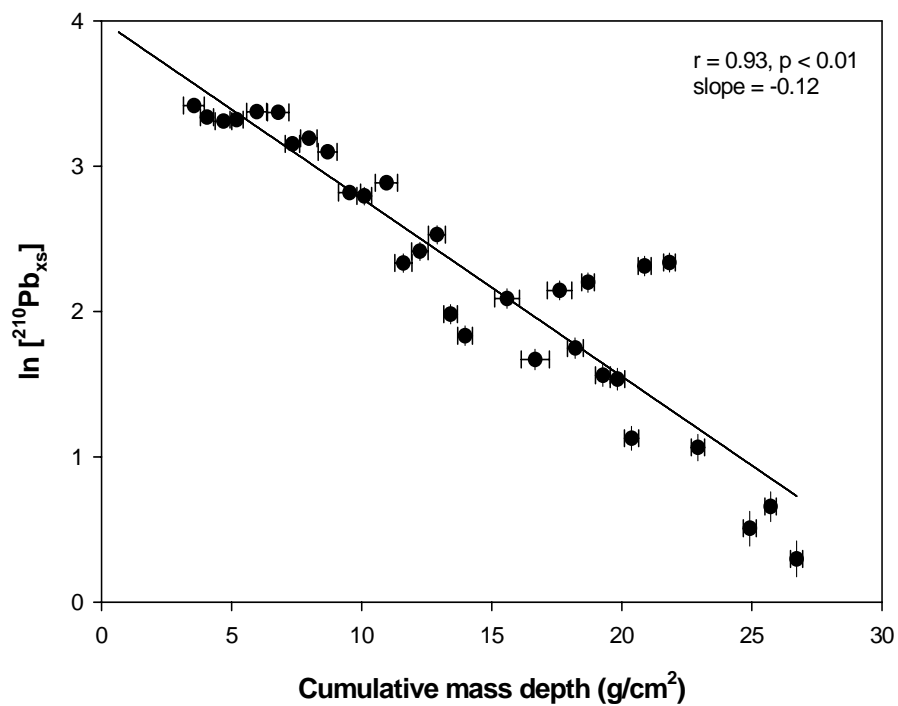


Figure 40: Semi-log plot of  $^{210}\text{Pb}_{\text{xs}}$  data for Corpus Christi Bay core 5.

desorption losses of  $^{137}\text{Cs}$  (e.g., Santschi *et al.* 2001a,b) than in the landward delta region (see Table 5 and related discussion).  $^{210}\text{Pb}_{\text{xs}}$  inventories are in most cases equal to or greater than the expected fallout inventory.

The interpretation of sediment supply to this estuary system as dominated by terrestrial inputs, with little discernible input from marine sources, based on sediment grain size and discrete lithogenic isotope data is further supported by sedimentation accumulation rates for Nueces and Corpus Christi Bays when examined in spatial context. Mean sediment accumulation rates versus distance from the Nueces River mouth consistently and significantly decrease moving towards the GOM, implying that the Nueces River is the most significant source of sediment to the system and that sediment accumulation does not increase even with close proximity to the GOM, which would be expected if significant sediment was derived from marine sources here (Fig. 6, 41).

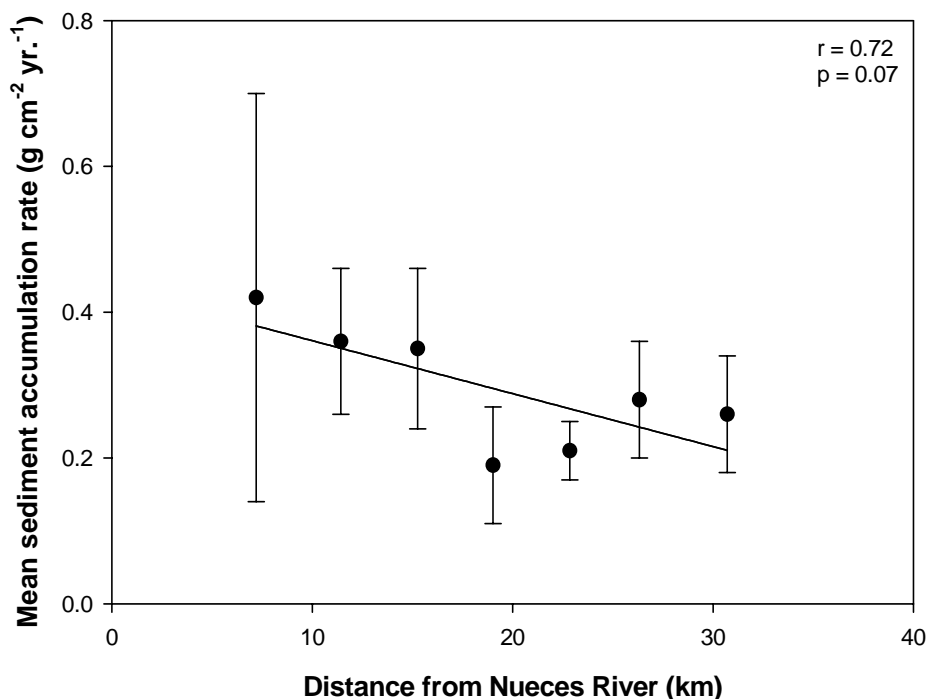


Figure 41: Mean sediment accumulation rate for each bay core versus distance from the Nueces River mouth.

## 5. CONCLUSIONS

### 5.1 Summary

This study sought to apply radiochemical and complimentary techniques to distinguish between terrestrial and marine sources of sediment to the greater Nueces-Corpus Christi Estuary in southwest Texas. An ancillary objective included the determination of sediment accumulation rates and mixing within the Nueces Delta and Nueces and Corpus Christi Bays. The study area included the lower parts of the Nueces River basin, Nueces Delta, Nueces-Corpus Christi Estuary, Gulf Intracoastal Waterway (GIW) and Gulf of Mexico (GOM). This region is appropriate for this research due to many and varied considerations, not least of which are the difficult and complex problems facing the region in the forms of increasing population, increased hydrologic management to meet increasing needs for freshwater resources and the delicate balance between these needs

and those presented by the regions natural systems, whose reliance on these same resources has put them at risk. Based on extensive field sampling of representative sediments and laboratory analyses, the principle findings of this research are summarized as follows:

1. While variability in surface sediment grain size distributions (sand:silt:clay) are observed, it is clear that the GOM sediments and those from the GIW are dominantly sands and conversely, those sediments from Corpus Christi Bay are dominantly clays. Sediments from both the Nueces Delta and Bay are similar to the terrestrial sediment types in that they have a more even distribution of the three size fractions. These data suggest that near shore oceanic sediments are sands derived predominantly from long shore transport in the littoral zone in association with the barrier island system. Similarly, GIW sands are likely sourced from a combination of long shore transport and wash over the barrier island system in association with high energy storm events and wave action. Bed load and suspended sediments sourced from a combination of the Nueces River inflow and ephemeral tributaries, particularly to the east of the estuary, provide sand and fines to the Nueces Delta and Bay, where the coarser size fractions are effectively retained, as reflected by the size distributions of sediments from those areas. These data suggest that marine sediment sources from the GOM or GIW do not provide a significant amount of sediment to the estuary system.
2. Lithogenic isotope ratios determined in surface sediments throughout the system are very similar and not statistically distinguishable. This is true for both small (discrete terrestrial or marine compartments) and large scale (terrestrial versus estuarine versus marine compartments) sample populations. Consequently, a numeric approach to discerning the importance of each of the two large scale sediment source areas (terrestrial and marine) to sediments within Nueces and Corpus Christi Bays is not possible here.
3. A stepwise, graphical examination of discrete lithogenic isotope signatures for surface sediments shows considerably more promise. Plots of sediment source compartment and bay sediment means for  $^{226}\text{Ra}$  versus  $^{232}\text{Th}$ ,  $^{226}\text{Ra}$  versus  $^{230}\text{Th}$  and  $^{228}\text{Ra}$  versus  $^{232}\text{Th}$  clearly show that terrestrial and marine sediment source components have significantly different signatures, even when consisting of mostly sands, and that sediment deposited in Nueces and Corpus Christi Bays are indistinguishable from the terrestrial component, suggesting they are composed mostly of sediment derived from terrestrial sources. Important supporting evidence is provided by the particle-bound thorium isotopes. Plots of  $^{230}\text{Th}$  versus  $^{232}\text{Th}$ ,  $^{228}\text{Th}$  versus  $^{232}\text{Th}$  and  $^{228}\text{Th}$  versus  $^{230}\text{Th}$  depict the same scenario. The fact that both Ra/Th and Th/Th isotopic data are in unanimous agreement, suggests that these isotopic signatures are reflective of differences in the sediment source compartments themselves and not a function of geochemical processes which are known to affect the elements considered in starkly contrasting ways.
4. The influence of upper basin geology on isotope ratio signatures does appear. Examination of alluvial sediment signatures of  $^{226}\text{Ra}/^{232}\text{Th}$ ,  $^{230}\text{Th}/^{232}\text{Th}$  and  $^{226}\text{Ra}/^{228}\text{Ra}$  all show consistent change moving inland, a likely effect of proximity to the uranium rich rocks of the upper coastal plain of Texas (e.g., the Catahoula Fm.), where lithogenic isotopic signatures would be expected to contrast with those derived from other rocks of the coastal plain.
5. Nueces Delta sediment cores were composed of predominantly fine grained sediments throughout (silts and clays), with the exception of cores 1 and 2, which had a considerable sand fraction, particularly in the upper region of the cores. The sediment accumulation rates determined by  $^{137}\text{Cs}$  and  $^{210}\text{Pb}_{\text{xs}}$  are in close agreement and are well within the range of those presented for the Nueces Delta by other researchers. A subtle gradient in sediment accumulation across the delta is evident, with rates that are generally lower in the west and progressively higher moving east. This is likely a reflection of contrasts in land use and topography on either side of the Nueces Delta here. The western side has a comparatively subdued topography and is dominated by industrial and residential land uses whereas the eastern border of the delta is delineated by a sharp bluff line, with mixed agricultural land at its summit.

6. The Nueces Bay sediment cores differ from those collected in Corpus Christi Bay in two ways; 1) sands comprise a larger percentage of their composition, particularly over the first 10 – 20 cm, and 2) they are mixed over greater depth. These differences are most likely attributable to geographic and physiographic effects, 1) proximity of Nueces Bay to the Nueces River and terrestrial sources of sandy sediment and 2) Nueces Bay, being shallower and in direct communication with the Nueces River, is more easily mixed by physical processes (wind, high river discharge, etc.) as compared to Corpus Christi Bay. Sediment accumulation rates determined by  $^{137}\text{Cs}$  and  $^{210}\text{Pb}_{\text{xs}}$  are in close agreement and when plotted versus distance from the Nueces River mouth consistently and significantly decrease moving towards the GOM, implying that the Nueces River is the most significant source of sediment to the system and that sediment accumulation does not increase even with close proximity to the GOM, which would be expected if significant sediment was derived from marine sources here.

Our overall interpretation of sediment supply to this estuary system as dominated by terrestrial inputs, with little discernible input from marine sources, is based on three complimentary sets of data, 1) sediment grain size distributions, 2) discrete lithogenic isotope data (both Ra/Th and Th/Th) and 3) sediment accumulation rates for Nueces and Corpus Christi Bays when examined in spatial context. Marine sources of sediment are often important in estuaries that have wide, un-obstructed openings to the sea, experience significant tidal variation or are well mixed due to a combination of significant tidal variation, wind action and the influence of shelf or open ocean currents. The Nueces-Corpus Christi Estuary, in contrast, can be characterized as micro-tidal, has an extensive barrier island system armoring and restricting communication with the GOM and is not significantly affected by shelf or open ocean currents. Based on these considerations, the evidence suggests that marine sources of sediment to this estuary are insignificant.

## 5.2 Recommendations

The vitality and sustainability of Texas coastal ecosystems is dependent upon many variables, not least of which is freshwater supply. This system has been heavily impacted by hydrologic management and much research has been published regarding the impacts of this management, which has been deleterious in most cases. Formulation of a management plan that will assure an adequate freshwater supply to this and other Texas estuaries is our foremost recommendation. Adequate sediment supply, particularly to a system where essentially all of the sediment is derived from terrestrial sources, is dependent upon freshwater inflow, in this case, from the Nueces River. Specific recommendations formulated from the results of this work include the following:

1. Support for additional research in this and related systems, focused principally on the development of new methodologies and applications of existing methodologies to accurately determine sources of sediment and the overall sediment budget. This information is essential in formulating a plan to arrest, or at least mitigate loss of coastline by erosion as well as in determining sources and fates of particle-associated contaminants.
2. Investigate the relative quantities of sediment supplied to the Nueces Delta from lateral sources. Contrasts in land usage as well as physiographic variables can be important in predicting where high rates of erosion will develop or continue. These data are essential in formulating management practices to mitigate such losses.
3. Support research that addresses the importance of sediment resuspension in Texas estuaries. These data are essential for estimating the inputs and outputs of sediment, the role of physical mixing in contaminant bio-availability and impacts on commercially important fish and shellfish populations.

## 6. REFERENCES

- Ames, L.L., McGarrah, J.E. and Walker, B.A., 1983. Sorption of trace constituents from aqueous solutions onto secondary minerals II: Radium, Clays and Clay Minerals, 31, 335-342.
- Baskaran, M., and Santschi, P.H., 1993. The role of particles and colloids in the transport of radionuclides in coastal environments of Texas, *Marine Chemistry*, 43: 95-114.
- Baskaran, M., Coleman, C.H. and Santschi, P.H., 1993. Atmospheric depositional fluxes of  $^7\text{Be}$  and  $^{210}\text{Pb}$  at Galveston and College Station, Texas, *Journal of Geophysical Research* 98 (D11), 20,555-20,571.
- Benoit, G., Rozan, T.F., Patton, P.C., Arnold, C.L., 1999. Trace metals and radionuclides reveal sediment sources and accumulation rates in Jordan Cove, Connecticut, *Estuaries* 22 (1), 65-80.
- Binford, M.W., 1990. Calculation and uncertainty analysis of  $^{210}\text{Pb}$  dates for PIRLA project lake sediment cores, *Journal of Paleolimnology* 3, 253-267.
- Brock, D.A., 2001. Nitrogen Budget for Low and High Freshwater Inflows, Nueces Estuary, Texas, *Estuaries* 24 (4), 509-521.
- Brown, L.F. Jr., Morton, R.A., McGowen, J.H., Kreitler C.W. and Fisher, W.L., 1974. Natural hazards of the Texas coastal zone, Bureau of Economic Geology, University of Texas at Austin, Austin, TX, 13p.
- Buckner, H.D., Carrillo, E.R. and Davidson, H.D., 1986. Water resources data, Texas: water year 1985, vol. 3, Colorado River Basin, Lavaca River Basin, Guadalupe River Basin, Nueces River Basin, Rio Grande Basin and intervening basins, U.S. Geological Survey Water-Data Report TX-85-3, 447p.
- Buesseler, K.O., Cochran, J.K., Bacon, M.P., Livingston, H.D., Casso, S.A., Hirschberg, D., Hartman, M.C. and Fler, A.P., 1992. Determination of thorium isotopes in seawater by non-destructive and radiochemical procedures. *Deep Sea Research* 39, 1103-1114.
- Cooper, J.A.G., 2001. Geomorphological variability among microtidal estuaries from the wave-dominated South African coast, *Geomorphology* 40, 99-122.
- Craft, C.B. and Richardson, C.J., 1993. Peat accretion and N, P, and organic accumulation in nutrient-enriched and unenriched Everglades peatlands, *Journal of Applied Ecology* 3, 446-458.
- Curtis, W.F., Culbertson, J.K. and Chase, E.B., 1973. Fluvial sediment discharge to the oceans from the conterminous United States: U.S. Geological Survey Circular 670, 17p.
- Elsinger, R.J. and Moore, W.S., 1984.  $^{226}\text{Ra}$  and  $^{228}\text{Ra}$  in the mixing zone of the Pee Dee River-Winyah Bay, Yangtze River and Delaware Bay estuaries. *Estuarine, Coastal and Shelf Science* 18, 601-613.
- Eyre, B., Hossain, S. and McKee, L., 1998. A suspended sediment budget for the modified subtropical Brisbane River Estuary, Australia, *Estuarine, Coastal and Shelf Science* 47, 513-522.
- Folk, R.L., 1965. *Petrology of Sedimentary Rocks*, Hemphill Publishing Company, Austin, TX, 178 p.
- Galloway, W.E., 1977. Catahoula Formation of the Texas Coastal Plain: depositional systems, composition, structural development, groundwater flow history, and uranium distribution. Bureau of Economic Geology, University of Texas, Austin, Report Investigation No. 87.
- Hallstadius, L., 1984. A Method for the Electrodeposition of Actinides. *Nuclear Instruments and Methods in Physics Research* 223, Section A, 266-267.
- Hancock, G.J., 2000. Identifying resuspended sediment in an estuary using the  $^{228}\text{Th}/^{232}\text{Th}$  activity ratio: the fate of lagoon sediment in the Bega River estuary, Australia. *Marine and Freshwater Research* 51, 659-667.
- He, Q. and Owens, P., 1995. Determination of suspended sediment provenance using caesium-137, unsupported lead-210 and radium-226: A numerical mixing model approach, in *Sediment and Water Quality in River Catchments*, edited by A. Gurnell, B. Webb, and I. Foster, pp. 207-227, John Wiley & Sons, New York.
- Hobday, D.K. and Galloway, W.E., 1999. Groundwater processes acid sedimentary uranium deposits. *Journal of Hydrogeology* 7(1), 127-138.
- Huntley, S.L., Wenning, R.J., Su, S.H., Bonnevie, N.L., Paustenbach, D.J., 1995. Geochronology and Sedimentology of the Lower Passaic River, New Jersey, *Estuaries* 18 (2), 351-361.
- Ivanovich, M. and Harmon, R.S., 1982. *Uranium Series Disequilibrium: Applications to Environmental Problems*, 571 pp., Clarendon Press, Oxford, UK.

- Ivanovich, M. and Harmon, R.S., 1992. Uranium-Series Disequilibrium: Applications to Earth, Marine, and Environmental Sciences, 910 pp., Clarendon Press, Oxford, UK.
- Jenkins, P.A., Duck, R.W., Rowan, J.S. and Walden, J., 2002. Fingerprinting of bed sediment in the Tay Estuary, Scotland: an environmental magnetism approach, *Hydrology and Earth System Sciences* 6(6), 1007-1016.
- Kaufman, A., 1969. Thorium-232 concentration of surface ocean water, *Geochimica et Cosmochimica Acta* 33, 717-724.
- Kendall, C. and McDonnell, J.J. (Eds.), 1998. *Isotope Tracers in Catchment Hydrology*, 872 pp., Elsevier, New York, NY, USA.
- Key, R.M., Stallard, R.F., Moore, W.S. and Sarmiento, J.L., 1985. Distribution and flux of Ra-226 and Ra-228 in the Amazon River Estuary, *Journal of Geophysical Research* 90, 6995-7004.
- Leibbrand, N.F., 1987. Estimated sediment deposition in Lake Corpus Christi, Texas, 1977-1985, U.S. Geological Survey Open File Report 87-239, 26p.
- Li, Y.H., Mathieu, G.G., Biscaye, P. and Simpson, H.J., 1977. The flux of Ra-226 from estuarine and continental shelf sediments, *Earth and Planetary Science Letters* 37, 237-241.
- Longley, W.L. (Ed.), 1994. Freshwater inflows to Texas bays and estuaries: ecological relationships and methods for determination of needs. Texas Water Development Board and Texas Parks and Wildlife Department, Austin, TX, 386p.
- Megumi, K., Oka, T., Yaskawa, K. and Sakanoue, M., 1982. Contents of natural radioactive nuclides in soil in relation to their surface area, *Journal of Geophysical Research* 87, 10,857-10,860.
- Morton, R.A. and Paine, J.G., 1984. Historical shoreline changes in Corpus Christi, Oso, and Nueces bays, Texas Gulf coast, Geological Circular 84-6, Bureau of Economic Geology, University of Texas at Austin, Austin, TX, 66 p.
- Murray, A.S., Caitcheon, G., Olley, J. and Crockford, H., 1990. Methods for Determining the Sources of Sediments Reaching Reservoirs: Targeting Soil Conservation, *Ancold Bulletin* 85, 61-70.
- Murray, A.S., Olley, J.M. and Wallbrink, P.J., 1991. Radionuclides for analysis of sediments in water supply catchments, Rep. 91/8, 35 pp., Commonwealth Scientific and Industrial Research Organization (CSIRO), Canberra, Australia.
- Oktay, S.D., Santschi, P.H., Moran, J.E. and Sharma, P., 2000. The <sup>129</sup>Iodine bomb pulse recorded in Mississippi River Delta sediments: results from isotopes of I, Pu, Cs, Pb and C, *Geochimica et Cosmochimica Acta* 64 (6), 989-996.
- Olley, J.M., Murray, A.S., Mackenzie, D.H. and Edwards, K., 1993. Identifying Sediment Sources in a Gullied Catchment Using Natural and Anthropogenic Radioactivity, *Water Resources Research* 29(4), 1037-1043.
- Olley, J. M. and Murray, A.S., 1994. Origins of the variability in the <sup>230</sup>Th/<sup>232</sup>Th ratio in sediments, in *Variability in Stream Erosion and Sediment Transport*, edited by L. J. Olive, R.J. Loughran and J.A. Kesby, IAHS publication 224, 65-70.
- Olley, J.M., Roberts, R.G. and Murray, A.S., 1997. A novel method for determining residence times of river and lake sediments based on disequilibrium in the thorium decay series, *Water Resources Research* 33(6), 1319-1326.
- Paola, C.G., Parker, R., Seal, R., Sinha, S.K., Southard, J.B. and Wilcock, P.R., 1992. Downstream fining by selective deposition in a laboratory flume, *Science* 258, 1757-1760.
- Ratzlaff, K.W., 1980. Land surface subsidence in the Texas coastal region, U.S. Geological Survey, Open-File Report 80-969, 19p.
- Ravichandran, M., Baskaran, M., Santschi, P.H. and Bianchi, T.S., 1995a. Geochronology of sediments of Sabine-Neches Estuary, Texas, *Chemical Geology* 125, 291-306.
- Ravichandran, M., Baskaran, M., Santschi, P.H. and Bianchi, T.S., 1995b. History of trace metal pollution in Sabine-Neches Estuary, Texas. *Environmental Science and Technology* 29, 1495-1503.

- Riese, A.C., 1982. Adsorption of Radium and Thorium onto Quartz and Kaolinite: A Comparison of Solution/Surface Equilibria Models, Ph.D. Dissertation, Colorado School of Mines, Golden, CO, USA.
- Roberts, H. M. and Plater, A.J., 1999. U-and Th-series disequilibria in coastal infill sediments from Praia da Rocha (Algarve Region, Portugal): a contribution to the study of late Quaternary weathering and erosion, *Geomorphology* 26, 223-238.
- Robbins, J.A., 1978. Geochemical and geophysical applications of radioactive lead. In: Nriagu, J.O. (Ed.) *The biogeochemistry of lead in the environment*, Elsevier, 285-393.
- Santschi, P.H., Li, Y.H., Bell, J., Trier, R.M., Kawtaluk, K., 1980. Plutonium in the coastal marine environment. *Earth and Planetary Science Letters* 51, 248-265.
- Santschi, P.H., Allison, M., Asbill, S., Perlet, A.B., Cappellino, S., Dobbs, C., McShea, L., 1999. Sediment transport and Hg recovery in Lavaca Bay, as evaluated from radionuclide and Hg distributions. *Environmental Science and Technology* 33, 378-391.
- Santschi, P.H., Guo, L., Asbill, S., Allison, M., Kepple, A.B. and Wen, L.W., 2001a. Accumulation rates and sources of sediments and organic carbon on the Palos Verde shelf based on radioisotope tracers ( $^{137}\text{Cs}$ ,  $^{239,240}\text{Pu}$ ,  $^{210}\text{Pb}$ ,  $^{234}\text{Th}$ ,  $^{238}\text{U}$  and  $^{14}\text{C}$ ), *Marine Chemistry* 73, 125-152.
- Santschi, P.H., Presley, B.J., Wade, T.L., Garcia-Romero, B. and Baskaran, M., 2001b. Historical contamination of PAHs, PCBs, DDTs, and heavy metals in Mississippi River Delta, Galveston Bay and Tampa Bay sediment cores, *Marine Environmental Research* 52, 51-79.
- Tanner, A.B., 1964. Physical and chemical controls on distribution of Radium-226 and radon-222 in ground water near Great Salt Lake, Utah, *Natural Radiation Environment*, in Proc. Int. Symp. Houston, 1963, edited by J.S. Adams and W.M. Lowder, University of Chicago Press, Chicago, IL, USA, 253-276 pp.
- Texas Water Development Board (TWDB), 1997. *Water for Texas: A Consensus-Based Update to the State Water Plan. Volume II*, Texas Water Development Board, Austin, Texas.
- Valero-Garces, B., Navas, A., Machin, J., Walling, D., 1999. Sediment sources and siltation in mountain reservoirs: a case study from the Central Spanish Pyrenees, *Geomorphology* 28, 23-41.
- Walker, H.J. and Coleman, J.M., 1987. Atlantic and Gulf Coastal Province, in Graf, W.L. (ed.) *Geomorphic Systems of North America: Boulder, Colorado*, Geological Society of America, Centennial Special Volume 2.
- Walsh, J.P. and Nittrouer, C.A., 2003. Contrasting styles of off-shelf sediment accumulation in New Guinea, *Marine Geology* 196, 105-125.
- Webster, I. T., Hancock, G.J. and Murray, A.S., 1995. Modelling the effect of salinity on radium desorption from sediments, *Geochimica et Cosmochimica Acta* 59(12), 2469-2476.
- White, W.A. and Calnan, T.R., 1990a. Sedimentation in fluvial-deltaic wetlands and estuarine areas, Texas Gulf coast: literature synthesis, Report to Texas Parks and Wildlife Department by the Bureau of Economic Geology, University of Texas at Austin, Austin, TX, 260 p.
- White, W.A. and Calnan, T.R., 1990b. Sedimentation and historical changes in fluvial-deltaic wetlands along the Texas Gulf coast with emphasis on the Colorado and Trinity River deltas, Report to the Texas Wildlife Department by Bureau of Economic Geology, University of Texas at Austin, Austin, TX, 124p.
- White, W.A., Morton, R.A. and Holmes, C.W., 2002. A comparison of factors controlling sedimentation rates and wetland loss in fluvial-deltaic systems, Texas Gulf coast, *Geomorphology*, vol. 44, p. 47-66.
- Winkels, H., Kroonenberg, S., Lychagin, M., Marin, G., Rusakov, G., Kasimov, N., 1998. Geochronology of priority pollutants in sedimentation zones of the Volga and Danube delta in comparison with the Rhine delta, *Applied Geochemistry* 13(5), 581-591.
- Yeager, K.M., Santschi, P.H., Phillips, J.D. and Herbert, B.E., 2002. Sources of alluvium in a coastal plain stream based on radionuclide signatures from the  $^{238}\text{U}$  and  $^{232}\text{Th}$  decay series, *Water Resources Research*, vol. 38, no. 11, p. 24-1 - 24-11.
- Yeager, K.M. and Santschi, P.H., 2003. Invariance of isotope ratios of lithogenic radionuclides: more evidence for their use as sediment source tracers. *Journal of Environmental Radioactivity*, vol. 69, p. 159-176.
- Yeager, K.M., Santschi, P.H., Phillips, J.D. and Herbert, B.E., 2004 (in press) Suspended sediment sources and tributary effects in the lower reaches of a coastal plain stream as indicated by radionuclides, Loco Bayou, Texas. *Environmental Geology*.

## **7. ACKNOWLEDGMENTS**

The following individuals contributed to this project by assisting in field work, laboratory work and/or by providing technical advice or support. Their contributions are greatly appreciated.

Dr. David Brock, TWDB, Austin

Ms. Kimberly Schindler, Texas A&M University at Galveston, Department of Ocean and Coastal Resources

Mr. Michael Andres, Texas A&M University at Galveston, Department of Marine Biology

Ms. Erin Weaver, Texas A&M University at Galveston, Department of Ocean and Coastal Resources

Ms. Michelle Spinelli, Texas A&M University at Galveston, Department of Marine Science

Dr. Timothy Dellapenna, Texas A&M University at Galveston, Department of Marine Sciences

**APPENDIX I: Nueces Delta sediment cores physical and radiochemical data**

Table AI1: Summary physical and radiochemical data for Nueces Delta core 1.

Depth (cm)	Cumulative mass depth (g/cm <sup>2</sup> )	Porosity	Total <sup>210</sup> Pb (mBq/g)	<sup>137</sup> Cs (mBq/g)	<sup>210</sup> Pb <sub>xs</sub> (mBq/g)	% Sand	% Silt	% Clay
1	1.47	0.41	66.99 ± 0.09	5.00 ± 0.50	53.79 ± 0.10	45.3	34.5	20.2
2	2.57	0.56	49.86 ± 0.08	5.55 ± 0.53	36.67 ± 0.09	--	--	--
3	4.57	0.20	43.75 ± 0.08	6.49 ± 0.55	30.55 ± 0.09	49.0	29.5	21.5
4	5.76	0.52	37.18 ± 0.06	8.43 ± 0.83	23.99 ± 0.08	--	--	--
5	7.51	0.30	33.90 ± 0.06	9.03 ± 0.90	20.70 ± 0.08	47.3	29.5	23.2
6	8.86	0.46	31.76 ± 0.09	10.74 ± 0.92	18.57 ± 0.10	--	--	--
7	10.50	0.35	32.75 ± 0.07	9.83 ± 0.91	19.55 ± 0.09	29.5	34.9	35.6
8	12.23	0.31	31.11 ± 0.06	9.26 ± 0.86	17.92 ± 0.08	--	--	--
9	13.53	0.48	26.58 ± 0.08	6.92 ± 0.67	13.38 ± 0.10	17.1	42.0	40.9
10	15.37	0.26	27.31 ± 0.06	4.68 ± 0.42	14.11 ± 0.08	--	--	--
11	16.66	0.49	24.29 ± 0.05	3.01 ± 0.28	11.10 ± 0.08	12.5	41.1	46.4
12	17.78	0.55	27.23 ± 0.07	0	14.03 ± 0.09	--	--	--
13	19.32	0.38	25.62 ± 0.06	--	12.43 ± 0.08	11.0	38.4	50.6
14	20.98	0.34	23.44 ± 0.07	--	10.24 ± 0.09	--	--	--
15	22.31	0.47	20.79 ± 0.05	--	7.60 ± 0.07	9.3	42.1	48.6
16	23.98	0.33	21.24 ± 0.06	--	8.04 ± 0.08	--	--	--
17	25.66	0.33	24.41 ± 0.06	--	11.21 ± 0.08	8.9	41.5	49.6
18	27.37	0.32	25.24 ± 0.06	--	12.05 ± 0.08	--	--	--
19	29.08	0.32	23.08 ± 0.04	--	9.89 ± 0.07	8.7	41.5	49.8
20	30.38	0.48	14.14 ± 0.05	--	0.95 ± 0.07	--	--	--
21	31.94	0.38	--	--	--	8.6	35.9	55.5
22	33.57	0.35	--	--	--	--	--	--
23	35.03	0.41	--	--	--	9.3	34.5	56.2
24	36.53	0.40	--	--	--	--	--	--
25	37.88	0.46	--	--	--	9.6	34.7	55.7
25-27	40.81	0.41	--	--	--	9.6	33.0	57.4
27-29	43.73	0.42	--	--	--	11.4	35.5	53.1
29-31	46.80	0.39	--	--	--	12.6	35.7	51.7
41-43	64.19	0.45	13.20 ± 0.05	--	0	--	--	--

Table AI2: Summary physical and radiochemical data for Nueces Delta core 2.

Depth (cm)	Cumulative mass depth (g/cm <sup>2</sup> )	Porosity	Total <sup>210</sup> Pb (mBq/g)	<sup>137</sup> Cs (mBq/g)	<sup>210</sup> Pb <sub>xs</sub> (mBq/g)	% Sand	% Silt	% Clay
1	2.35	0.06	26.98 ± 0.06	1.85 ± 0.18	14.18 ± 0.08	57.3	34.2	8.5
2	4.28	0.23	23.63 ± 0.04	2.68 ± 0.25	10.82 ± 0.06	--	--	--
3	5.95	0.33	25.23 ± 0.05	2.80 ± 0.26	12.43 ± 0.07	60.4	30.5	9.2
4	7.65	0.32	23.88 ± 0.04	1.91 ± 0.20	11.08 ± 0.06	--	--	--
5	9.58	0.23	19.83 ± 0.04	1.79 ± 0.17	7.03 ± 0.06	80.8	9.5	9.8
6	11.60	0.19	27.70 ± 0.04	2.82 ± 0.23	14.90 ± 0.06	--	--	--
7	13.39	0.28	30.40 ± 0.07	5.56 ± 0.48	17.60 ± 0.08	65.2	17.9	16.9
8	14.91	0.39	26.71 ± 0.05	3.47 ± 0.29	13.91 ± 0.06	--	--	--
9	17.33	0.03	27.05 ± 0.04	4.92 ± 0.42	14.25 ± 0.06	67.8	16.6	15.6
10	18.66	0.47	25.28 ± 0.04	6.43 ± 0.55	12.48 ± 0.06	--	--	--
11	21.17	0.00	26.26 ± 0.05	5.04 ± 0.46	13.46 ± 0.07	52.6	21.1	26.3
12	23.04	0.25	23.99 ± 0.05	2.39 ± 0.22	11.19 ± 0.07	--	--	--
13	24.40	0.46	22.92 ± 0.04	0	10.12 ± 0.06	24.0	28.8	47.1
14	25.65	0.50	24.09 ± 0.04	--	11.29 ± 0.06	--	--	--
15	27.39	0.30	23.78 ± 0.04	--	10.98 ± 0.06	21.5	29.6	48.9
16	28.87	0.41	26.21 ± 0.07	--	13.41 ± 0.09	--	--	--
17	30.27	0.44	14.89 ± 0.05	--	2.09 ± 0.06	19.6	30.7	49.7
18	31.99	0.31	24.01 ± 0.06	--	11.21 ± 0.07	--	--	--
19	34.04	0.18	22.34 ± 0.07	--	9.54 ± 0.08	21.4	31.5	47.0
20	35.33	0.48	26.32 ± 0.05	--	13.52 ± 0.06	--	--	--
21	37.50	0.13	15.20 ± 0.05	--	2.40 ± 0.07	21.4	35.3	43.4
22	39.26	0.30	14.57 ± 0.05	--	1.77 ± 0.07	--	--	--
23	40.87	0.36	15.02 ± 0.05	--	2.22 ± 0.07	22.6	40.6	36.7
24	42.43	0.38	12.34 ± 0.04	--	0	--	--	--
25	44.27	0.26	12.80 ± 0.04	--	0	19.7	32.4	47.9
25-27	47.82	0.29	--	--	--	17.3	32.4	50.2
27-29	51.15	0.33	--	--	--	18.4	50.1	31.4
29-31	54.18	0.39	--	--	--	19.6	71.1	9.3
31-33	57.70	0.29	--	--	--	--	--	--
33-34.5	60.64	0.22	--	--	--	--	--	--
34.5-37.5	63.80	0.58	--	--	--	--	--	--

Table AI3: Summary physical and radiochemical data for Nueces Delta core 3.

Depth (cm)	Cumulative mass depth (g/cm <sup>2</sup> )	Porosity	Total <sup>210</sup> Pb (mBq/g)	<sup>137</sup> Cs (mBq/g)	<sup>210</sup> Pb <sub>xs</sub> (mBq/g)	% Sand	% Silt	% Clay
1	1.57	0.37	92.75 ± 0.19	10.41 ± 0.94	75.54 ± 0.21	9.8	27.8	62.4
2	2.69	0.55	65.48 ± 0.13	12.23 ± 1.13	48.27 ± 0.16	--	--	--
3	4.31	0.35	61.36 ± 0.13	14.41 ± 1.28	44.15 ± 0.16	1.2	27.2	71.6
4	5.40	0.57	57.45 ± 0.13	20.45 ± 1.90	40.24 ± 0.15	--	--	--
5	6.32	0.63	54.80 ± 0.10	17.08 ± 1.37	37.59 ± 0.14	1.0	19.1	79.9
6	7.65	0.47	47.44 ± 0.08	12.51 ± 1.15	30.23 ± 0.12	--	--	--
7	9.19	0.38	45.12 ± 0.08	9.37 ± 0.90	27.91 ± 0.12	1.2	18.4	80.3
8	10.73	0.38	43.95 ± 0.11	6.49 ± 0.55	26.74 ± 0.14	--	--	--
9	11.51	0.69	34.51 ± 0.10	4.29 ± 0.39	17.31 ± 0.13	1.0	14.7	84.3
10	12.44	0.63	37.80 ± 0.09	3.31 ± 0.32	20.59 ± 0.13	--	--	--
11	13.74	0.48	34.62 ± 0.09	2.79 ± 0.27	17.41 ± 0.12	1.0	19.6	79.4
12	14.66	0.63	37.24 ± 0.10	1.35 ± 0.13	20.03 ± 0.14	--	--	--
13	15.61	0.62	35.84 ± 0.09	1.63 ± 0.17	18.64 ± 0.12	1.4	22.4	76.2
14	16.51	0.64	37.40 ± 0.09	0.90 ± 0.10	20.19 ± 0.13	--	--	--
15	17.95	0.42	31.58 ± 0.07	0.69 ± 0.08	14.37 ± 0.11	2.2	24.4	73.4
16	19.19	0.51	33.02 ± 0.09	--	15.81 ± 0.13	--	--	--
17	20.54	0.46	27.85 ± 0.06	--	10.64 ± 0.11	6.3	24.9	68.8
18	21.73	0.52	25.18 ± 0.09	--	7.97 ± 0.13	--	--	--
19	22.95	0.51	24.62 ± 0.07	--	7.42 ± 0.11	8.6	23.2	68.2
20	23.96	0.60	22.59 ± 0.05	0	5.38 ± 0.10	--	--	--
21	25.30	0.47	18.18 ± 0.05	--	0.97 ± 0.10	9.2	29.6	61.1
22	26.60	0.48	--	--	--	--	--	--
23	28.09	0.41	15.09 ± 0.06	--	0	9.1	28.9	62.1
24	29.48	0.44	--	--	--	--	--	--
25	30.74	0.50	19.65 ± 0.05	--	2.44 ± 0.10	9.0	26.1	64.8
25-27	33.47	0.45	--	--	--	9.6	19.6	70.8
27-29	36.38	0.42	20.40 ± 0.09	--	3.19 ± 0.13	10.6	26.0	63.4
29-31	39.19	0.44	--	--	--	11.1	27.4	61.6
31-33	41.98	0.44	17.77 ± 0.05	--	0.56 ± 0.10	--	--	--
35-37	47.70	0.42	17.21 ± 0.09	--	0	--	--	--

Table AI4: Summary physical and radiochemical data for Nueces Delta core 4.

Depth (cm)	Cumulative mass depth (g/cm <sup>2</sup> )	Porosity	Total <sup>210</sup> Pb (mBq/g)	<sup>137</sup> Cs (mBq/g)	<sup>210</sup> Pb <sub>xs</sub> (mBq/g)	% Sand	% Silt	% Clay
1	0.67	0.73	40.27 ± 0.12	2.73 ± 0.22	17.66 ± 0.14	4.1	30.5	65.4
2	1.31	0.75	41.93 ± 0.12	2.58 ± 0.21	19.31 ± 0.14	--	--	--
3	1.85	0.78	45.85 ± 0.13	2.45 ± 0.18	23.23 ± 0.15	1.6	28.2	70.2
4	2.42	0.77	62.08 ± 0.16	4.24 ± 0.34	39.47 ± 0.18	--	--	--
5	2.80	0.85	61.35 ± 0.17	5.26 ± 0.42	38.73 ± 0.19	2.0	18.3	79.7
6	3.50	0.72	52.27 ± 0.14	3.92 ± 0.33	29.66 ± 0.16	--	--	--
7	4.38	0.65	48.53 ± 0.14	2.88 ± 0.23	25.92 ± 0.16	16.9	18.0	65.2
8	5.12	0.70	54.38 ± 0.16	2.91 ± 0.27	31.76 ± 0.17	--	--	--
9	6.23	0.56	36.63 ± 0.11	2.27 ± 0.20	14.02 ± 0.13	24.8	24.5	50.7
10	7.45	0.51	29.80 ± 0.10	0.84 ± 0.08	7.19 ± 0.12	--	--	--
11	8.56	0.55	25.96 ± 0.08	--	3.35 ± 0.11	25.3	17.6	57.1
12	9.68	0.56	28.80 ± 0.08	--	6.19 ± 0.11	--	--	--
13	10.91	0.51	31.02 ± 0.09	--	8.41 ± 0.12	3.9	20.9	75.2
14	12.04	0.55	27.81 ± 0.09	--	5.20 ± 0.11	--	--	--
15	13.67	0.35	27.72 ± 0.08	0	5.10 ± 0.11	2.3	17.9	79.8
16	14.64	0.61	28.04 ± 0.08	--	5.43 ± 0.11	--	--	--
17	15.90	0.49	28.02 ± 0.08	--	5.41 ± 0.11	1.4	21.7	76.9
18	17.26	0.46	29.31 ± 0.08	--	6.69 ± 0.11	--	--	--
19	18.46	0.52	29.31 ± 0.09	--	6.70 ± 0.12	1.6	22.7	75.7
20	19.83	0.45	26.72 ± 0.08	--	4.11 ± 0.11	--	--	--
21	21.18	0.46	--	--	--	2.3	27.1	70.6
22	22.75	0.37	--	--	--	--	--	--
23	24.31	0.38	--	--	--	2.9	28.9	68.2
24	25.73	0.43	--	--	--	--	--	--
25	27.11	0.45	--	--	--	5.7	35.1	59.2
25-27	30.09	0.40	--	--	--	3.1	29.0	67.9
27-29	32.62	0.49	--	--	--	1.4	37.6	61.0
29-31	35.68	0.39	--	--	--	1.6	31.5	66.9
31-33	38.48	0.44	25.25 ± 0.07	--	2.64 ± 0.10	--	--	--
35-37	44.00	0.47	28.96 ± 0.12	--	6.35 ± 0.14	--	--	--
39-41	50.10	0.37	25.41 ± 0.11	--	2.80 ± 0.13	--	--	--
43-45	55.91	0.39	28.13 ± 0.14	--	5.51 ± 0.16	--	--	--
47-49	61.77	0.43	30.37 ± 0.17	--	7.76 ± 0.18	--	--	--
51-53	67.23	0.47	24.11 ± 0.07	--	1.50 ± 0.10	--	--	--
55-57	72.08	0.57	29.58 ± 0.09	--	6.97 ± 0.12	--	--	--
57-59	73.64	0.69	33.75 ± 0.11	--	11.14 ± 0.13	--	--	--
59-61	74.45	0.84	22.61 ± 0.07	--	0	--	--	--

Table AI5: Summary physical and radiochemical data for Nueces Delta core 5.

Depth (cm)	Cumulative mass depth (g/cm <sup>2</sup> )	Porosity	Total <sup>210</sup> Pb (mBq/g)	<sup>137</sup> Cs (mBq/g)	<sup>210</sup> Pb <sub>xs</sub> (mBq/g)	% Sand	% Silt	% Clay
1	0.92	0.63	29.26 ± 0.08	1.95 ± 0.19	10.07 ± 0.11	8.9	43.1	47.9
2	1.58	0.74	37.75 ± 0.11	3.41 ± 0.32	18.55 ± 0.13	--	--	--
3	2.12	0.78	62.36 ± 0.23	4.33 ± 0.43	43.16 ± 0.24	5.4	20.6	74.1
4	2.74	0.75	61.57 ± 0.22	4.69 ± 0.39	42.37 ± 0.23	--	--	--
5	3.50	0.69	48.52 ± 0.17	3.13 ± 0.30	29.32 ± 0.18	0.8	22.1	77.0
6	4.25	0.70	49.56 ± 0.15	3.82 ± 0.34	30.36 ± 0.16	--	--	--
7	5.00	0.70	53.41 ± 0.17	4.08 ± 0.35	34.21 ± 0.19	0.9	23.0	76.1
8	5.64	0.75	60.24 ± 0.16	3.20 ± 0.28	41.04 ± 0.17	--	--	--
9	6.33	0.72	57.89 ± 0.15	3.97 ± 0.38	38.69 ± 0.17	3.1	21.0	75.9
10	7.23	0.64	55.05 ± 0.14	4.09 ± 0.41	35.86 ± 0.16	--	--	--
11	7.73	0.80	54.90 ± 0.19	3.74 ± 0.34	35.71 ± 0.20	1.8	12.6	85.6
12	8.59	0.65	45.38 ± 0.16	3.85 ± 0.33	26.19 ± 0.17	--	--	--
13	9.68	0.57	36.77 ± 0.12	3.01 ± 0.29	17.57 ± 0.14	24.7	19.9	55.4
14	10.98	0.48	35.77 ± 0.10	2.77 ± 0.23	16.58 ± 0.12	--	--	--
15	11.94	0.62	35.82 ± 0.12	3.68 ± 0.29	16.63 ± 0.14	33.9	13.6	52.5
16	13.29	0.46	36.43 ± 0.11	4.37 ± 0.38	17.23 ± 0.13	--	--	--
17	14.55	0.49	36.84 ± 0.10	4.68 ± 0.46	17.65 ± 0.12	18.9	19.0	62.1
18	15.43	0.65	42.20 ± 0.13	7.53 ± 0.68	23.00 ± 0.15	--	--	--
19	16.27	0.66	36.97 ± 0.12	6.56 ± 0.57	17.77 ± 0.14	7.3	15.1	77.6
20	17.15	0.65	36.58 ± 0.12	5.70 ± 0.59	17.38 ± 0.14	--	--	--
21	17.99	0.66	32.54 ± 0.10	6.49 ± 0.75	13.34 ± 0.12	13.6	17.3	69.1
22	18.98	0.60	40.44 ± 0.14	6.77 ± 0.78	21.24 ± 0.16	--	--	--
23	20.07	0.57	29.68 ± 0.10	--	10.48 ± 0.12	15.3	32.8	51.9
24	21.56	0.40	18.54 ± 0.07	--	0	--	--	--
25	22.74	0.53	19.89 ± 0.08	--	0.69 ± 0.11	45.0	15.7	39.3
25-27	24.80	0.59	19.89 ± 0.09	--	0.69 ± 0.11	33.8	16.3	49.8
27-29	26.79	0.60	26.89 ± 0.12	--	7.70 ± 0.14	22.0	17.5	60.5
29-31	28.90	0.58	21.36 ± 0.10	--	2.16 ± 0.12	15.5	18.6	65.9
69-71	68.76	0.68	19.20 ± 0.07	--	0	--	--	--

**APPENDIX II: Nueces Bay and Corpus Christi Bay physical and radiochemical data, x-radiographs and supporting data**

Table AII1: Summary physical and radiochemical data for Nueces Bay Core 1.

Depth (cm)	Cumulative mass depth (g/cm <sup>2</sup> )	Porosity	Total <sup>210</sup> Pb (mBq/g)	<sup>137</sup> Cs (mBq/g)	<sup>210</sup> Pb <sub>xs</sub> (mBq/g)	% Sand	% Silt	% Clay
1	0.86	0.66	22.07 ± 0.07	0.66 ± 0.04	--	50.1	13.0	36.9
2	2.03	0.53	22.34 ± 0.07	--	--	--	--	--
3	3.43	0.44	22.05 ± 0.07	0.49 ± 0.04	--	46.6	37.0	16.4
4	4.68	0.50	26.91 ± 0.08	--	--	--	--	--
5	5.90	0.51	26.75 ± 0.08	0.89 ± 0.08	--	47.0	31.9	21.1
6	7.10	0.52	24.60 ± 0.07	--	--	--	--	--
7	8.32	0.52	24.59 ± 0.09	--	--	48.1	28.1	23.8
8	9.46	0.54	27.46 ± 0.09	--	--	--	--	--
9	10.67	0.51	25.77 ± 0.08	--	--	45.8	26.5	27.6
10	11.82	0.54	27.34 ± 0.09	1.33 ± 0.12	--	--	--	--
11	12.95	0.55	24.19 ± 0.08	--	--	44.9	27.0	28.1
12	14.02	0.57	24.80 ± 0.08	--	--	--	--	--
13	14.87	0.66	26.02 ± 0.08	--	--	41.9	24.7	33.4
14	15.61	0.70	24.60 ± 0.07	--	--	--	--	--
15	16.53	0.63	23.87 ± 0.07	1.13 ± 0.08	--	39.6	28.4	32.0
16	17.38	0.66	20.32 ± 0.07	--	--	--	--	--
17	18.30	0.63	25.79 ± 0.08	--	--	37.8	26.5	35.6
18	19.10	0.68	23.99 ± 0.07	--	--	--	--	--
19	19.88	0.69	26.32 ± 0.09	--	--	34.7	27.4	37.8
20	20.72	0.66	30.27 ± 0.10	--	--	--	--	--
21	21.54	0.68	23.98 ± 0.08	--	--	13.6	22.4	64.0
22	22.43	0.64	23.33 ± 0.08	--	--	--	--	--
23	23.08	0.74	26.32 ± 0.07	--	--	17.8	18.9	63.3
24	23.78	0.72	25.82 ± 0.08	--	--	--	--	--
25	24.52	0.70	24.90 ± 0.08	--	--	9.3	19.8	70.9
26	25.27	0.70	24.36 ± 0.07	--	--	--	--	--
27	26.00	0.71	26.14 ± 0.07	--	--	11.8	22.1	66.1
28	26.68	0.73	25.86 ± 0.06	--	--	--	--	--
29	27.54	0.65	26.90 ± 0.06	--	--	6.3	22.2	71.4
30	28.22	0.73	17.13 ± 0.06	--	--	--	--	--
31	28.92	0.72	--	--	--	8.3	17.3	74.5
37	33.55	0.75	26.14 ± 0.13	--	--	--	--	--
43	38.15	0.69	25.51 ± 0.12	--	--	--	--	--
49	43.05	0.74	20.63 ± 0.07	--	--	--	--	--

Table AII2: Summary physical and radiochemical data for Nueces Bay Core 2.

Depth (cm)	Cumulative mass depth (g/cm <sup>2</sup> )	Porosity	Total <sup>210</sup> Pb (mBq/g)	<sup>137</sup> Cs (mBq/g)	<sup>210</sup> Pb <sub>xs</sub> (mBq/g)	% Sand	% Silt	% Clay
1	0.89	0.64	18.82 ± 0.06	1.22 ± 0.11	0	68.5	9.9	21.7
2	2.00	0.55	19.90 ± 0.07	1.45 ± 0.12	0	--	--	--
3	3.31	0.48	23.20 ± 0.08	0.87 ± 0.06	2.98 ± 0.12	59.2	15.8	25.0
4	4.46	0.54	23.12 ± 0.08	1.23 ± 0.08	2.91 ± 0.12	--	--	--
5	5.55	0.56	25.34 ± 0.09	1.82 ± 0.14	5.13 ± 0.13	52.1	18.6	29.4
6	6.59	0.59	23.01 ± 0.07	1.88 ± 0.19	2.80 ± 0.12	--	--	--
7	7.63	0.58	25.58 ± 0.08	1.31 ± 0.10	5.36 ± 0.12	48.5	21.2	30.3
8	8.66	0.59	22.22 ± 0.07	1.04 ± 0.09	2.00 ± 0.12	--	--	--
9	9.62	0.61	25.14 ± 0.08	1.92 ± 0.16	4.93 ± 0.13	40.6	21.0	38.4
10	10.54	0.63	27.61 ± 0.09	2.28 ± 0.16	7.39 ± 0.13	--	--	--
11	11.39	0.66	31.65 ± 0.09	2.81 ± 0.19	11.44 ± 0.13	28.0	26.7	45.3
12	12.25	0.65	31.85 ± 0.10	2.32 ± 0.17	11.64 ± 0.14	--	--	--
13	12.95	0.72	30.37 ± 0.09	3.29 ± 0.28	10.16 ± 0.13	18.1	29.4	52.5
14	13.75	0.68	33.79 ± 0.09	3.06 ± 0.20	13.58 ± 0.14	--	--	--
15	14.47	0.71	36.46 ± 0.10	--	16.24 ± 0.14	17.3	29.6	53.2
16	15.13	0.74	36.82 ± 0.10	--	16.61 ± 0.14	--	--	--
17	15.79	0.74	35.34 ± 0.12	--	15.13 ± 0.16	12.5	27.4	60.1
18	16.55	0.69	32.59 ± 0.09	--	12.38 ± 0.13	--	--	--
19	17.24	0.72	32.96 ± 0.10	--	12.75 ± 0.14	11.3	28.2	60.6
20	17.88	0.75	33.59 ± 0.12	--	13.38 ± 0.15	--	--	--
21	18.51	0.75	30.97 ± 0.09	--	10.76 ± 0.13	7.5	29.5	63.0
22	19.08	0.77	33.06 ± 0.09	--	12.85 ± 0.13	--	--	--
23	19.67	0.77	34.01 ± 0.09	--	13.80 ± 0.13	4.4	27.7	67.9
24	20.20	0.79	34.78 ± 0.10	--	14.56 ± 0.14	--	--	--
25	20.77	0.77	32.82 ± 0.09	--	12.61 ± 0.13	4.3	21.2	74.5
26	21.23	0.81	36.72 ± 0.10	--	16.51 ± 0.14	--	--	--
27	21.70	0.81	37.15 ± 0.10	--	16.93 ± 0.14	4.9	19.9	75.2
28	22.30	0.76	42.09 ± 0.11	--	21.88 ± 0.15	--	--	--
29	22.80	0.80	38.94 ± 0.11	--	18.73 ± 0.15	3.3	25.4	71.2
30	23.32	0.80	37.85 ± 0.09	--	17.63 ± 0.13	--	--	--
31	23.86	0.78	35.33 ± 0.09	--	15.12 ± 0.13	0.4	26.3	73.3
32	24.39	0.79	36.90 ± 0.10	--	16.69 ± 0.14	--	--	--
33	24.87	0.81	29.32 ± 0.09	--	9.11 ± 0.13	--	--	--
34	25.38	0.80	37.99 ± 0.11	--	17.78 ± 0.14	--	--	--
35	26.03	0.74	33.28 ± 0.10	--	13.06 ± 0.14	--	--	--
36	26.59	0.78	32.37 ± 0.10	--	12.16 ± 0.14	--	--	--
37	27.17	0.77	33.88 ± 0.12	--	13.67 ± 0.15	--	--	--

Table AII2: Summary physical and radiochemical data for Nueces Bay Core 2 (continued).

Depth (cm)	Cumulative mass depth (g/cm <sup>2</sup> )	Porosity	Total <sup>210</sup> Pb (mBq/g)	<sup>137</sup> Cs (mBq/g)	<sup>210</sup> Pb <sub>xs</sub> (mBq/g)	% Sand	% Silt	% Clay
38	27.83	0.74	33.16 ± 0.10	--	12.95 ± 0.14	--	--	--
39	28.51	0.73	32.20 ± 0.11	--	11.98 ± 0.14	--	--	--
40	29.31	0.68	27.26 ± 0.09	--	7.05 ± 0.13	--	--	--
41	29.98	0.73	31.80 ± 0.15	--	11.58 ± 0.18	--	--	--
42	30.56	0.77	19.53 ± 0.09	--	0	--	--	--
43	31.12	0.78	21.46 ± 0.10	--	1.24 ± 0.14	--	--	--
44	31.58	0.81	23.79 ± 0.10	--	3.58 ± 0.14	--	--	--
45	32.20	0.75	28.94 ± 0.13	--	8.73 ± 0.16	--	--	--
46	32.70	0.80	39.14 ± 0.17	--	18.92 ± 0.20	--	--	--
47	33.18	0.81	31.63 ± 0.12	--	11.42 ± 0.16	--	--	--
48	33.72	0.79	30.21 ± 0.12	--	10.00 ± 0.15	--	--	--
49	34.31	0.76	33.60 ± 0.16	--	13.38 ± 0.19	--	--	--
50	34.95	0.75	30.30 ± 0.14	--	10.09 ± 0.17	--	--	--
51	35.43	0.81	21.30 ± 0.10	--	1.08 ± 0.14	--	--	--
52	36.06	0.75	27.11 ± 0.11	--	6.89 ± 0.15	--	--	--
53	36.69	0.75	28.50 ± 0.10	--	8.29 ± 0.14	--	--	--
54	37.29	0.76	21.89 ± 0.10	--	1.68 ± 0.14	--	--	--
55	38.03	0.71	20.21 ± 0.10	--	0	--	--	--

Table AII3: Summary physical and radiochemical data for Nueces Bay Core 3.

Depth (cm)	Cumulative mass depth (g/cm <sup>2</sup> )	Porosity	Total <sup>210</sup> Pb (mBq/g)	<sup>137</sup> Cs (mBq/g)	<sup>210</sup> Pb <sub>xs</sub> (mBq/g)	% Sand	% Silt	% Clay
1	0.87	0.65	9.39 ± 0.03	0	0.98 ± 0.05	84.9	5.6	9.6
2	2.24	0.45	10.84 ± 0.03	0	2.42 ± 0.05	--	--	--
3	3.63	0.45	14.14 ± 0.04	0.75 ± 0.07	5.73 ± 0.05	76.0	8.0	16.0
4	4.89	0.50	15.24 ± 0.05	0	6.83 ± 0.06	--	--	--
5	6.13	0.50	14.33 ± 0.04	0	5.92 ± 0.05	70.9	9.4	19.8
6	7.26	0.55	16.48 ± 0.05	0.67 ± 0.05	8.07 ± 0.06	--	--	--
7	8.35	0.56	17.12 ± 0.05	0.33 ± 0.02	8.70 ± 0.06	63.3	10.9	25.8
8	9.54	0.53	18.64 ± 0.05	0.66 ± 0.06	10.23 ± 0.06	--	--	--
9	10.61	0.57	17.36 ± 0.05	0	8.94 ± 0.06	59.3	11.9	28.8
10	11.76	0.54	15.99 ± 0.05	0.76 ± 0.11	7.58 ± 0.06	--	--	--
11	13.10	0.46	21.21 ± 0.07	1.97 ± 0.18	12.79 ± 0.08	56.8	12.3	30.8
12	14.28	0.53	15.41 ± 0.05	1.37 ± 0.10	7.00 ± 0.06	--	--	--
13	15.61	0.47	18.43 ± 0.05	1.43 ± 0.12	10.01 ± 0.06	58.8	12.8	28.4
14	16.77	0.54	16.88 ± 0.05	0.89 ± 0.09	8.47 ± 0.06	--	--	--
15	18.04	0.49	16.54 ± 0.05	1.32 ± 0.15	8.13 ± 0.06	61.5	10.5	28.0
16	19.29	0.50	17.00 ± 0.05	1.02 ± 0.09	8.59 ± 0.06	--	--	--
17	20.52	0.51	16.94 ± 0.06	0.26 ± 0.06	8.53 ± 0.07	61.5	11.1	27.4
18	21.79	0.49	17.15 ± 0.06	1.04 ± 0.09	8.74 ± 0.07	--	--	--
19	23.17	0.45	15.76 ± 0.05	--	7.34 ± 0.06	66.3	10.0	23.7
20	24.47	0.48	14.22 ± 0.04	--	5.80 ± 0.06	--	--	--
21	25.71	0.50	6.79 ± 0.02	--	0	67.3	9.2	23.5
22	26.99	0.49	6.85 ± 0.02	--	0	--	--	--
23	28.34	0.46	6.55 ± 0.03	--	0	72.4	7.5	20.1
24	29.92	0.37	5.75 ± 0.02	--	0	--	--	--
25	31.29	0.45	7.19 ± 0.03	--	0	75.9	6.6	17.4
26	32.50	0.51	10.14 ± 0.03	--	1.73 ± 0.05	--	--	--
27	33.96	0.42	10.51 ± 0.04	--	2.09 ± 0.05	72.1	6.8	21.1
28	35.56	0.36	8.37 ± 0.03	--	0	--	--	--
29	37.04	0.41	10.22 ± 0.03	--	1.81 ± 0.05	66.9	8.3	24.9
30	38.58	0.38	--	--	--	--	--	--
31	40.02	0.43	--	--	--	67.8	8.4	23.8
51	67.13	0.55	8.79 ± 0.04	--	0	--	--	--
52	68.29	0.54	8.41 ± 0.04	--	0	--	--	--

Table AII4: Summary physical and radiochemical data for Corpus Christi Bay Core 1.

Depth (cm)	Cumulative mass depth (g/cm <sup>2</sup> )	Porosity	Total <sup>210</sup> Pb (mBq/g)	<sup>137</sup> Cs (mBq/g)	<sup>210</sup> Pb <sub>xs</sub> (mBq/g)	% Sand	% Silt	% Clay
1	0.66	0.74	33.31 ± 0.12	2.62 ± 0.20	23.74 ± 0.12	5.6	44.5	49.9
2	1.44	0.68	33.35 ± 0.10	2.78 ± 0.17	23.78 ± 0.11	--	--	--
3	2.11	0.73	32.82 ± 0.10	2.29 ± 0.20	23.25 ± 0.11	5.4	52.0	42.6
4	2.76	0.74	33.59 ± 0.11	2.32 ± 0.16	24.02 ± 0.12	--	--	--
5	3.55	0.68	35.16 ± 0.12	2.62 ± 0.17	25.58 ± 0.13	5.2	47.6	47.3
6	4.05	0.80	34.14 ± 0.10	2.37 ± 0.17	24.56 ± 0.11	--	--	--
7	4.69	0.75	27.47 ± 0.09	2.52 ± 0.18	17.90 ± 0.10	1.9	42.2	55.9
8	5.19	0.80	33.47 ± 1.96	2.88 ± 0.16	23.90 ± 1.96	--	--	--
9	5.96	0.69	34.81 ± 0.12	3.04 ± 0.27	25.23 ± 0.13	2.7	43.2	54.1
10	6.79	0.67	34.49 ± 0.12	2.96 ± 0.26	24.92 ± 0.12	--	--	--
11	7.34	0.78	31.04 ± 0.07	2.61 ± 0.18	21.47 ± 0.08	2.5	44.7	52.8
12	7.97	0.75	28.79 ± 0.07	2.84 ± 0.25	19.22 ± 0.08	--	--	--
13	8.69	0.71	29.05 ± 0.09	2.85 ± 0.25	19.48 ± 0.10	2.0	33.3	64.7
14	9.53	0.66	27.64 ± 0.10	2.63 ± 0.23	18.07 ± 0.11	--	--	--
15	10.10	0.77	24.59 ± 0.07	3.00 ± 0.27	15.02 ± 0.07	1.6	34.4	63.9
16	10.95	0.66	25.84 ± 0.06	2.53 ± 0.28	16.27 ± 0.07	--	--	--
17	11.60	0.74	24.99 ± 0.07	3.07 ± 0.27	15.42 ± 0.07	1.7	31.3	67.0
18	12.24	0.75	21.17 ± 0.07	3.16 ± 0.34	11.59 ± 0.08	--	--	--
19	12.89	0.74	26.14 ± 0.10	2.60 ± 0.26	16.56 ± 0.11	1.0	24.2	74.8
20	13.41	0.79	25.11 ± 0.06	2.24 ± 0.20	15.54 ± 0.07	--	--	--
21	13.98	0.77	23.98 ± 0.08	--	14.41 ± 0.08	0.5	18.6	80.9
22	14.64	0.74	23.33 ± 0.08	--	13.75 ± 0.08	--	--	--
23	15.59	0.62	15.69 ± 0.05	--	6.12 ± 0.06	3.3	39.2	57.5
24	16.67	0.57	25.82 ± 0.08	--	16.25 ± 0.09	--	--	--
25	17.61	0.63	24.90 ± 0.08	--	15.32 ± 0.08	15.3	31.4	53.3
26	18.21	0.76	24.36 ± 0.07	--	14.78 ± 0.08	--	--	--
27	18.70	0.80	16.98 ± 0.08	--	7.19 ± 0.09	12.4	23.7	63.9
28	19.27	0.77	14.72 ± 0.06	--	5.15 ± 0.07	--	--	--
29	19.83	0.78	16.98 ± 0.08	--	7.41 ± 0.08	3.3	18.1	78.6
30	20.38	0.78	16.43 ± 0.05	--	6.85 ± 0.06	--	--	--
31	20.88	0.80	16.34 ± 0.05	--	6.77 ± 0.06	2.7	8.5	88.8
32	21.38	0.80	16.02 ± 0.05	--	6.45 ± 0.06	--	--	--
33	21.83	0.82	17.94 ± 0.05	--	8.37 ± 0.06	--	--	--
34	22.41	0.77	12.13 ± 0.04	--	2.56 ± 0.05	--	--	--
35	22.92	0.80	16.90 ± 0.05	--	7.33 ± 0.06	--	--	--
37	23.96	0.80	15.40 ± 0.06	--	5.82 ± 0.07	--	--	--
39	24.92	0.80	14.46 ± 0.07	--	4.88 ± 0.08	--	--	--

Table AII4: Summary physical and radiochemical data for Corpus Christi Bay Core 1 (continued).

Depth (cm)	Cumulative mass depth (g/cm <sup>2</sup> )	Porosity	Total <sup>210</sup> Pb (mBq/g)	<sup>137</sup> Cs (mBq/g)	<sup>210</sup> Pb <sub>xs</sub> (mBq/g)	% Sand	% Silt	% Clay
41	25.72	0.83	11.84 ± 0.05	--	2.27 ± 0.06	--	--	--
43	26.72	0.82	13.67 ± 0.06	--	4.09 ± 0.07	--	--	--
45	27.78	0.77	13.89 ± 0.06	--	4.32 ± 0.07	--	--	--
47	28.75	0.83	12.12 ± 0.04	--	2.55 ± 0.05	--	--	--
49	29.61	0.82	12.81 ± 0.06	--	3.24 ± 0.07	--	--	--
51	30.43	0.86	14.78 ± 0.05	--	5.21 ± 0.06	--	--	--
53	31.47	0.79	12.57 ± 0.04	--	3.00 ± 0.05	--	--	--
55	32.95	0.67	9.57 ± 0.03	--	0	--	--	--

Table AII5: Summary physical and radiochemical data for Corpus Christi Bay Core 2.

Depth (cm)	Cumulative mass depth (g/cm <sup>2</sup> )	Porosity	Total <sup>210</sup> Pb (mBq/g)	<sup>137</sup> Cs (mBq/g)	<sup>210</sup> Pb <sub>xs</sub> (mBq/g)	% Sand	% Silt	% Clay
1	0.32	0.87	37.12 ± 0.11	2.64 ± 0.24	26.11 ± 0.11	7.8	40.2	52.0
2	0.97	0.74	39.22 ± 0.10	1.94 ± 0.16	28.21 ± 0.11	--	--	--
3	1.66	0.72	37.49 ± 0.11	2.37 ± 0.20	26.48 ± 0.11	7.1	42.0	50.9
4	2.47	0.68	30.46 ± 0.08	2.60 ± 0.21	19.45 ± 0.09	--	--	--
5	3.10	0.75	33.19 ± 0.09	1.95 ± 0.16	22.18 ± 0.10	6.7	38.6	54.7
6	3.89	0.68	30.33 ± 0.08	2.31 ± 0.25	19.32 ± 0.09	--	--	--
7	4.64	0.70	33.02 ± 0.10	2.38 ± 0.20	22.02 ± 0.10	5.0	32.9	62.1
8	5.44	0.68	33.99 ± 0.10	2.02 ± 0.23	22.98 ± 0.10	--	--	--
9	6.23	0.68	27.30 ± 0.08	3.37 ± 0.31	16.29 ± 0.09	4.0	37.0	59.0
10	7.08	0.66	30.63 ± 0.09	1.67 ± 0.42	19.62 ± 0.10	--	--	--
11	7.92	0.67	28.85 ± 0.08	2.18 ± 0.27	17.85 ± 0.09	3.2	36.2	60.7
12	8.83	0.64	27.98 ± 0.08	1.55 ± 0.15	16.97 ± 0.09	--	--	--
13	9.42	0.76	22.01 ± 0.07	2.06 ± 0.20	11.00 ± 0.08	2.9	35.2	62.0
14	10.36	0.63	16.99 ± 0.05	--	5.99 ± 0.07	--	--	--
15	11.19	0.67	17.32 ± 0.05	--	6.31 ± 0.07	7.5	35.0	57.5
16	12.02	0.66	22.47 ± 0.07	--	11.46 ± 0.08	--	--	--
17	12.81	0.69	18.92 ± 0.06	--	7.91 ± 0.07	12.0	32.8	55.1
18	13.71	0.64	17.02 ± 0.05	--	6.01 ± 0.07	--	--	--
19	14.52	0.68	17.58 ± 0.06	--	6.57 ± 0.07	5.9	29.6	64.5
20	15.23	0.72	18.33 ± 0.06	--	7.33 ± 0.07	--	--	--
21	15.86	0.75	13.01 ± 0.05	--	2.01 ± 0.06	7.5	24.3	68.2
22	16.33	0.81	13.62 ± 0.05	--	2.61 ± 0.06	--	--	--
23	16.81	0.81	13.06 ± 0.04	--	2.05 ± 0.06	2.8	16.6	80.5
24	17.42	0.76	12.19 ± 0.04	--	1.18 ± 0.06	--	--	--
25	17.88	0.82	12.30 ± 0.04	--	1.29 ± 0.06	3.8	20.8	75.4
26	18.39	0.79	10.93 ± 0.04	--	0	--	--	--
27	18.92	0.79	10.47 ± 0.04	--	0	3.1	16.4	80.5
28	19.42	0.80	10.17 ± 0.04	--	0	--	--	--
29	19.94	0.79	11.13 ± 0.04	--	0	0.6	4.8	94.6
30	20.44	0.80	11.01 ± 0.04	--	0	--	--	--
31	20.94	0.80	--	--	--	1.2	24.4	74.4
48	30.88	0.75	14.90 ± 0.06	--	--	--	--	--
50	32.22	0.74	12.42 ± 0.04	--	--	--	--	--

Table AII6: Summary physical and radiochemical data for Corpus Christi Bay Core 3.

Depth (cm)	Cumulative mass depth (g/cm <sup>2</sup> )	Porosity	Total <sup>210</sup> Pb (mBq/g)	<sup>137</sup> Cs (mBq/g)	<sup>210</sup> Pb <sub>xs</sub> (mBq/g)	% Sand	% Silt	% Clay
1	0.25	0.90	37.85 ± 0.10	2.15 ± 0.23	28.86 ± 0.10	2.3	74.6	23.1
2	0.70	0.82	37.19 ± 0.10	2.93 ± 0.29	28.21 ± 0.10	--	--	--
3	1.43	0.71	35.93 ± 0.10	2.59 ± 0.36	26.94 ± 0.10	8.1	31.5	60.4
4	1.93	0.80	35.67 ± 0.10	2.84 ± 0.21	26.69 ± 0.10	--	--	--
5	2.48	0.78	36.78 ± 0.10	2.25 ± 0.22	27.79 ± 0.10	6.2	28.8	65.0
6	3.14	0.73	35.36 ± 0.09	2.43 ± 0.22	26.37 ± 0.10	--	--	--
7	3.79	0.74	41.17 ± 0.11	2.42 ± 0.24	32.19 ± 0.12	4.7	29.9	65.5
8	4.40	0.76	34.24 ± 0.10	2.64 ± 0.27	25.25 ± 0.10	--	--	--
9	4.99	0.76	36.39 ± 0.10	3.23 ± 0.43	27.41 ± 0.10	3.8	29.9	66.4
10	5.55	0.77	32.37 ± 0.11	3.18 ± 0.32	23.39 ± 0.11	--	--	--
11	6.16	0.76	33.45 ± 0.11	3.21 ± 0.38	24.46 ± 0.11	2.7	27.6	69.7
12	6.79	0.75	30.58 ± 0.09	2.98 ± 0.26	21.60 ± 0.09	--	--	--
13	7.48	0.72	28.49 ± 0.10	3.85 ± 0.55	19.51 ± 0.10	3.6	26.3	70.2
14	8.17	0.73	26.92 ± 0.09	2.49 ± 0.19	17.93 ± 0.09	--	--	--
15	8.85	0.73	25.60 ± 0.09	2.39 ± 0.22	16.62 ± 0.09	2.7	27.2	70.2
16	9.51	0.74	22.29 ± 0.98	2.55 ± 0.23	13.31 ± 0.98	--	--	--
17	10.19	0.73	25.01 ± 0.08	2.48 ± 0.25	16.03 ± 0.09	3.5	26.4	70.1
18	10.88	0.72	21.38 ± 0.06	--	12.40 ± 0.07	--	--	--
19	11.38	0.80	21.22 ± 0.07	--	12.24 ± 0.08	5.4	21.9	72.6
20	12.09	0.72	16.97 ± 0.06	2.00 ± 0.17	7.98 ± 0.07	--	--	--
21	12.73	0.75	20.50 ± 0.06	--	11.52 ± 0.07	13.9	20.3	65.7
22	13.36	0.74	21.14 ± 0.06	--	12.16 ± 0.07	--	--	--
23	13.97	0.76	18.18 ± 0.06	--	9.20 ± 0.07	15.4	21.9	62.6
24	14.65	0.73	16.89 ± 0.05	--	7.91 ± 0.06	--	--	--
25	15.39	0.71	13.96 ± 0.04	--	4.98 ± 0.05	24.7	18.3	57.0
26	16.06	0.73	14.27 ± 0.05	--	5.29 ± 0.06	--	--	--
27	16.87	0.68	14.43 ± 0.04	--	5.45 ± 0.05	18.8	16.4	64.8
28	17.66	0.68	14.09 ± 0.04	--	5.11 ± 0.05	--	--	--
29	18.41	0.70	13.23 ± 0.04	--	4.25 ± 0.05	31.2	16.3	52.5
30	19.17	0.70	9.45 ± 0.03	--	0.47 ± 0.04	--	--	--
31	20.01	0.66	8.04 ± 0.03	--	0	39.1	11.4	49.5
32	20.62	0.75	9.50 ± 0.03	--	0.52 ± 0.05	--	--	--
33	21.21	0.76	8.66 ± 0.03	--	0	--	--	--
34	21.85	0.74	9.19 ± 0.03	--	0	--	--	--
35	22.49	0.74	9.95 ± 0.03	--	0.97 ± 0.04	--	--	--
36	22.94	0.82	8.56 ± 0.03	--	0	--	--	--

Table AII7: Summary physical and radiochemical data for Corpus Christi Bay Core 4.

Depth (cm)	Cumulative mass depth (g/cm <sup>2</sup> )	Porosity	Total <sup>210</sup> Pb (mBq/g)	<sup>137</sup> Cs (mBq/g)	<sup>210</sup> Pb <sub>xs</sub> (mBq/g)	% Sand	% Silt	% Clay
1	0.74	0.70	29.43 ± 0.10	--	14.78 ± 0.11	24.1	25.6	50.3
2	1.62	0.65	31.53 ± 0.11	--	16.88 ± 0.12	--	--	--
3	2.35	0.71	30.33 ± 0.09	--	15.68 ± 0.10	18.9	27.9	53.2
4	3.28	0.63	30.94 ± 0.10	--	16.28 ± 0.11	--	--	--
5	3.95	0.73	29.27 ± 0.11	--	14.62 ± 0.12	13.7	26.1	60.2
6	4.70	0.70	29.56 ± 0.08	--	14.90 ± 0.10	--	--	--
7	5.53	0.67	27.31 ± 0.09	--	12.66 ± 0.10	10.2	24.3	65.5
8	6.28	0.70	25.48 ± 0.08	--	10.83 ± 0.09	--	--	--
9	6.93	0.74	24.89 ± 0.08	--	10.24 ± 0.09	6.1	28.1	65.8
10	7.69	0.69	22.74 ± 0.07	--	8.09 ± 0.08	--	--	--
11	8.44	0.70	23.31 ± 0.07	--	8.66 ± 0.09	4.7	25.2	70.1
12	9.28	0.67	24.52 ± 0.07	--	9.87 ± 0.09	--	--	--
13	10.16	0.65	22.10 ± 0.06	--	7.45 ± 0.08	5.2	26.7	68.1
14	11.04	0.65	24.20 ± 0.07	--	9.55 ± 0.09	--	--	--
15	11.70	0.74	22.67 ± 0.07	--	8.02 ± 0.08	4.3	26.2	69.5
16	12.50	0.68	22.37 ± 0.06	--	7.71 ± 0.08	--	--	--
17	13.36	0.66	22.84 ± 0.07	--	8.18 ± 0.09	3.9	26.4	69.7
18	14.17	0.67	21.17 ± 0.06	--	6.52 ± 0.08	--	--	--
19	14.93	0.70	20.81 ± 0.06	--	6.16 ± 0.08	3.4	27.3	69.3
20	15.86	0.63	21.62 ± 0.06	--	6.96 ± 0.08	--	--	--
21	16.64	0.69	13.80 ± 0.05	--	0	3.2	25.6	71.2
22	17.58	0.62	15.06 ± 0.06	--	0.41 ± 0.08	--	--	--
23	18.34	0.70	16.35 ± 0.06	--	1.69 ± 0.08	4.4	27.9	67.7
24	19.17	0.67	16.11 ± 0.06	--	1.45 ± 0.08	--	--	--
25	20.00	0.67	15.36 ± 0.06	--	0.71 ± 0.07	3.4	22.8	73.8
26	20.82	0.67	14.06 ± 0.05	--	0	--	--	--
27	21.60	0.69	14.00 ± 0.05	--	0	4.2	22.2	73.6
28	22.27	0.73	14.27 ± 0.05	--	0	--	--	--
29	22.91	0.74	14.25 ± 0.05	--	0	8.5	18.3	73.2
30	23.68	0.70	14.65 ± 0.05	--	0	--	--	--
31	24.44	0.69	--	--	0	8.0	23.2	68.8

Table AII8: Summary physical and radiochemical data for Corpus Christi Bay Core 5.

Depth (cm)	Cumulative mass depth (g/cm <sup>2</sup> )	Porosity	Total <sup>210</sup> Pb (mBq/g)	<sup>137</sup> Cs (mBq/g)	<sup>210</sup> Pb <sub>xs</sub> (mBq/g)	% Sand	% Silt	% Clay
1	0.66	0.74	41.75 ± 0.10	--	28.44 ± 0.12	2.3	29.3	68.4
2	1.44	0.68	39.89 ± 0.10	--	26.58 ± 0.12	--	--	--
3	2.11	0.73	42.48 ± 0.10	--	29.18 ± 0.13	2.0	30.5	67.5
4	2.76	0.74	42.35 ± 0.10	--	29.05 ± 0.12	--	--	--
5	3.55	0.68	43.77 ± 0.12	--	30.47 ± 0.14	2.9	61.4	35.7
6	4.05	0.80	41.44 ± 0.11	--	28.14 ± 0.13	--	--	--
7	4.69	0.75	40.65 ± 0.11	--	27.35 ± 0.13	3.5	35.2	61.4
8	5.19	0.80	40.95 ± 0.11	--	27.64 ± 0.13	--	--	--
9	5.96	0.69	42.50 ± 0.12	--	29.19 ± 0.14	3.4	25.7	70.9
10	6.79	0.67	42.37 ± 0.12	--	29.06 ± 0.14	--	--	--
11	7.34	0.78	36.69 ± 0.11	--	23.39 ± 0.13	2.7	25.0	72.2
12	7.97	0.75	37.62 ± 0.12	--	24.31 ± 0.14	--	--	--
13	8.69	0.71	35.45 ± 0.12	--	22.14 ± 0.14	2.8	26.6	70.7
14	9.53	0.66	30.03 ± 0.09	--	16.73 ± 0.11	--	--	--
15	10.10	0.77	29.66 ± 0.09	--	16.35 ± 0.12	3.1	28.7	68.2
16	10.95	0.66	31.22 ± 0.10	--	17.92 ± 0.12	--	--	--
17	11.60	0.74	23.61 ± 0.08	--	10.31 ± 0.11	1.7	27.4	70.9
18	12.24	0.75	24.49 ± 0.08	--	11.19 ± 0.10	--	--	--
19	12.89	0.74	25.85 ± 0.09	--	12.54 ± 0.11	2.5	25.0	72.5
20	13.41	0.79	20.56 ± 0.07	--	7.25 ± 0.10	--	--	--
21	13.98	0.77	19.56 ± 0.07	--	6.25 ± 0.10	4.7	24.5	70.8
22	14.64	0.74	12.04 ± 0.04	--	0	--	--	--
23	15.59	0.62	21.38 ± 0.08	--	8.08 ± 0.11	4.2	26.6	69.2
24	16.67	0.57	18.61 ± 0.06	--	5.31 ± 0.09	--	--	--
25	17.61	0.63	21.85 ± 0.07	--	8.54 ± 0.10	4.0	28.7	67.3
26	18.21	0.76	19.05 ± 0.06	--	5.75 ± 0.10	--	--	--
27	18.70	0.80	22.33 ± 0.09	--	9.03 ± 0.12	3.0	23.9	73.1
28	19.27	0.77	18.07 ± 0.07	--	4.76 ± 0.10	--	--	--
29	19.83	0.78	17.94 ± 0.06	--	4.64 ± 0.09	3.7	27.9	68.4
30	20.38	0.78	16.39 ± 0.06	--	3.09 ± 0.09	--	--	--
31	20.88	0.80	23.40 ± 0.13	--	10.10 ± 0.15	0.8	24.8	74.3
33	21.83	0.82	23.65 ± 0.10	--	10.34 ± 0.12	--	--	--
35	22.92	0.80	16.20 ± 0.08	--	2.90 ± 0.11	--	--	--
39	24.92	0.80	14.97 ± 0.08	--	1.66 ± 0.11	--	--	--
41	25.72	0.83	15.24 ± 0.07	--	1.93 ± 0.10	--	--	--
43	26.72	0.82	14.65 ± 0.06	--	1.35 ± 0.09	--	--	--
45	27.78	0.77	13.30 ± 0.07	--	0	--	--	--

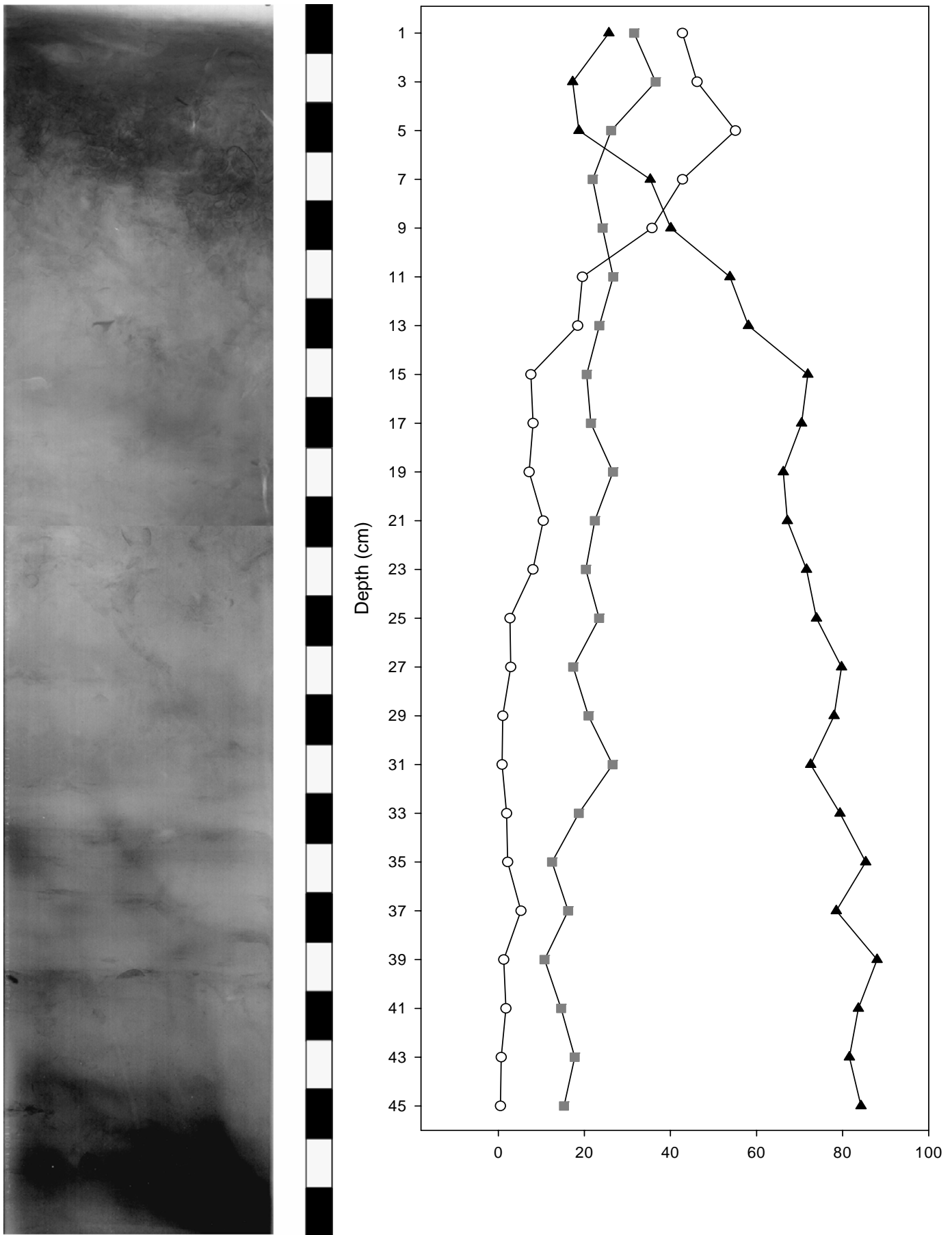


Figure AIII: X-radiography and grain size distribution for Nueces Bay core 1, open circles denote % sand, grey boxes denote % silt and solid triangles denote % clay.

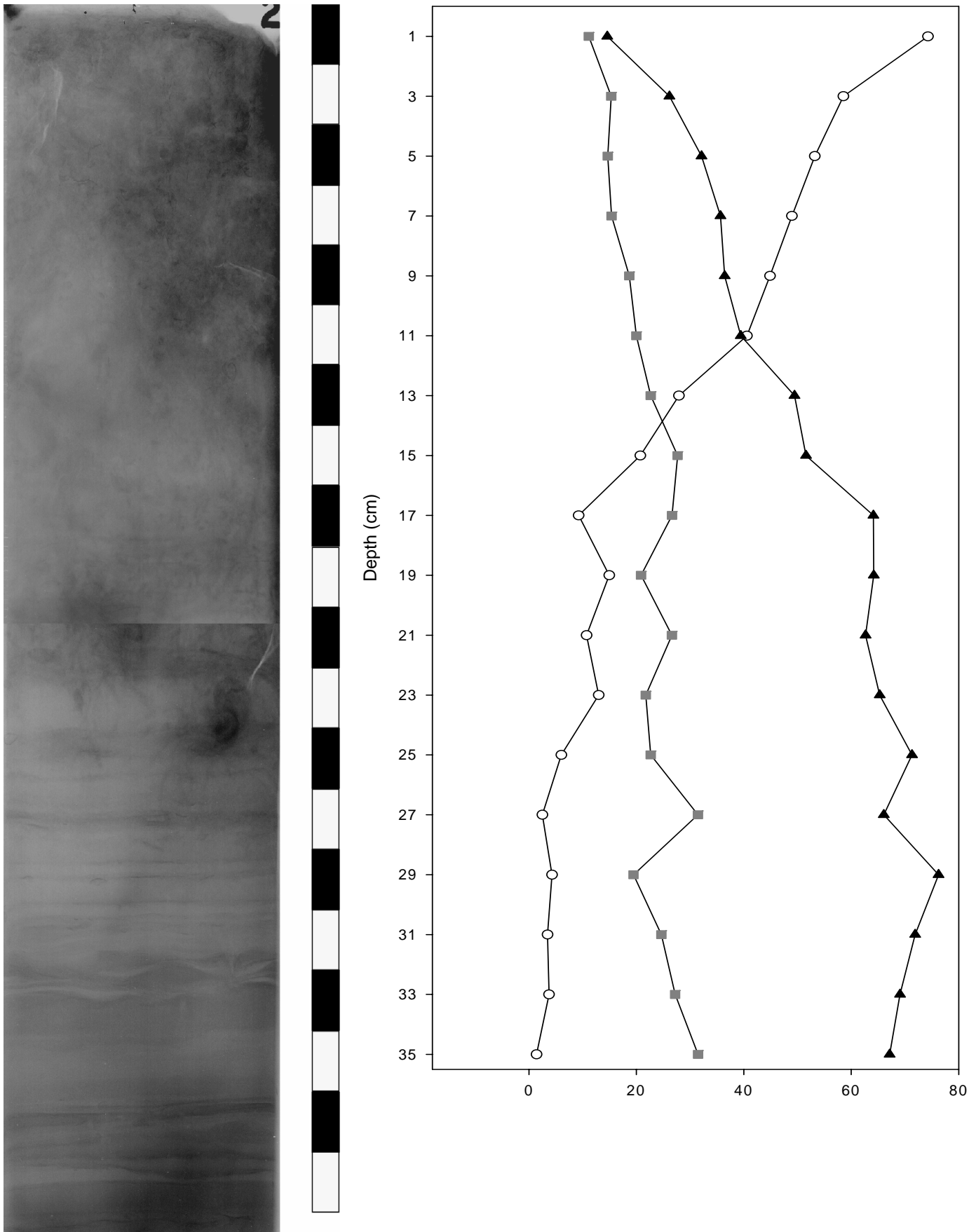


Figure AII2: X-radiography and grain size distribution for Nueces Bay core 2, open circles denote % sand, grey boxes denote % silt and solid triangles denote % clay.

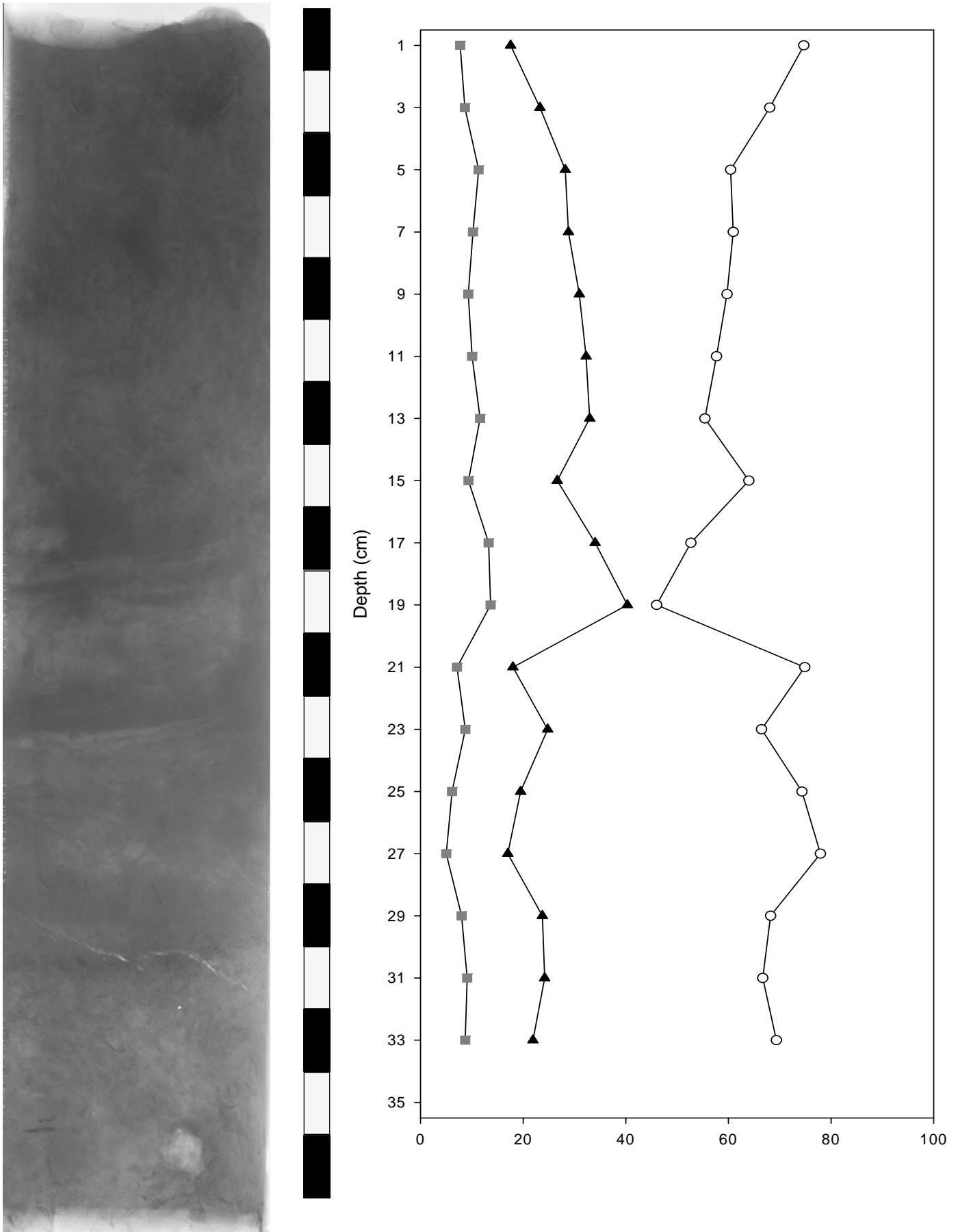


Figure AII3: X-radiography and grain size distribution for Nueces Bay core 3, open circles denote % sand, grey boxes denote % silt and solid triangles denote % clay.

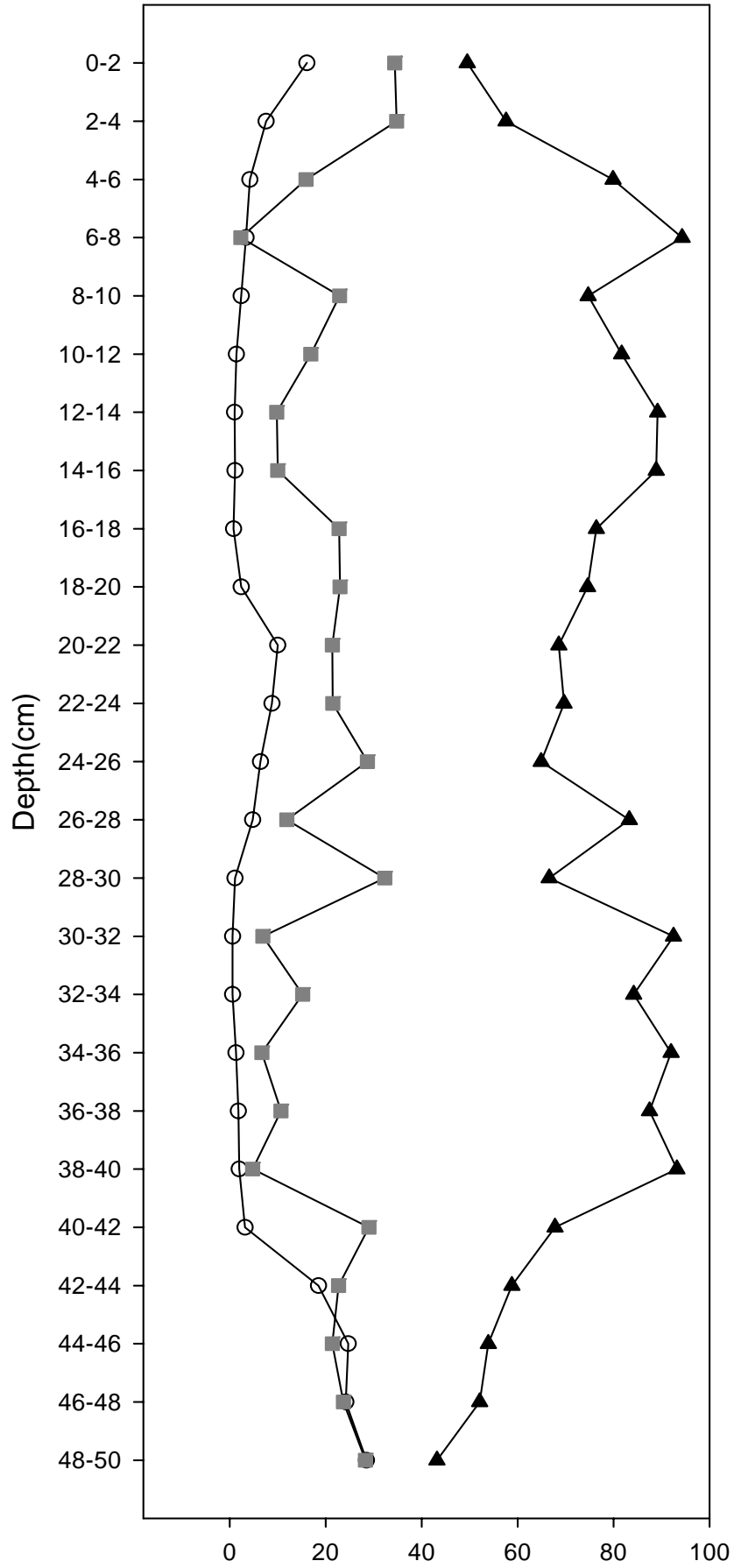


Figure AII4: X-radiography and grain size distribution for Corpus Christi Bay core 1, open circles denote % sand, grey boxes denote % silt and solid triangles denote % clay.

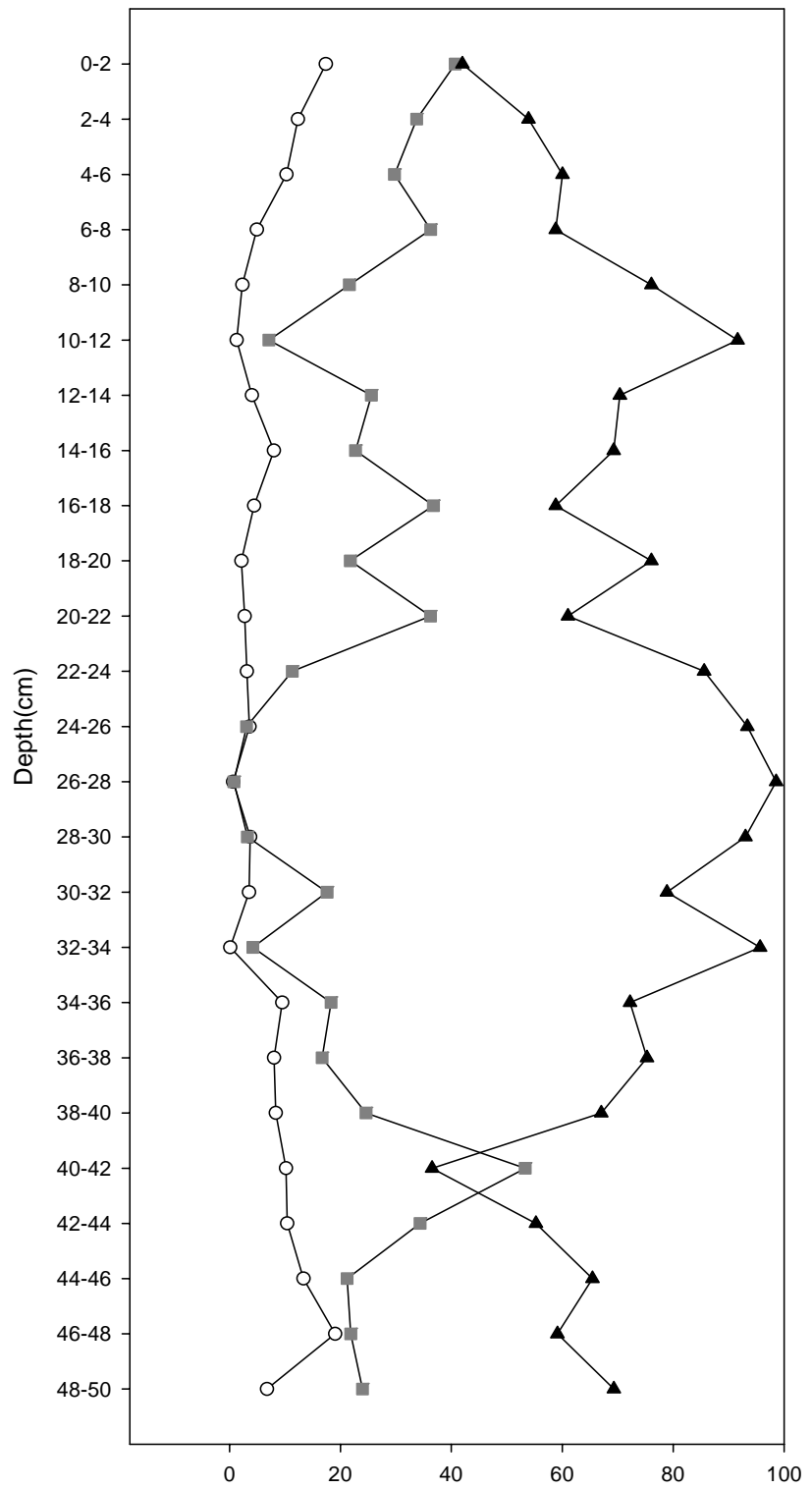


Figure AII5: X-radiography and grain size distribution for Corpus Christi Bay core 2, open circles denote % sand, grey boxes denote % silt and solid triangles denote % clay.

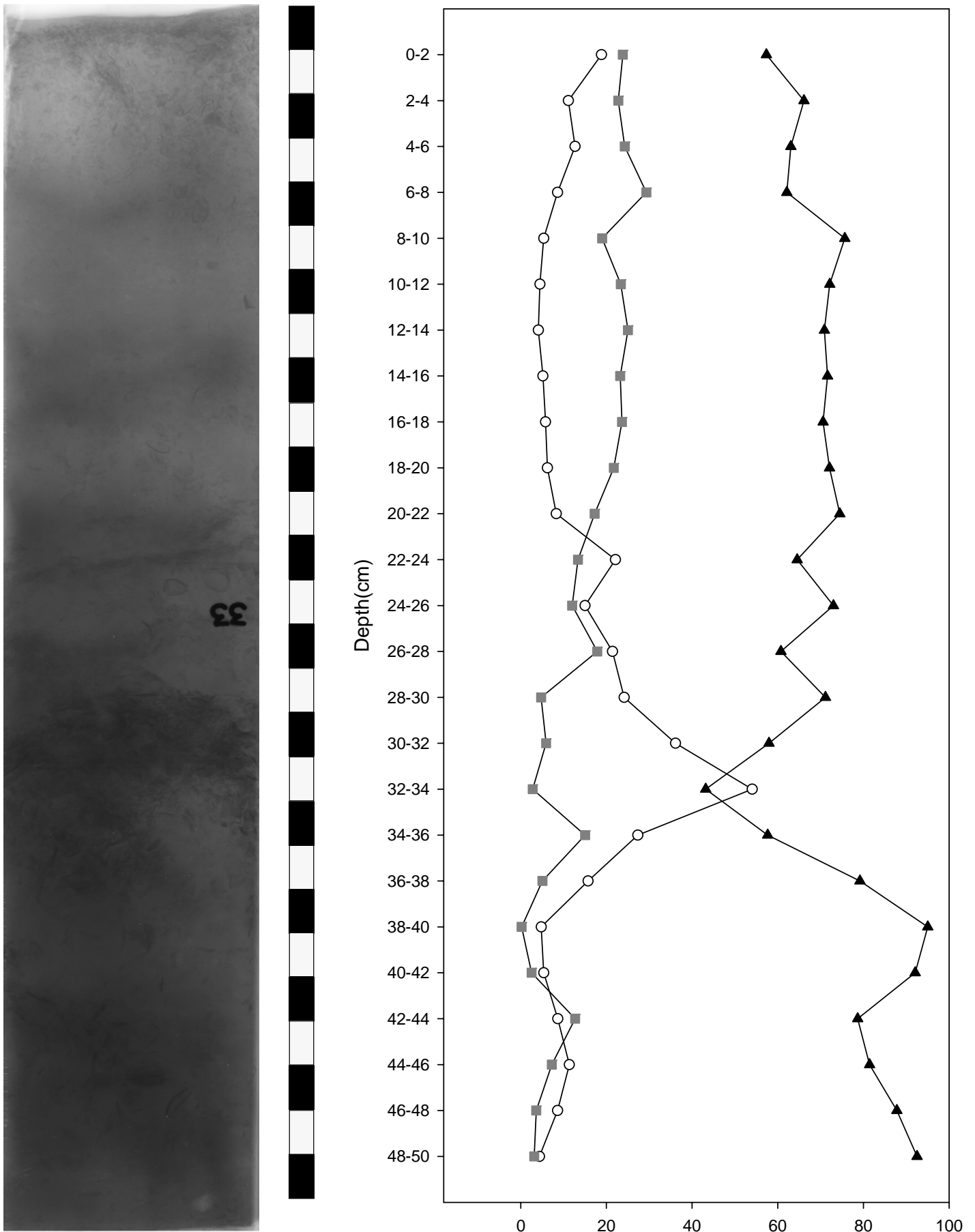


Figure AII6: X-radiography and grain size distribution for Corpus Christi Bay core 3, open circles denote % sand, grey boxes denote % silt and solid triangles denote % clay.

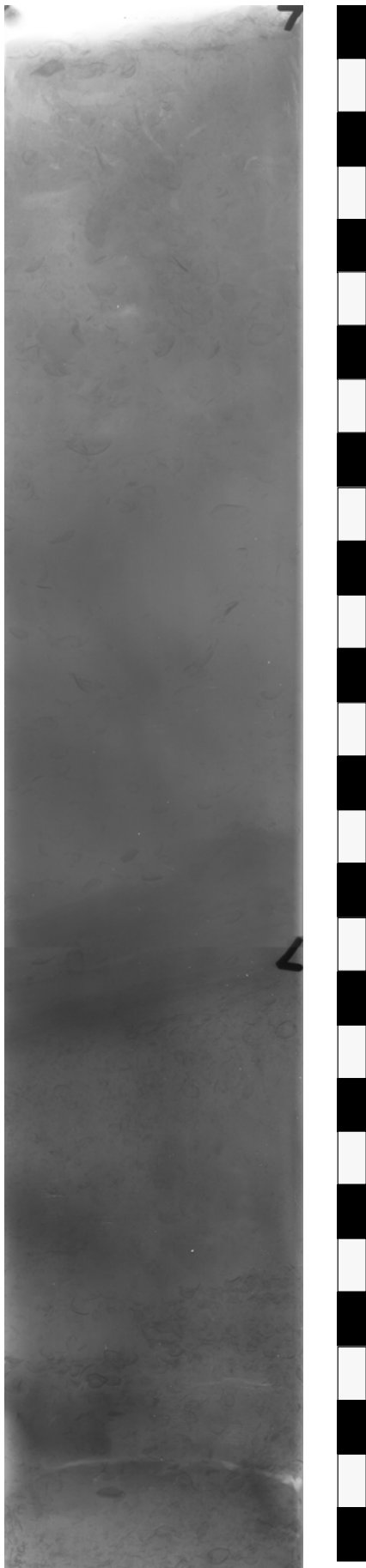


Figure AII7: X-radiography and grain size distribution for Corpus Christi Bay core 4, open circles denote % sand, grey boxes denote % silt and solid triangles denote % clay.

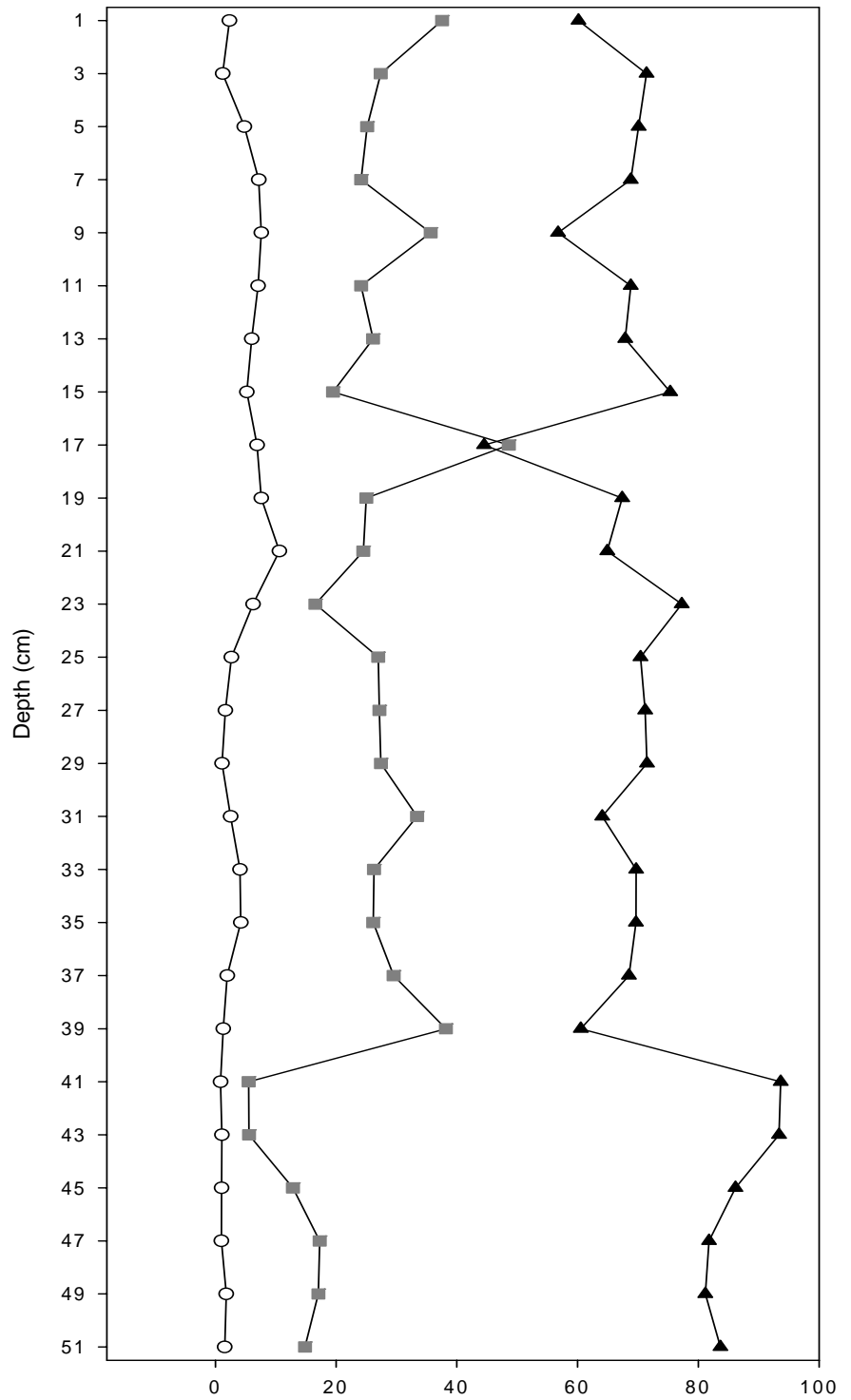
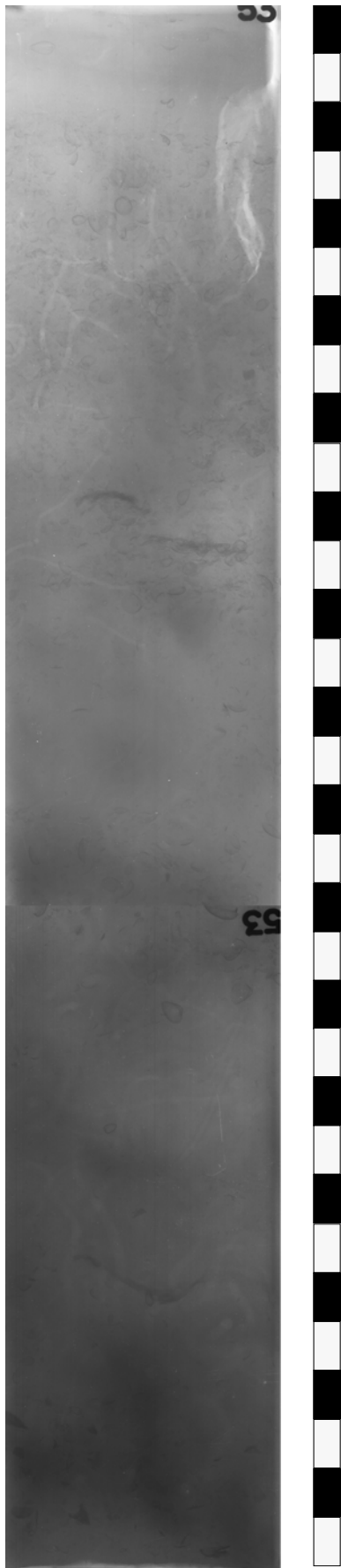


Figure AII8: X-radiography and grain size distribution for Corpus Christ Bay core 5, open circles denote % sand, grey boxes denote % silt and solid triangles denote % clay.

Table AII9: Summary grain size data for Nueces Bay cores 1, 2 and 3 x-radiography sections.

(1) Depth (cm)	% Sand	% Silt	% Clay	(2) Depth (cm)	% Sand	% Silt	% Clay	(3) Depth (cm)	% Sand	% Silt	% Clay
0 - 2	42.8	31.5	25.7	0 - 2	74.3	11.1	14.6	0 - 2	74.7	7.7	17.6
2 - 4	46.2	36.6	17.3	2 - 4	58.5	15.3	26.1	2 - 4	68.1	8.7	23.3
4 - 6	55.1	26.2	18.7	4 - 6	53.2	14.7	32.1	4 - 6	60.4	11.3	28.2
6 - 8	42.8	21.9	35.3	6 - 8	49.0	15.4	35.7	6 - 8	60.9	10.2	28.8
8 - 10	35.7	24.2	40.1	8 - 10	44.9	18.7	36.4	8 - 10	59.7	9.3	31.0
10 - 12	19.5	26.7	53.8	10 - 12	40.6	20.0	39.4	10 - 12	57.7	10.0	32.3
12 - 14	18.4	23.5	58.1	12 - 14	27.9	22.7	49.4	12 - 14	55.4	11.6	33.0
14 - 16	7.5	20.5	71.9	14 - 16	20.7	27.7	51.6	14 - 16	64.0	9.4	26.6
16 - 18	8.0	21.5	70.5	16 - 18	9.2	26.6	64.1	16 - 18	52.7	13.3	34.0
18 - 20	7.1	26.6	66.2	18 - 20	14.9	20.9	64.2	18 - 20	46.0	13.7	40.3
20 - 22	10.4	22.4	67.2	20 - 22	10.7	26.6	62.7	20 - 22	74.9	7.1	18.0
22 - 24	8.0	20.3	71.6	22 - 24	13.0	21.7	65.3	22 - 24	66.5	8.8	24.8
24 - 26	2.7	23.4	73.9	24 - 26	6.0	22.7	71.3	24 - 26	74.3	6.2	19.5
26 - 28	2.9	17.4	79.7	26 - 28	2.5	31.5	66.1	26 - 28	77.9	5.0	17.0
28 - 30	1.0	20.9	78.0	28 - 30	4.3	19.5	76.2	28 - 30	68.2	8.0	23.8
30 - 32	0.9	26.5	72.6	30 - 32	3.4	24.7	71.9	30 - 32	66.7	9.1	24.2
32 - 34	1.9	18.7	79.4	32 - 34	3.7	27.2	69.1	32 - 34	69.4	8.7	21.9
34 - 36	2.2	12.5	85.4	34 - 36	1.4	31.5	67.1	34 - 36	66.1	8.0	25.9
36 - 38	5.3	16.2	78.5	36 - 38	--	--	--	36 - 38	--	--	--
38 - 40	1.2	10.7	88.0	38 - 40	--	--	--	38 - 40	--	--	--
40 - 42	1.8	14.6	83.7	40 - 42	--	--	--	40 - 42	--	--	--
42 - 44	0.7	17.7	81.6	42 - 44	--	--	--	42 - 44	--	--	--
44 - 46	0.5	15.2	84.3	44 - 46	--	--	--	44 - 46	--	--	--
46 - 48	--	--	--	46 - 48	--	--	--	46 - 48	--	--	--
48 - 50	--	--	--	48 - 50	--	--	--	48 - 50	--	--	--

Table AIII10: Summary grain size data for Corpus Christi Bay cores 1, 2 and 3 x-radiography sections.

(1) Depth (cm)	% Sand	% Silt	% Clay	(2) Depth (cm)	% Sand	% Silt	% Clay	(3) Depth (cm)	% Sand	% Silt	% Clay
0 - 2	16.1	34.4	49.5	0 - 2	17.3	30.5	52.2	0 - 2	18.8	23.8	57.4
2 - 4	7.6	34.9	57.6	2 - 4	12.3	33.8	53.9	2 - 4	11.1	22.8	66.1
4 - 6	4.2	15.9	79.9	4 - 6	10.2	29.7	60.0	4 - 6	12.7	24.3	63.1
6 - 8	3.4	2.3	94.4	6 - 8	4.9	36.3	58.8	6 - 8	8.6	29.3	62.1
8 - 10	2.4	22.9	74.7	8 - 10	2.3	21.6	76.1	8 - 10	5.4	19.0	75.6
10 - 12	1.4	16.9	81.7	10 - 12	1.3	7.1	91.6	10 - 12	4.5	23.4	72.2
12 - 14	1.0	9.8	89.2	12 - 14	4.0	25.6	70.4	12 - 14	4.1	25.0	70.9
14 - 16	1.1	10.0	88.9	14 - 16	8.0	22.7	69.3	14 - 16	5.2	23.2	71.6
16 - 18	0.8	22.8	76.3	16 - 18	4.4	36.8	58.8	16 - 18	5.8	23.6	70.6
18 - 20	2.4	23.0	74.6	18 - 20	2.2	21.8	76.1	18 - 20	6.2	21.7	72.1
20 - 22	10.0	21.4	68.6	20 - 22	2.7	36.2	61.0	20 - 22	8.3	17.3	74.5
22 - 24	8.8	21.5	69.7	22 - 24	3.1	11.3	85.6	22 - 24	22.1	13.3	64.5
24 - 26	6.4	28.7	64.9	24 - 26	3.6	3.0	93.4	24 - 26	15.0	12.0	73.0
26 - 28	4.8	11.9	83.3	26 - 28	0.6	0.8	98.6	26 - 28	21.4	17.9	60.7
28 - 30	1.0	32.3	66.6	28 - 30	3.7	3.2	93.0	28 - 30	24.1	4.7	71.1
30 - 32	0.6	6.9	92.5	30 - 32	3.5	17.6	78.9	30 - 32	36.1	5.9	58.0
32 - 34	0.6	15.2	84.2	32 - 34	0.1	4.2	95.7	32 - 34	54.0	2.8	43.2
34 - 36	1.3	6.7	92.0	34 - 36	9.5	18.3	72.2	34 - 36	27.3	15.0	57.6
36 - 38	1.8	10.7	87.5	36 - 38	8.0	16.7	75.3	36 - 38	15.7	5.1	79.2
38 - 40	2.0	4.8	93.2	38 - 40	8.3	24.6	67.0	38 - 40	4.8	0.2	95.0
40 - 42	3.2	29.0	67.8	40 - 42	10.2	53.3	36.5	40 - 42	5.4	2.5	92.1
42 - 44	18.5	22.7	58.8	42 - 44	10.4	34.4	55.3	42 - 44	8.7	12.7	78.7
44 - 46	24.7	21.4	53.9	44 - 46	13.3	21.2	65.5	44 - 46	11.3	7.2	81.4
46 - 48	24.2	23.7	52.0	46 - 48	19.0	21.8	59.1	46 - 48	8.6	3.6	87.8
48 - 50	28.5	28.3	43.2	48 - 50	6.7	24.0	69.3	48 - 50	4.4	3.1	92.5

Table AIII1: Summary grain size data for Corpus Christi Bay cores 4 and 5 x-radiography sections.

(4) Depth (cm)	% Sand	% Silt	% Clay	(5) Depth (cm)	% Sand	% Silt	% Clay
0 - 2	21.8	21.4	56.8	0 - 2	2.3	37.5	60.2
2 - 4	15.2	16.6	68.2	2 - 4	1.2	27.4	71.4
4 - 6	14.7	20.9	64.3	4 - 6	4.8	25.1	70.1
6 - 8	12.7	15.9	71.4	6 - 8	7.2	25.2	67.7
8 - 10	8.9	14.4	76.7	8 - 10	7.6	35.6	56.8
10 - 12	10.3	21.4	68.3	10 - 12	7.1	24.1	68.8
12 - 14	8.1	26.1	65.8	12 - 14	6.0	26.1	67.9
14 - 16	9.1	24.6	66.3	14 - 16	5.2	19.5	75.3
16 - 18	4.9	14.5	80.6	16 - 18	6.9	48.6	44.5
18 - 20	3.1	17.9	79.1	18 - 20	7.6	25.0	67.4
20 - 22	4.2	18.1	77.8	20 - 22	10.6	24.5	64.9
22 - 24	4.0	26.3	69.8	22 - 24	6.2	16.6	77.2
24 - 26	4.4	19.8	75.8	24 - 26	2.6	27.0	70.4
26 - 28	8.5	19.5	72.0	26 - 28	1.6	27.2	71.2
28 - 30	15.2	24.9	59.9	28 - 30	1.1	27.4	71.5
30 - 32	13.1	28.1	58.8	30 - 32	2.5	33.4	64.1
32 - 34	14.4	18.1	67.6	32 - 34	4.0	26.3	69.7
34 - 36	13.8	20.5	65.6	34 - 36	4.2	26.1	69.7
36 - 38	8.3	15.7	76.0	36 - 38	2.0	29.5	68.5
38 - 40	12.4	12.9	74.7	38 - 40	1.3	38.2	60.5
40 - 42	--	--	--	40 - 42	0.8	5.5	93.6
42 - 44	--	--	--	42 - 44	1.1	5.6	93.4
44 - 46	--	--	--	44 - 46	1.0	12.8	86.1
46 - 48	--	--	--	46 - 48	1.0	17.3	81.8
48 - 50	--	--	--	48 - 50	1.8	17.1	81.1